Report No. K-TRAN: KU-22-6 ▪ FINAL REPORT ▪ October 2025

Mitigating Concentrated Sheet Flow of Water at Ends of Superelevated Curves

Adam Alani
Joshua Roundy, Ph.D., P.E.
Alexandra Kondyli, Ph.D.

The University of Kansas

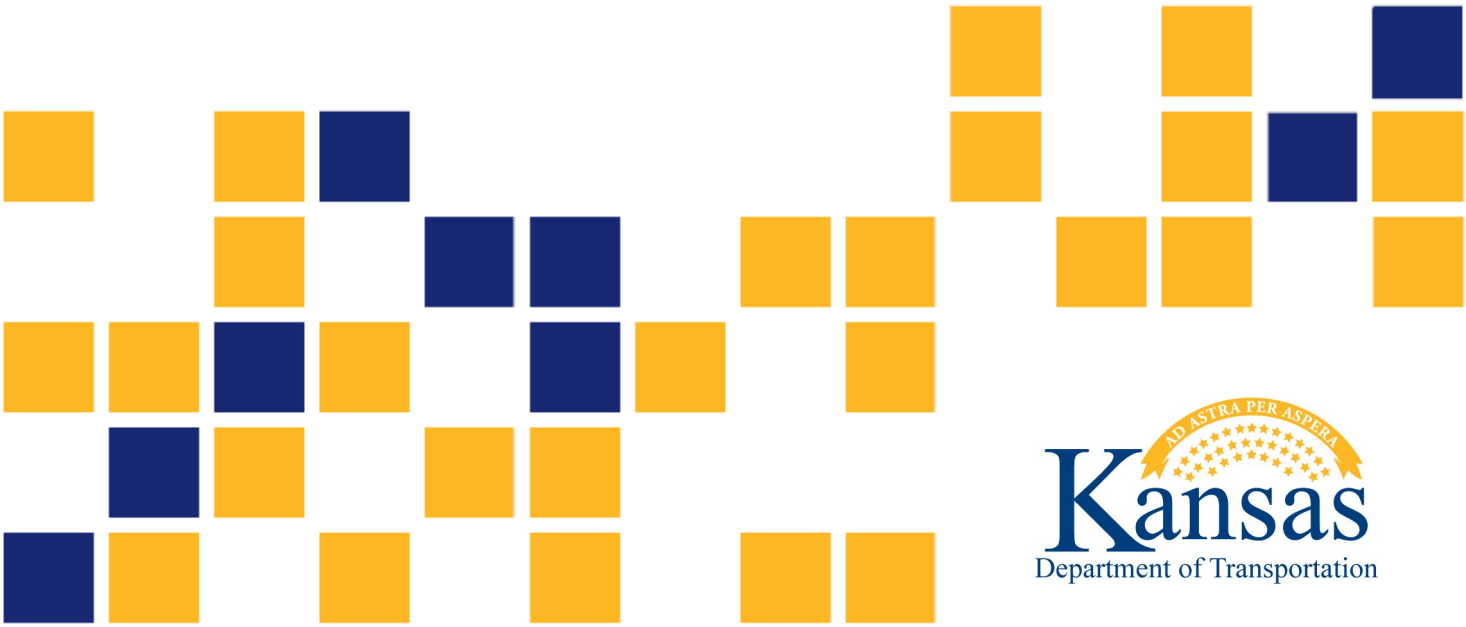

Kansas
Department of Transportation

1 Report No. K-TRAN: KU-22-6	**2 Government Accession No.**	**3 Recipient Catalog No.**
4 Title and Subtitle Mitigating Concentrated Sheet Flow of Water at Ends of Superelevated Curves		**5 Report Date** October 2025 **6 Performing Organization Code**
7 Author(s) Adam Alani; Joshua Roundy, Ph.D., P.E.; Alexandra Kondyli, Ph.D.		**8 Performing Organization Report No.**
9 Performing Organization Name and Address The University of Kansas Department of Civil, Environmental & Architectural Engineering 1530 West 15th St Lawrence, Kansas 66045-7609		**10 Work Unit No. (TRAIS)** **11 Contract or Grant No.** C2192
12 Sponsoring Agency Name and Address Kansas Department of Transportation Bureau of Research 2300 SW Van Buren Topeka, Kansas 66611-1195		**13 Type of Report and Period Covered** Final Report August 2021 – January 2023 **14 Sponsoring Agency Code** RE-0834-01
15 Supplementary Notes For more information write to address in block 9.		

16 Abstract

Superelevated highway transitions experience an area of zero-cross slope as one side of the roadway transitions from a normal crown cross slope to superelevation. These areas of minimal transverse cross slope combined with minimal longitudinal grade can cause an increase in water accumulation on highways, which can increase the likelihood for hydroplaning. This research investigates hydroplaning and its causes using the current design literature from state departments of transportation regarding the improvement of pavement drainage to reduce the potential for hydroplaning. Engineers at the Kansas Department of Transportation identified several locations with potentially poor pavement drainage in areas of superelevation transitions, and then these locations were used to identify potential areas of problematic hydroplaning. The potentially problematic locations were then analyzed using data from digital terrain mapping and laser crack measuring systems to pinpoint specific areas near superelevated highway transitions where water accumulates to a sufficient depth; thereby, increasing the potential for hydroplaning. Several mitigation strategies are discussed for these locations, including the use of slope flow path minimization at transition areas to mediate water accumulation issues.

17 Key Words Fluid Dynamics, Hydroplaning, Drainage, Hydraulics, Runoff		**18 Distribution Statement** No restrictions. This document is available to the public through the National Technical Information Service www.ntis.gov.	
19 Security Classification (of this report) Unclassified	**20 Security Classification (of this page)** Unclassified	**21 No. of pages** 113	**22 Price**

Form DOT F 1700.7 (8-72)

This page intentionally left blank.

Mitigating Concentrated Sheet Flow of Water at Ends of Superelevated Curves

Final Report

Prepared by

Adam Alani
Joshua Roundy, Ph.D., P.E.
Alexandra Kondyli, Ph.D.

The University of Kansas

A Report on Research Sponsored by

THE KANSAS DEPARTMENT OF TRANSPORTATION
TOPEKA, KANSAS

and

THE UNIVERSITY OF KANSAS
LAWRENCE, KANSAS

October 2025

PREFACE

The Kansas Department of Transportation's (KDOT) Kansas Transportation Research and New-Developments (K-TRAN) Research Program funded this research project. It is an ongoing, cooperative and comprehensive research program addressing transportation needs of the state of Kansas utilizing academic and research resources from KDOT, Kansas State University and the University of Kansas. Transportation professionals in KDOT and the universities jointly develop the projects included in the research program.

NOTICE

The authors and the state of Kansas do not endorse products or manufacturers. Trade and manufacturers names appear herein solely because they are considered essential to the object of this report.

This information is available in alternative accessible formats. To obtain an alternative format, contact the Office of Public Affairs, Kansas Department of Transportation, 700 SW Harrison, 2nd Floor – West Wing, Topeka, Kansas 66603-3745 or phone (785) 296-3585 (Voice) (TDD).

DISCLAIMER

The contents of this report reflect the views of the authors who are responsible for the facts and accuracy of the data presented herein. The contents do not necessarily reflect the views or the policies of the state of Kansas. This report does not constitute a standard, specification or regulation.

Abstract

Superelevated highway transitions experience an area of zero-cross slope as one side of the roadway transitions from a normal crown cross slope to superelevation. These areas of minimal transverse cross slope combined with minimal longitudinal grade can cause an increase in water accumulation on highways, which can increase the likelihood for hydroplaning. This research investigates hydroplaning and its causes using the current design literature from state departments of transportation regarding the improvement of pavement drainage to reduce the potential for hydroplaning. Engineers at the Kansas Department of Transportation identified several locations with potentially poor pavement drainage in areas of superelevation transitions, and then these locations were used to identify potential areas of problematic hydroplaning. The potentially problematic locations were then analyzed using data from digital terrain mapping and laser crack measuring systems to pinpoint specific areas near superelevated highway transitions where water accumulates to a sufficient depth, thereby increasing the potential for hydroplaning. Several mitigation strategies are discussed for these locations, including the use of slope flow path minimization at transition areas to mediate water accumulation issues.

Acknowledgments

Financial support was provided by the Kansas Department of Transportation. The opinions and conclusions presented herein are those of the writers and do not necessarily represent those of the sponsoring organization.

Table of Contents

Abstract v
Acknowledgments vi
Table of Contents vii
List of Tables x
List of Figures xi
Chapter 1: Introduction 1
1.1 Problem Statement 1
1.2 Objectives 2
1.3 Methodology 2
Chapter 2: Literature Review 3
2.1 Hydroplaning 3
2.2 Hydroplaning Characteristics 3
2.3 Water Film Thickness Models and Equations 4
2.4 Hydroplaning Models and Equations 6
2.5 DOT Design Tools 9
2.6 Surface Texture 10
2.6.1 Roadway Texture and Hydroplaning 11
2.6.2 Pavement Texture and Grooving 12
2.6.3 High Friction Surface Treatments 16
2.7 DOT Highway and Drainage Design Manuals 17
Chapter 3: Datasets and Methods 22
3.1 Study Locations 22
3.1.1 Site Visits 27
3.2 Datasets 31
3.2.1 Digital Terrain Mapping 32
3.2.2 Laser Crack Measuring System Data 32
3.2.3 State Crash Data 32
3.3 Methods 33
3.3.1 Hydroplaning Remediation 33
3.3.2 Flow Direction and Flow Accumulation 34

3.3.3 Roadway Texture and Slopes 34
3.3.4 Highway Redesign Using Slope-Path Length 35
Chapter 4: Digital Model Results 38
4.1 Analysis Results 38
4.1.1 Results for the 169-2 RP 79.2 Location 38
4.1.2 Results for the 70-84 RP 204.8 Location 41
4.1.3 Results for the 35-46 RP 214.7 Location 44
4.1.4 Results for the 35-46 RP 217.55 Location 47
4.1.5 Results for the 70-31 RP 295.2 Location 50
4.1.6 Results for the 50-9 RP 330.1 Location 53
4.1.7 Results from the 70-89 RP 357.7 Location 56
4.2 Overall Hydroplaning Potential and Mitigation 59
4.3 Crash Rate 59
4.4 Geometric Redesign to Mitigate Hydroplaning 61
4.4.1 Identifying Poor Drainage Using Flow Paths in ORD 61
4.4.2 Design Check of Slope Flow Path Length 69
Chapter 5: Discussion 74
5.1 Hydroplaning Remediation Recommendations for Study Locations 74
5.2 Geometric Redesign 74
Chapter 6: Summary and Recommendations 76
6.1 Summary 76
6.2 Recommendations and Best Practices 76
6.3 Uncertainty and Limitations 77
6.4 Future Directions 79
References 80
Appendix A: Relevant Literature from Departments of Transportation 88
A.1 Alabama Department of Transportation 88
A.2 Colorado Department of Transportation 88
A.3 Florida Department of Transportation 89
A.4 Georgia Department of Transportation 90
A.5 Idaho Transportation Department 91

A.6 Minnesota Department of Transportation 92
A.7 Nebraska Department of Transportation 93
A.8 North Carolina Department of Transportation 94
A.9 Oregon Department of Transportation 96
A.10 Texas Department of Transportation 96
A.11 Vermont Agency of Transportation 97
A.12 West Virginia Division of Highways 98

List of Tables

Table 2.1: Flexible and Concrete Pavement Treatment Strategies 12
Table 2.2: Typical Ranges of Macrotexture for New and Aged Surface Textures 14
Table 2.3: Texture Method and Ranking 14
Table 2.4: Texture and Friction Ranges of Concrete Surfaces 15
Table 2.5: Highway Design Manual Source and Superelevated Transition Design Reference Location 17
Table 2.6: Drainage Design Manual Source and Reference Location 19
Table 3.1: Study Locations in Kansas Identified by KDOT Engineers 22
Table 3.2: AADT, Design Speed, and Superelevation Information for Study Locations 22
Table 3.3: Transition Runout/Runoff Length and Horizontal Curve Information for Study Locations 23
Table 3.4: Methods of Hydroplaning Remediation 33
Table 4.1: Study Location Results 59
Table 4.2: All-Weather and Wet-Weather Crash Rates for Study Locations 60
Table 4.3: Comparison of Transition Designs For 70-31 RP 295. Location In ORD 65
Table 4.4: Minimum Acceleration Lane Lengths 68
Table 4.5: Slope Flow Path Length Comparison of Transition Redesign 70

List of Figures

Figure 2.1: Water Film Thickness (WFD), MTD, and Total Flow Thickness 11
Figure 3.1: Study Locations in Kansas (Blue Markers)..... 23
Figure 3.2: Approximate Superelevated Transitions at 169-2 RP 79.2 24
Figure 3.3: Approximate Superelevated Transitions at 70-84 RP 204.8 24
Figure 3.4: Approximate Superelevated Transitions at 35-46 RP 214.7 25
Figure 3.5: Approximate Superelevated Transitions at 35-46 RP 217.55 25
Figure 3.6: Approximate Superelevated Transitions at 70-31 RP 295.2 26
Figure 3.7: Approximate Superelevated Transitions at 50-9 RP 330.1 26
Figure 3.8: Approximate Superelevated Transitions at 70-89 RP 357.7 27
Figure 3.9: Gore Area Facing Southbound Direction Near 35-46 RP 214.7..... 28
Figure 3.10: Northbound Direction Near 35-46 RP 217.55 (Left) and Evident Dampness at the Southbound Direction Near 35-46 RP 217.55 (Right) 28
Figure 3.11: Washout Near Guardrail Near 35-46 RP 217.55..... 29
Figure 3.12: Eastbound (Left) and Westbound Direction (Right) Near 70-31 RP 295.2 29
Figure 3.13: Eastbound (Left) and Westbound Direction (Right) Near 50-9 RP 330.1 30
Figure 3.14: Westbound (Left) and Eastbound Direction (Right) Near 70-89 RP 357.7 30
Figure 3.15: Superelevated Transition at the 70-31 RP 295.4 Location..... 35
Figure 3.16: Horizontal Alignment of 70-31 RP 295.4 Location in ORD 36
Figure 3.17: 3D Corridor Model of 70-31 RP 295.4 Location in ORD 36
Figure 3.18: Superelevation Transition of the 70-31 RP 295.4 Location in ORD 37
Figure 4.1: Results for the 169-2 RP 79.2 Location: (a) Scan Locations, (b) MTD, (c) Cross Slope, and (d) Longitudinal Slope 39
Figure 4.2: (a) Flow Direction, (b) Flow Accumulation..... 40
Figure 4.3: Results for the 70-84 RP 204.8 Location: (a) Scan Locations, (b) MTD, (c) Cross Slope, and (d) Longitudinal Slope 42
Figure 4.4: (a) Flow Direction, (b) Flow Accumulation..... 43
Figure 4.5: Results for the 35-46 RP 214.7 Location: (a) Scan Locations, (b) MTD, (c) Cross Slope, and (d) Longitudinal Slope 45
Figure 4.6: (a) Flow Direction, (b) Flow Accumulation..... 46
Figure 4.7: Results for the 35-46 RP 217.55 Location: (a) Scan Locations, (b) MTD, (c) Cross Slope, and (d) Longitudinal Slope 48

Figure 4.8: (a) Flow Direction, (b) Enlarged View of Flow Direction, and (c) Flow Accumulation 49
Figure 4.9: Results for the 70-31 RP 295.2 Location: (a) Scan Locations, (b) MTD, (c) Cross Slope, and (d) Longitudinal Slope 51
Figure 4.10: (a) Flow Direction, (b) Flow Accumulation 52
Figure 4.11: Results for the 50-9 RP 330.1 Location: (a) Scan Locations, (b) MTD, (c) Cross Slope, and (d) Longitudinal Slope 54
Figure 4.12: (a) Flow Direction, (b) Flow Accumulation 55
Figure 4.13: Results for the 70-89 RP 357.7 Location: (a) Scan Locations, (b) MTD, (c) Cross Slope, and (d) Longitudinal Slope 57
Figure 4.14: (a) Flow Direction, (b) Flow Accumulation 58
Figure 4.15: All-Weather and Wet-Weather Crash Rates for Study Locations 61
Figure 4.16: Flow Slope Paths of Original 70-31 RP 295.2 Design 62
Figure 4.17: Flow Slope Path of Transition Area of Original 70-31 RP 295.2 Design 63
Figure 4.18: Flow Slope Path of Tangent Section of 70-31 RP 295.2 Location 63
Figure 4.19: Method to Attain Superelevation for Transition Redesign 64
Figure 4.20: Vertical Alignment for the 70-31 RP 295.2 Location 66
Figure 4.21: Entrance Terminal Examples 67
Figure 4.22: Entrance Types within Horizontal Curves 69
Figure 4.23: Flow Slope Paths of Minimum Transition Length for 70-31 RP 295.2 Location 70
Figure 4.24: Flow Slope Paths of Shortened Transition 1 for 70-31 RP 295.2 Location 70
Figure 4.25: Flow Slope Paths of Shortened Transition 2 for 70-31 RP 295.2 Location 71
Figure 4.26: Flow Slope Paths of 7.0% Superelevation Transition for 70-31 RP 295.2 Location 71
Figure 4.27: Flow Slope Paths of 67% Runoff Before the PC for 70-31 RP 295.2 Location 71
Figure 4.28: Flow Slope Paths of 50% Runoff Before the PC for 70-31 RP 295.2 Location 71
Figure 4.29: Flow Slope Paths of Shortened Transition 2 with 67% Runoff Before the PC for 70-31 RP 295.2 Location 72
Figure 4.30: Acceleration Lane Reconfiguration at 70-31 RP 295.2 Location 72
Figure 4.31: Slope Flow Path Length for Acceleration Lane Reconfiguration at 70-31 RP 295.2 Location 73

Chapter 1: Introduction

Vehicle crashes due to rainfall are primarily caused by reduced visibility for drivers and dynamic hydroplaning (Ong et al., 2005). Hydroplaning occurs when water buildup creates a water film that could provide enough lift to exceed the drainage capacity of a tire tread pattern to the surface of the roadway (AASHTO, 2018). Consequently, roadway infrastructure must effectively reduce the elements conducive to hydroplaning during rainfall events.

To effectively mitigate hydroplaning, the flow of rainwater, or sheet flow, over superelevated highway transitions can be modeled. A superelevation transition occurs as a roadway of a normal crown heads into a curve. The transition section contains an area of roadway in which the cross slope becomes zero and water is slow to drain from the roadway. The geometry at these transitions tends to direct runoff from a large surface area to a smaller cross section, leading to a runoff depth that may cause hydroplaning. Although many models have reproduced the flow of water over superelevated highway transitions, most models are unavailable for industry use. In addition, modeling water film thickness, and thus hydroplaning potential, for complicated highway profiles requires the synthesis of many areas of research, including hydroplaning mechanics, fluid mechanics, highway design, and material properties, to develop hydroplaning mitigation strategies.

Therefore, this project, which focuses on the hydraulics and drainage geometry at curve transitions, proposes methods to predict where hydroplaning is likely to occur and presents mitigation strategies and recommendations to evaluate the proposed strategies. This study also investigated various design considerations the Kansas Department of Transportation (KDOT) could utilize for general hydroplaning mitigation and hydroplaning mitigation at superelevated transition areas.

1.1 Problem Statement

Superelevated highway transitions require adequate design to ensure proper drainage to mitigate sheet flow and ponding on roadways and reduce hydroplaning.

1.2 Objectives

The objectives of this research were to identify the conditions that cause concentrated flow at superelevated curve transitions and propose mitigation strategies for current and future designs by modeling sheet flow through curve transitions to predict problematic locations.

1.3 Methodology

The multifaceted nature of hydroplaning requires any hydroplaning investigation to account for roadway characteristics such as geometry, texture, and drainage, as well as vehicle-roadway interactions. Therefore, this study conducted a literature review that included every highway and drainage design manual for each of the 50 state departments of transportation (DOTs) in the United States, with a focus on relevant hydroplaning mitigation. Two software tools commonly used by state DOTs were also used to study flow near superelevated highway transitions.

Chapter 2: Literature Review

Hydroplaning potential is an essential consideration of sheet flow mitigation on a roadway. Previous research has studied hydroplaning mechanics and types, hydroplaning methods and models, hydroplaning prevention tools, and methods to increase pavement texture to decrease hydroplaning potential. Recently, the American Association of State Highway and Transportation Officials (AASHTO) and state DOTs have issued guidance to improve drainage at areas of low roadway slope and reduce hydroplaning.

2.1 Hydroplaning

Horne (1968) and Browne (1975) describe the three types of hydroplaning for pneumatic-tired vehicles: dynamic hydroplaning, viscous hydroplaning, and reverted-rubber hydroplaning. Dynamic hydroplaning occurs when enough fluid is present on a roadway surface to separate the tires of a vehicle from the ground, specifically when a roadway is flooded. According to Browne (1975), dynamic hydroplaning occurs when "the tire exceeds the combined drainage capacity of the tread pattern and the pavement texture… in deep fluid layers where fluid inertial effects are dominant." Dynamic hydroplaning is the dominant focus of many hydroplaning models and equations. The second type, viscous hydroplaning, occurs on damp roadways with a very thin film of water that overwhelms the microtexture of the roadway. Since very small amounts of fluid can cause this type of hydroplaning, viscous hydroplaning can occur at any vehicle speed (Browne, 1975). Finally, reverted-rubber hydroplaning, which occurs on wet roadways with macrotexture but minimal microtexture, means the wheels of the vehicle lock when braking (usually at high speeds), causing the tire that is in contact with the roadway to heat up and begin to melt, resulting in lost traction (Browne, 1975). The fluid and tire become sufficiently hot enough to produce steam (Horne, 1968).

2.2 Hydroplaning Characteristics

Sufficient fluid on a roadway can lift the tires of a vehicle when the fluid force is equal to or exceeds the vertical force of a vehicle. As the velocity of a vehicle increases, tire pressure becomes equivalent to inertial forces of the water film, and the contact patch of the tire and

roadway buckle, meaning the film of water on the roadway supports the load of the vehicle (Flintsch et al., 2021). According to AASHTO (2018), "water depth, roadway geometrics, vehicle speed, tire tread design and depth, tire inflation pressure, pavement surface macrotexture, and the condition of the pavement surface" all impact hydroplaning and subsequent hydroplaning potential. Flintsch et al. (2021) suggests that, when considering hydroplaning, fluid lift forces be compared to wheel loads, or the vector of the lateral and longitudinal forces be compared to the force generated by the tire at the operating conditions. In the former consideration, wheel loads depend on vehicle characteristics and pavement characteristics, and an increased margin between wheel load and fluid lift forces improves turning and braking. The latter consideration describes available and necessary forces to prevent hydroplaning.

2.3 Water Film Thickness Models and Equations

The consideration of hydroplaning at superelevated highway transitions, however, requires methods and equations to estimate hydroplaning speed. Many hydroplaning models and equations have been developed using water film thickness (WFT) or water film depth (WFD) as input variables. WFT, or the height of flowing water over a surface, is significantly influenced by rainfall intensity, roadway geometry, roadway drainage, pavement porosity, and highway drainage (Flintsch et al., 2021). Many one-dimensional (1D) WFT models have been developed to estimate hydroplaning speed. For example, the 1D models by Gallaway et al. (1971) with the Texas DOT (TxDOT) and the PAVDRN by Anderson et al. (1998) are two of the most widely used models in the literature. The model first developed by Gallaway et al. (1971) was later updated to the following equation (i.e., empirical model) by Gallaway et al. (1979) based on experimentation at test locations:

$$WFT = 0.003726\, MTD^{0.125} L^{0.193} I^{0.562} S^{-0.364} - MTD \qquad \textbf{Equation 2.1}$$

Where:

WFT = water film thickness (in.),

MTD = mean texture depth of the pavement (in.),

L = length of the drainage path (ft),

I = rainfall intensity (in./h), and

S = cross slope of the roadway (ft/ft).

The PAVDRN model was based on the following kinetic wave equation:

$$\boldsymbol{WFT} = \left(\frac{\boldsymbol{nLI}}{\boldsymbol{36.1\,S^{0.5}}}\right) - \boldsymbol{MTD}$$

Equation 2.2

Where:

WFT = water film thickness (in.),

n = Manning's roughness coefficient (-),

L = length of drainage path (ft),

I = excess rainfall intensity (in./h) or rainfall rate (pavement permeability of the infiltration rate),

S = slope of the drainage path (in./in.), and

MTD = mean texture depth of the pavement (in.).

Li et al. (2023) developed a specific WFT equation for superelevation transitions that conserves mechanical energy while assuming open-channel flow and non-uniform gradient flow. Results showed strong correlation with the Gallaway equation, as shown in the following equation:

$$\boldsymbol{h} = \boldsymbol{v^{\frac{1}{12}}}\left(\frac{\boldsymbol{0.3164}}{\boldsymbol{8ig}}\right)^{\frac{1}{3}}(\boldsymbol{Il})^{\frac{7}{12}}$$

Equation 2.3

Where:

h = water depth (m),

v = kinematic viscosity at 20 °C (v = 1.003×10^{-6} m^2/s),

i = slope of the flow path (%),

g = gravitational constant (g = 9.8 m^2/s),

I = rainfall intensity (m/s), and

l = distance between the starting point and given section along the flow path (m).

Several notable two-dimensional (2D) and three-dimensional (3D) WFT models have also been developed over the years. For example, Ong and Fwa (2007) developed a 3D finite-element model based on mechanics and fluid dynamics. Charbeneau et al. (2008) developed a 2D diffusion wave model for superelevated highway transition, but it is not freely available and is therefore unlikely to be utilized by highway engineers. Work by Lottes et al. (2020) and Sitek and Lottes (2020) used computational fluid dynamics (CFDs) to calculate WFT. Although results from these studies agreed with the Gallaway model for WFT, the Gallaway model predicted higher WFT

results than the CFD models when rainfall exceeded 6 in./h and pavement roughness was considered.

2.4 Hydroplaning Models and Equations

As mentioned, many developed models can calculate WFT and hydroplaning speed. The most popular models include NASA hydroplaning equations developed by Dreher and Horne (1963) and expanded on by Horne (1968), TxDOT equations based on Gallaway et al. (1979), and PAVDRN equations based on Anderson et al. (1998). The following NASA equation yields hydroplaning speed based on empirical data:

$$v_p = 51.80 - 17.15(F_{AR}) + 0.72p$$

Equation 2.4

Where:
v_p = hydroplaning speed (mph),
F_{AR} = tire footprint aspect ratio, and
p = tire pressure (psi).

For heavyweight vehicles such as trucks or trailers, the tire aspect ratio decreases as the tire footprint aspect ratio decreases with added weight, as demonstrated in the following adjusted equation:

$$v_p = 7.95\sqrt{p(F_{AR})^{-1}}$$

Equation 2.5

Where:
v_p = hydroplaning speed (mph),
p = tire pressure (psi), and
F_{AR} = tire footprint aspect ratio.

The NASA equations were developed with an assumed WFT of 0.3 in. (7.62 mm), so a WFT was not included as an input parameter.

The Texas equations yield hydroplaning speeds based on empirical data. A relationship of hydroplaning speed was established as:

$$v_p = SD^{0.04} p^{0.3} (TD + 1)^{0.06} A$$

Equation 2.6

Where:

v_p = hydroplaning speed (mph),

$SD = \frac{\omega_d - \omega_w}{\omega_d} 100\%$ = spin-down ratio (unitless), assumed to be 10%,

ω_d = rotational velocity of the tire on dry pavement (rpm),

ω_w = rotational velocity of the tire on wet pavement (rpm),

p = tire pressure (psi),

TD = tire tread depth (recommended minimum tread depth is 2/32 in. (1.5 mm)) [in 32nds of an inch], and A is defined in the following equation:

$$A = max\left(3.507 + \frac{10.409}{WFT^{0.06}}, \left[\frac{28.952}{WFT^{0.06}} - 7.817\right] T^{0.14}\right)$$

Equation 2.7

Where:

WFT = water film thickness (in.), and

T = pavement texture depth (in.).

The PAVDRN empirical equation (Equation 2.8) presents a model that utilizes WFT less than 2.4 mm. For WFT greater than 2.4 mm, the model utilizes the hydroplaning equation developed by Gallaway et al. (1979) for the Texas DOT equations.

$$v_p = 26.04 WFT^{-0.259}$$

Equation 2.8

Where:

v_p = hydroplaning speed (mph), and

WFT = water film thickness (in.).

The following equation was developed by the Florida DOT (FDOT) using a unique hydroplaning speed based on research by Gunaratne et al. (2012) to create an analytical solution based on data by Ong and Fwa (2007) to produce a finite-element based fluid model:

$$v_p = WL^{0.2} p^{0.5} \left(\frac{0.82}{WFT^{0.06}} + 0.49\right)$$

Equation 2.9

Where:

v_p = hydroplaning speed (km/h),

WL = wheel load (N)

p = tire pressure (kPa), and

WFT = water film thickness (mm).

The following equation for trucks was also developed based on the NASA equation and the footprint aspect ratio of a vehicle from the study by Gunaratne et al. (2012):

$$v_p = 23.1(p)^{0.21}\left(\frac{1.4}{F_{AR}}\right)^{0.5}\left(\frac{0.268}{WFT^{0.651}}+1\right)$$

Equation 2.10

Where:

v_p = hydroplaning speed (km/h),

p = tire pressure (kPa),

F_{AR} = tire footprint aspect ratio, and

WFT = water film thickness (mm).

Li et al. (2023) developed the following equation to estimate the water depth for hydroplaning at superelevated transitions by considering a decrease in friction as it related to lubrication regimes of the roadway due to increased WFT.

$$h_t = r - \sqrt{\frac{N^2 cos^2\theta}{v^4 b^2 \rho^2}}$$

Equation 2.11

Where:

h_t = hydroplaning threshold water depth,

r = tire radius,

N = tire load,

θ = resultant gradient of the roadway section,

v = velocity of the fluid sheet,

b = tire width, and

ρ = density of water.

The older models of Horne (1968), Gallaway et al. (1979), and Anderson et al. (1998) rely on empirical regression and are not based on the mechanics of water flow, meaning these models cannot be applied outside the range of data used to generate them (Flintsch et al., 2021). More recent models, however, are based on principles of water flow, such as diffusion wave and kinematic wave models, that can be more accurately applied to roadway geometry. However, kinematic wave models cannot be used near superelevated highway transitions due to the location of the transition area and because the roadway slope nears zero percent (Jeong & Charbeneau, 2010). Therefore, models that utilize finite element analysis (Li et al., 2006) and computational

fluid dynamics (Ong & Fwa, 2007) reveal how tire-pavement interactions and vehicle dynamics impact hydroplaning. Although these models are accurate and robust, they are not readily available for engineering usage (Flintsch et al., 2021), and the incorporation of these models into the design process is not widespread. However, Flintsch et al. (2021) created a design beta version of a tool that focuses on the performance characteristics of vehicle varieties using the openly available 1D, WFT equation by Gallaway et al. (1979).

2.5 DOT Design Tools

Various highway design tools for roadway slope near superelevated transitions and hydroplaning potential have been created for DOTs. For example, the Iowa DOT created an Excel-based tool in 2014 to identify areas of low slope at superelevated transitions (Iowa DOT, 2019). The tool uses roadway type, runout and runoff lengths, horizontal-curve stationing, vertical curve stationing, vertical point of intersection, back grade, forward grade, and curve length as inputs to find the roadway slope near the location of zero cross slope. Using these inputs, the tool creates a graphical heatmap of slope along the highway map. Areas of highway have suitable drainage if resulting slopes are above 0.5%; highlighted areas below this threshold are reviewed and modified. This tool is relatively easy to use and is best suited for application on simple highway designs that only incorporate a highway curve.

In 2012, the FDOT developed a hydroplaning prediction tool based in Microsoft's Excel. In 2020, Lee and Ayyala (2020) created another multifunctional Excel-based tool that calculates WFT predictions on a highway profile of cross slope by lane, lane width, and longitudinal grade. These predictions can be calculated for a single cross section of a roadway or for a continuously changing length of roadway. Once the WFT is estimated using the Gallaway et al. (1979) WFT model, the U.K. Road Research Laboratory WFT model by Ross and Russam (1968), the modified New Zealand WFT model by Chesterton et al. (2006), or the PAVDRN WFT model by Anderson et al. (1998) and Huebner et al. (1997), the tool uses these WFT models to estimate a hydroplaning speed based on the Gallaway hydroplaning model by Gallaway et al. (1979), the PAVDRN hydroplaning model by Anderson et al. (1998), and the University of South Florida model by Gunaratne et al. (2012).

The FDOT tool provides many useful applications. For example, engineers can use the tool to conduct risk analysis, where hydroplaning speeds from the previous models are compared to expected speeds based on rainfall. This study used research by Jayasooriya and Gunaratne (2014) to predict if a driver will hydroplane on a roadway section during specific rainfall intensities. The FDOT hydroplaning tool also has a continuous analysis setting that allows users to process results for a stretch of roadway with a changing cross slope, grade, pavement texture, or rut depth. Additional support to export a .kml file for use in satellite imaging programs or websites to view results using GPS coordinates is also available. A probabilistic analysis can also be conducted with various combinations of input parameters (e.g., rainfall intensity, pavement temperature, axle weight, and tire pressure) using a Monte Carlo simulation to view variations of variables using a distribution so users can view likely WFTs and hydroplaning speeds over a distribution of various input parameters. Although the FDOT hydroplaning tool is beneficial for general hydroplaning estimation, it offers limited use for superelevated transition design, meaning more advanced models are needed for WFT and hydroplaning prediction in transition areas with complicated geometry.

2.6 Surface Texture

One of the most common measurements of surface texture is mean texture depth (MTD). A volumetric technique, such as the sand patch method (ASTM E965-15, 2019), is often used to determine the MTD, or average macrotexture of a surface. Recently, multi-laser collection vehicles have been employed to digitally collect MTD volumetrically (Drenth et al., 2017). Although the Technical Working Group (TWG) of the Federal Highway Administration (FHWA) recommends that concrete surfaces have an average minimum MTD of 0.03 in. (0.8 mm), with no individual test results less than 0.02 in. (0.5 mm) (Hibbs & Larson, 1996), state agencies have various acceptable MTD values based on pavement application (Snyder, 2006). Figure 2.1 shows the relationship of MTD and WFT.

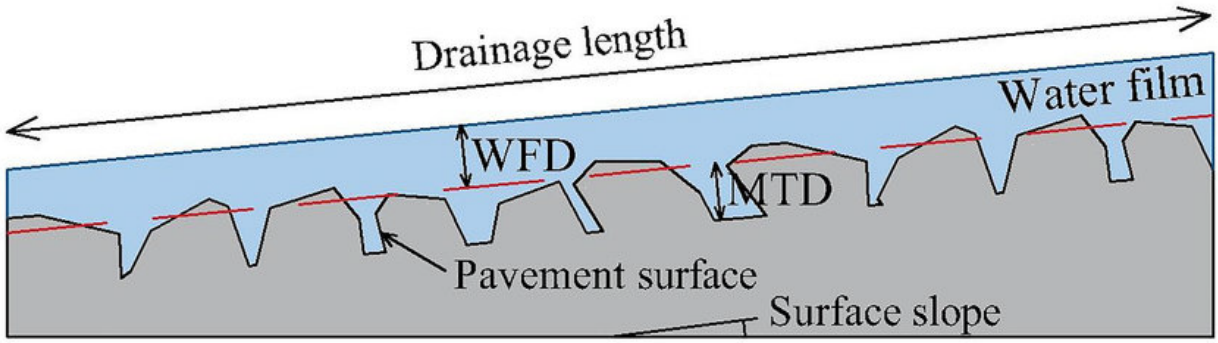

Figure 2.1: Water Film Thickness (WFD), MTD, and Total Flow Thickness
Source: Pourhassan et al., 2022. © Sage Publishing; reprinted by permission of Sage Publications.

Macrotexture and microtexture are related to frictional properties of a pavement surface (Kummer & Meyer, 1963), and texture depth uniquely impacts roadway performance depending on heights. Microtexture impacts friction at low speeds, while macrotexture significantly impacts high-speed friction, rolling resistance, and noise (Boulet et al., 1995). Macrotexture also creates porosity on roadway surfaces; thereby, increasing water drainage and reducing WFD (Pranjić & Deluka-Tibljaš, 2022).

2.6.1 Roadway Texture and Hydroplaning

High pavement texture plays a significant role in hydroplaning scenarios. In areas of high friction demand, such as transition areas, pavement can wear quickly, leading to decreased surface texture (Merritt et al., 2021). Texture management is essential for reducing hydroplaning, especially in rehabilitation methods. Roadway friction is often quantified as the friction number (FN), where 100 times the force required to slide locked, braking wheels of a trailer over a pavement surface is divided by the effective wheel loads (Snyder, 2019). The FN is not directly related to MTD because the variety of parameters (vehicle speed, aggregate type, roadway moisture, etc.) involved in its measurement prevents a simple association of the two (Zuniga-Garcia & Prozzi, 2019). However, researchers agree that macrotexture and microtexture are the primary contributors to pavement performance at high and low vehicle speeds (Henry, 2000), and surface texture is the primary property that controls skid resistance, preventing tires from sliding on pavement surfaces (Rajaei et al., 2017).

2.6.2 Pavement Texture and Grooving

Several techniques are commonly used to increase roadway texture. For example, pavement texturing and grooving are often applied to concrete and asphalt roadways as well as existing or newly constructed roads. Table 2.1 lists low-cost treatments used to improve pavement safety performance, as adapted from Merritt et al. (2015).

Table 2.1: Flexible and Concrete Pavement Treatment Strategies

Flexible Pavement Treatment Strategies	Concrete Pavement Strategies
Thin HMA Overlay	Thin HMA Overlay
Open-Graded Friction Course (OGFC)	Open-Graded Friction Course (OGFC)
Ultra-Thin Bonded Wearing Course (UTBWC)	Ultra-Thin Bonded Wearing Course (UTBWC)
Microsurfacing	Microsurfacing
Shotblasting/Abrading	Shotblasting/Abrading
High Friction Surface Treatment (HFST)	High Friction Surface Treatment (HFST)
Chip Seal (various binder types)	Diamond Grinding
Cape Seal	Grooving
Scrub Seal	Next Generation Concrete Surface
Slurry Seal	
Micro-Milling	

Source: (Merritt et al., 2015)

Thin hot mix asphalt (HMA) can be applied to concrete or asphalt pavement to improve friction and correct minor ruts in a roadway. Open-graded friction courses (OGFCs) use a porous overlay to increase drainage, while ultra-thin bonded wearing courses (UTBWCs) use an emulsion layer as a binder for asphalt on top of concrete or asphalt. Slurry seals are comprised of a mixture of emulsified asphalt, water, fine aggregate, and mineral filler that are applied to pavement surfaces in a thin layer. A cape seal is a chip seal with a slurry seal placed on top. Microsurfacing is similar to a slurry seal, but the binder is modified with a polymer. Shotblasting occurs when steel pellets are blasted at the roadway surface to add texture (Merritt et al., 2015). Each of these measures can improve roadway texture.

Texturing options for existing pavement include diamond grinding, diamond grooving, and next-generation concrete surfacing, which increase MTD by removing the top layers of concrete. These treatments are typically applied in the longitudinal direction. However, diamond-ground

surfaces tend to wear quickly compared to other remediation options. Milling, overlays, and cross-section overbuilds are also texturing strategies for existing roadways. Similar to grinding, milling removes the top layer of pavement and can be used to correct slopes in areas of poor surface drainage. Overlays can be used after milling to provide a new roadway surface to correct rutting, poor slope, and subsequent problematic drainage (Flintsch et al., 2021).

Pavement rehabilitation techniques differ by location and even within states. In Kansas, for example, the city of Salina uses microsurfacing, chip sealing, UTBWCs, asphalt mills and overlays, diamond grinding, and concrete overlays (City of Salina, 2020). Comparatively, the city of Lenexa uses microsurfacing, chip sealing with granite, UTBWCs, and mills and overlays (City of Lenexa, n.d.).

Pavement grooving and various forms of texture drags can also be used to increase MTD on roadways. Burlap bag drags, turf drags, and broom drags can be used on new pavement, while tining, grooving, and exposed aggregate concrete are strategies for new and existing pavement. Research has shown that grooves should be parallel to water flow to reduce hydroplaning and increase drainage, and grooves should be parallel to the pavement slope to maximize hydroplaning reduction and improve drainage (Flintsch et al., 2021). Table 2.2 compares the texture of new pavement and existing pavement restoration.

Table 2.2: Typical Ranges of Macrotexture for New and Aged Surface Textures

Texture Type	Typical MTD for Newly Created Textures, mm	Typical MTD for Aged/Trafficked Textures, mm
New Pavement		
Burlap, Broom, and Standard Turf Drags	0.35 to 0.50	0.30 to 0.45
Heavy Turf Drag	0.50 to 0.90	0.40 to 0.80
Transverse and Transverse Skewed Tine	0.60 to 1.25	0.50 to 1.15
Longitudinal Tine	0.60 to 1.25	0.50 to 1.15
Longitudinal Diamond Grind	0.70 to 1.40	0.50 to 1.25
Longitudinal Grooving	0.80 to 1.50	0.70 to 1.40
EAC	0.90 to 1.60	0.75 to 1.50
Porous PCC	1.20 to 2.50	0.90 to 2.25
Restoration of Existing Pavement		
Longitudinal Diamond Grind	0.70 to 1.40	0.50 to 1.25
Longitudinal Grooving	0.80 to 1.50	0.70 to 1.40
Shotblasted PCC	1.00 to 1.50	0.80 to 1.40
HMA (dense-graded fine)	0.40 to 0.75	0.30 to 0.70
HMA (dense-graded coarse)	0.60 to 1.20	0.50 to 1.10
Ultra-thin Bonded Wearing Course	1.00 to 1.75	0.80 to 1.50

Source: Hall et al. (2009)

A National Cooperative Highway Research Program (NCHRP) report by Hall et al. (2009) describes concrete texturing resources and their uses throughout the United States, including in Kansas. Table 2.3 lists concrete pavement surface textures and rankings of their benefits.

Table 2.3: Texture Method and Ranking

Method	Friction	Exterior Noise	Cost	Constructability
Transverse tine (0.75-in. spacing)	1	8	1	2
Transverse tine (0.5-in. spacing)	1	6	1	2
Transverse tine (variable spacing)	1	7	1	2
Transverse groove	1	7	4	3
Transverse drag	2	6	–	2
Longitudinal tine	1	4	1	1
Longitudinal groove	1	5	3	3
Longitudinal grind	1	3	3	3
Longitudinal burlap drag	4	3	1	1
Longitudinal turf drag	2	3	1	1
Longitudinal plastic brush	3	3	1	1
EAC	2	3	3	4
Shotblasted PCC	1	7	2	3
Porous PCC	1	1	5	4
Ultra-thin epoxied laminate	1	2	6	3
Ultra-thin bonded wearing course	2	2	3	3

Source: Hall et al. (2009)

Friction and noise relationships are important considerations when selecting the best method of pavement grooving. The texture, friction, and noise associated with texture methods are presented in Table 2.4.

Table 2.4: Texture and Friction Ranges of Concrete Surfaces

Method	Texture Range		Friction Range		Noise Range	
	MTD, mm	MPD, mm	FN40R	FN40S	CPX, dB (A)	CPB L_{max}, dB (A)
Transverse tine (0.75 in.)	0.53 to 1.1	0.50 to 0.52	41.0 to 56.0	30.6 to 34.4	100.4 to 104.8	83.0 to 84.0
Transverse tine (0.5 in.)		0.35 to 1.00	54.0 to 71.0	37.6 to 62.0		81.9 to 83.0
Transverse tine (variable)	1.14	0.42 to 1.02		50.0 to 69.5		81.0 to 87.3
Transverse groove	1.07			48.0 to 58.0		84.1 to 84.6
Transverse drag	0.76		22.0 to 46.0			
Longitudinal tine	1.22			36.0 to 76.6	96.6 to 103.5	79.0 to 85.0
Longitudinal groove	1.14			48.0 to 55.0	99.4 to 103.8	80.9
Longitudinal grind	0.30 to 1.20		35.0 to 51.0	29.9 to 46.8	95.5 to 102.5	81.2
Longitudinal burlap drag					101.4 to 101.5	
Longitudinal turf drag	0.53 to 1.00		23.0 to 55.6	20.0 to 38.0	97.4 to 98.6	83.7
Longitudinal plastic brush			48.0 to 52.0	23.0 to 24.0	101.8 to 102.2	
EAC	0.9 to 1.1		35.0 to 42.0			
Shot abraded PCC	1.2 to 2.0			34.3 to 46.2		84.3
Porous PCC						
Ultra-thin epoxied laminate	1.4					79.8
Ultra-thin bonded wearing course	0.97 to 1.98		26.0 to 27.0		95.0 to 99.0	

Source: Hall et al. (2009)

In Kansas, KDOT uses a longitudinal tine with 0.75 in. (19 mm) spacing and 0.15 in. (3.8 mm) depth with a burlap or a longitudinal turf drag to texture new concrete pavement. Hall et al. (2009) found that various pavement locations in Kansas also have been treated with longitudinal diamond grinding, resulting in high friction rankings; thereby, proving the cost-effectiveness of this replacement for HMA resurfacings. Diamond grinding, however, increases wheel-to-road noise and microtexture deterioration due to the use of limestone aggregate on roadways in Kansas.

Research has shown that the stability of motorcycle riders is also specifically impacted by longitudinal and transverse cut tining and grooves. A laboratory study by Martinez et al. (1976) studied the safety of motorcycle riders using pavement grooves of various configurations. Three motorcycle riders of various skill levels reported feeling uncertain when riding on longitudinally grooved pavement. Riders claimed a slight wobble developed at speeds above 70 mph on this pavement, but the conclusion was made that pavement grooving is not hazardous to experienced riders traveling below 70 mph. Transverse grooving perpendicular to the direction of travel did not impact the riding experience, and riders claimed no discernable difference between grooved roadways and roads with no grooves (Martinez et al., 1976).

2.6.3 High Friction Surface Treatments

Unlike other pavement treatment options, high friction surface treatments (HFSTs) are used almost exclusively to increase roadway safety (Merritt et al., 2015). In Kansas, Zahir et al. (2017) increased friction on roadway surfaces using an epoxy or polymer resin binder sprayed onto an existing surface with surface-bonded aggregate cured by heat. Aggregate in the treatment layer provided friction on the roadway surface and increased texture depth. HFSTs can also be used in locations with poor roadway geometry or variable superelevation, including exit-entrance ramps, horizontal curves, intersections, bridge decks, crosswalks, school crossings, corners, steep grades, bus lanes, roundabouts, toll plazas, and other skid-hazard areas. Most states that use HFSTs terminate them at the tangent point along a curve. Ride noise, ride quality, and durability remain the same as untreated pavement surfaces. The FHWA guidebook by Merritt et al. (2021) describes HFST feasibility, design and field verification, installation, and performance monitoring.

In terms of HFST application, research has shown that open-graded friction course or grooved concrete may require two layers of application to thoroughly bind to the pavement and create proper texture depth. According to Merritt et al. (2021), treatments must be applied to good quality pavements that are clean and dry. Setting times for HFSTs range from 15 minutes to 2 hours, depending on the usage of a hot or cold application method, respectively, and the service lives of HFSTs are 7–10 years, depending on traffic volumes, traffic type, roadway type, and

geometric condition. HFSTs have a negligible environmental impact, so they do not require long approval periods since they are only applied to road surfaces.

During trial applications, states with applied HFSTs had a 57%–100% decrease in crashes, no matter the weather. For example, 60 locations in Kentucky had an 85% crash reduction for dry weather, and wet-weather crashes decreased 78% (Merritt et al., 2015). Based on this and other DOT data, a 20%–30% reduction in crashes overall and a 50% reduction in wet-weather crashes for general HFST applications is expected (Merritt et al., 2015). A KDOT study (Zahir et al., 2017) of two on-ramps and one off-ramp found a 20% increase in texture depth on asphalt sections and a 55% increase in texture depth on concrete sections after application with resulting MTDs increased to greater than 1.0 mm. However, the same KDOT study found a decrease in texture depth after 1 year at an off-ramp from Interstate 70 (I-70) to northbound K-177.

2.7 DOT Highway and Drainage Design Manuals

To determine optimal design for superelevated highway transitions and hydroplaning mitigation, this research studied design manuals from every state DOT that includes the manual on the DOT website. Highway design manuals (HDMs) and drainage design manuals (DDMs) were compiled, with a focus on drainage at areas of low slope and hydroplaning mitigation. Tables 2.5 and 2.6 list the HDM and DDM references, respectively, and summaries of state DOT manuals that contain information related to research areas are presented in Appendix A.

Table 2.5: Highway Design Manual Source and Superelevated Transition Design Reference Location

State	HDM Link	Guidance Reference Page, Section, or Chapter of Superelevation Transition Design
Alabama	N/A	N/A
Alaska	N/A	N/A
Arizona	https://azdot.gov/business/engineering-and-construction/roadway-engineering/roadway-design/roadway-design-guidelines	Pg. 200-9, Sec. 202.3
Arkansas	N/A	N/A
California	https://dot.ca.gov/programs/design/manual-highway-design-manual-hdm	Pg. 200-19, Sec. 202.5
Colorado	https://web.archive.org/web/20240330094251/https://www.codot.gov/business/designsupport/bulletins_manuals/cdot-roadway-design-guide-2018/cdot-rdg-2018	Pg. 3-23, Sec. 3.2.3.3

State	HDM Link	Guidance Reference Page, Section, or Chapter of Superelevation Transition Design
Connecticut	https://portal.ct.gov/dot/-/media/dot/aec/manuals/highway-design-manual_2024-10.pdf	Pg. 8-2(8), Sec. 8-2.03.02
Delaware	https://roaddesignmanual.deldot.gov/index.php/Manual	Pg. 5-14, Sec. 5.3.2
Florida	https://www.fdot.gov/roadway/fdm/default.shtm	Pg. 54, Sec. 210.9.1
Georgia	https://www.dot.ga.gov/GDOT/pages/DesignManualsGuides.aspx	Pg. 4-30, Sec. 4.5.4 & Pg. 6-24, Sec. 6.15
Hawaii	N/A	N/A
Idaho	https://apps.itd.idaho.gov/apps/manuals/manualsonline.html	Sec. 534.04
Illinois	https://idot.illinois.gov/doing-business/procurements/engineering-architectural-professional-services/Consultants-Resources/index	Sec. 2.4.1
Indiana	https://www.in.gov/indot/design-manual/	Pg. 15, Sec. 43-3.0
Iowa	https://iowadot.gov/design/design-manual	Pg. 2A-4 & Pg. 21M-51
Kansas	https://kart.ksdot.gov/	Pg.7-19, Sec. 7.3.5
Kentucky	https://transportation.ky.gov/Highway-Design/Pages/default.aspx	Sec. HD-702.5
Louisiana	http://wwwsp.dotd.la.gov/Inside_LaDOTD/Divisions/Engineering/Road_Design/Pages/Road-Design-Manual.aspx	Pg. 4-18, Sec. 4.6.3
Maine	https://www.maine.gov/mdot/engineering/highway/	Sec. "Horizontal Design"
Maryland	https://roads.maryland.gov/mdotsha/pages/Index.aspx?PageId=65	N/A
Massachusetts	https://www.mass.gov/lists/design-guides-and-manuals	Pg. 4-18, Sec. 4.2.5
Michigan	https://mdotjboss.state.mi.us/stdplan/englishroadmanual.htm	Pg. 3.04.02
Minnesota	https://roaddesign.dot.state.mn.us/	Pg. 3-3(9), Sec. 3-3.03
Mississippi	https://mdot.ms.gov/portal/engineering_standards_guides_manuals	Pg. 3-9, Sec. 3-4.02
Missouri	N/A	N/A
Montana	https://www.mdt.mt.gov/publications/manuals.aspx	Pg. 3-8, Sec. 3.3
Nebraska	https://dot.nebraska.gov/business-center/design-consultant/rd-manuals/	Pg. 3-5, Sec. 2.B.1
Nevada	https://www.dot.nv.gov/doing-business/about-ndot/ndot-divisions/engineering/design/standard-specifications-and-plans	Pg. 29, Sec. 3.5
New Hampshire	https://www.dot.nh.gov/doing-business-nhdot/engineers-consultants/highway-design-manual	Pg. 4-15
New Jersey	https://www.state.nj.us/transportation/eng/documents/RDM/	Pg. 4.3.2, Sec. 4-11
New Mexico	https://www.dot.nm.gov/infrastructure/engineering-publications/design-manual/	Sec. 1000.5.4.1
New York	https://www.dot.ny.gov/divisions/engineering/design/dqab/hdm	Pg. 5-56, Sec 5.7.3.3
North Carolina	https://connect.ncdot.gov/projects/roadway/roadway%20design%20manual/forms/allitems.aspx	Sec 1-15 & Sec 1-16
North Dakota	https://www.dot.nd.gov/manuals/design/designmanual/designmanual.htm	N/A
Ohio	https://www.transportation.ohio.gov/working/engineering/roadway/manuals-standards/location-design-vol-1/location-design-vol-1	Pg. 44, Sec. 202.4.5
Oklahoma	https://oklahoma.gov/odot/business-center/pre-construction-design/roadway-design.html	N/A

State	HDM Link	Guidance Reference Page, Section, or Chapter of Superelevation Transition Design
Oregon	https://www.oregon.gov/odot/Engineering/Pages/Hwy-Design-Manual.aspx	Pg. 183, Sec. 218.8
Pennsylvania	https://www.pa.gov/content/dam/copapwp-pagov/en/penndot/documents/public/pubsforms/publications/pub-13m/pub%2013m%20title%20page.pdf	Pg. 2 - 14, Sec. D
Rhode Island	http://www.dot.ri.gov/business/highwaydesignmanual.php	Sec. 420.03
South Carolina	https://www.scdot.org/business/road-design.aspx	Pg. 5.3-10, Sec. 5.3.4
South Dakota	https://dot.sd.gov/doing-business/engineering/design-services/forms-manuals	Pg. 5-13
Tennessee	https://www.tn.gov/tdot/engineering-division/engineering-production-support/design-standards/design-guidelines2.html	Pg. 2-1, Sec. 2-101.01
Texas	https://onlinemanuals.txdot.gov/TxDOTOnlineManuals/txdotmanuals/rdw/rdw.pdf	Pg. 2-23
Utah	https://www.udot.utah.gov/connect/business/design/roadway-design/	Pg. 3-2, Sec. 3.3.3
Vermont	https://vtrans.vermont.gov/docs#Manual	Pg. & 5-8
Virginia	https://www.vdot.virginia.gov/doing-business/technical-guidance-and-support/technical-guidance-documents/road-design-manual/	N/A
Washington	https://wsdot.wa.gov/engineering-standards/all-manuals-and-standards/manuals/design-manual	Pg. 1250-5, Sec. 1250.05
West Virginia	https://transportation.wv.gov/highways/engineering/Pages/Manuals.aspx	N/A
Wisconsin	N/A	N/A
Wyoming	https://www.dot.state.wy.us/home/engineering_technical_programs/manuals_publications/road_design_manual.html	Pg. 16, Sec. 3-02

Table 2.6: Drainage Design Manual Source and Reference Location

State	DDM Link	Guidance Reference Page, Section, or Chapter
Alabama	https://www.dot.state.al.us/publications/Design/pdf/HydraulicManual.pdf	Sec. 6.1.2 & Sec. 6.6.5
Alaska	https://dot.alaska.gov/stwddes/desbridge/pop_hwydrnman.shtml	N/A
Arizona	https://azdot.gov/business/engineering-and-construction/roadway-engineering/drainage-design/manuals-drainage-design	N/A
Arkansas	N/A	N/A
California	Included in HDM	Pg. 830-7, Sec. 833.2
Colorado	https://www.codot.gov/business/hydraulics/drainage-design-manual	N/A
Connecticut	https://portal.ct.gov/dot/bureaus/engineering-and-construction/engineering/bridges/soils-foundation-hydraulics-and-drainage/drainage-manual	N/A
Delaware	Included in HDM	Sec. 6.8.2.3
Florida	https://www.fdot.gov/roadway/drainage/manualsandhandbooks.shtm	Pg. 3-9

State	DDM Link	Guidance Reference Page, Section, or Chapter
Georgia	https://www.dot.ga.gov/GDOT/pages/DesignManualsGuides.aspx	Pg. 6-1, Sec. 6.1.2
Hawaii	https://hidot.hawaii.gov/stormwater/storm-water-management/maui/swmp/	N/A
Idaho	N/A	N/A
Illinois	https://idot.illinois.gov/doing-business/procurements/engineering-architectural-professional-services/Consultants-Resources/index	Pg. 44, Sec. 9.3
Indiana	https://www.in.gov/indot/design-manual/	N/A
Iowa	https://iowadot.gov/design/design-manual	Sec. 4A-3
Kansas	https://kart.ksdot.gov/	N/A
Kentucky	N/A	N/A
Louisiana	http://wwwsp.dotd.la.gov/Inside_LaDOTD/Divisions/Engineering/Public_Works/Hydraulics/Pages/default.aspx	Pg. 8(A) - 7, Sec. 8-A.7.1
Maine	https://www.maine.gov/mdot/engineering/highway/	Pg. "Design", Sec. "Drainage Design"
Maryland	https://roads.maryland.gov/mdotsha/pages/Index.aspx?PageId=65	Sec. I-4-A-1
Massachusetts	https://www.mass.gov/doc/storm-water-handbook-for-highways-and-bridges	N/A
Michigan	N/A	N/A
Minnesota	https://www.dot.state.mn.us/bridge/hydraulics/drainagemanual.html	Sec. 8.5.2
Mississippi	N/A	N/A
Missouri	N/A	N/A
Montana	https://www.mdt.mt.gov/publications/manuals.aspx	N/A
Nebraska	https://dot.nebraska.gov/business-center/design-consultant/rd-manuals/	N/A
Nevada	https://www.dot.nv.gov/doing-business/about-ndot/ndot-divisions/engineering/design/drainage-manual	Pg. 3-7, Sec. 3.3.2.2.1
New Hampshire	Included in HDM	Pg. 6-7
New Jersey	Included in HDM	Sec. 10.5.9
New Mexico	https://www.dot.nm.gov/infrastructure/program-management/drainage-design/	Pg. 5-56, Spec. 504.2
New York	Included in HDM	Pg. 81-9, Sec. 8.7.4.4
North Carolina	Included in HDM	Pg. 1-16
North Dakota	Included in HDM	N/A
Ohio	https://www.transportation.ohio.gov/working/engineering/hydraulic/location-design-vol-2	N/A
Oklahoma	https://oklahoma.gov/odot/business-center/pre-construction-design/roadway-design/support-units/oklahoma-roadway-drainage-manual.html	Pg. 10.12-1
Oregon	https://www.oregon.gov/odot/hydraulics/pages/hydraulics-manual.aspx	Pg. 200-66, Sec. 218.3
Pennsylvania	https://www.pa.gov/agencies/penndot/programs-and-doing-business/environment/hydrology-and-hydraulics.html	Pg. 13 - 9, Sec. 13.5
Rhode Island	Included in HDM	N/A

State	DDM Link	Guidance Reference Page, Section, or Chapter
South Carolina	Included in HDM	N/A
South Dakota	https://dot.sd.gov/doing-business/engineering/design-services/forms-manuals#listItemLink_1187	Pg. 12-13, Sec. 12.6.3.2
Tennessee	https://www.tn.gov/content/tn/tdot/engineering-division/engineering-production-support/design-standards/drainage-manual.html	Pg. 7-5, Sec. 7.03.1
Texas	https://onlinemanuals.txdot.gov/TxDOTOnlineManuals/txdotmanuals/hyd/index.htm	Ch. 10, Sec. 4
Utah	https://www.udot.utah.gov/connect/business/design/drainage-design-hydraulics/	Pg. 8-3
Vermont	https://vtrans.vermont.gov/highway/structures-hydraulics/hydraulics2	Pg. 8-5, Sec. 8.3.4.4
Virginia	https://www.vdot.virginia.gov/doing-business/technical-guidance-and-support/technical-guidance-documents/drainage-manual/	Ch. 9, Sec. 9.4.3.2
Washington	https://wsdot.wa.gov/engineering-standards/all-manuals-and-standards/manuals/hydraulics-manual	Pg. 5-1
West Virginia	https://transportation.wv.gov/highways/engineering/Pages/Manuals.aspx	Pg. 5-11, Sec. 5.3.2.7
Wisconsin	N/A	N/A
Wyoming	Included in HDM	N/A

Chapter 3: Datasets and Methods

3.1 Study Locations

KDOT identified the highway locations of superelevated transitions listed in Tables 3.1–3.3 and Figure 3.1 as having increased hydroplaning potential. All annual average daily traffic (AADT) in this study was taken from state traffic count maps from 2021 (KDOT, 2021a). In the tables and figures, locations are shown with their mile marker or relative reference point (RP).

Table 3.1: Study Locations in Kansas Identified by KDOT Engineers

Location of Interest (Route and Project)	Reference Point (RP)	Coordinate Location	County in Kansas	Highway Route	Direction of Interest (Northbound, Southbound, Eastbound, Westbound)
169-2 K-4420-01	79.2	38.06701, -95.37934	Anderson	US-169	Northbound, Southbound
70-84 I-70-3(3)19	204.8	38.84857, -98.48842	Russel	I-70	Eastbound
35-46 K 9014-01	214.7	38.84523, -94.82853	Johnson	I-35	Southbound
35-46 K 4088-02	217.55	38.87682, -94.79362	Johnson	I-35	Southbound
70-31 K 2611-01	295.2	38.99928, -96.85764	Geary	I-70	Eastbound
50-9 K 2438-01	330.1	38.40531, -96.49143	Chase	US-50	Eastbound, Westbound
70-89 K-2446-01	357.7	39.06494, -95.73569	Shawnee	I-70	Westbound

Table 3.2: AADT, Design Speed, and Superelevation Information for Study Locations

Reference Point (RP)	AADT as of 2021 (Vehicles/Day)	Design Speed (mph)	Design Superelevation (%)	Superelevation Rotation Method
79.2	4160	70	1.6 (Rotated Crown)	Center Line
204.8	13500	70	1.5 (Rotated Crown)	Center Line
214.7	52800	70	2.3	Center Line
217.55	62900	70	7.0	Center Line
295.2	26800	70	6.5	Center Line
330.1	5180	60	3.0	Inside Edge
357.7	57800	65	4.1	Outside Edge

Table 3.3: Transition Runout/Runoff Length and Horizontal Curve Information for Study Locations

Location Reference Point (RP)	Transition Runout Length (ft)	Transition Runoff Length (ft)	Horizontal Curve Length (ft)	Horizontal Curve Radius (ft)
79.2	75	200	6484.99	11459.16
204.8	75	150	1200.00	17188.76
214.7	23	91	339.35	2772.77
217.55	284	840	1421.53	2864.79
295.2	75	275	1655.50	2864.79
330.1	75	175	2703.33	5729.63
357.7	25	275	338.57	3819.72

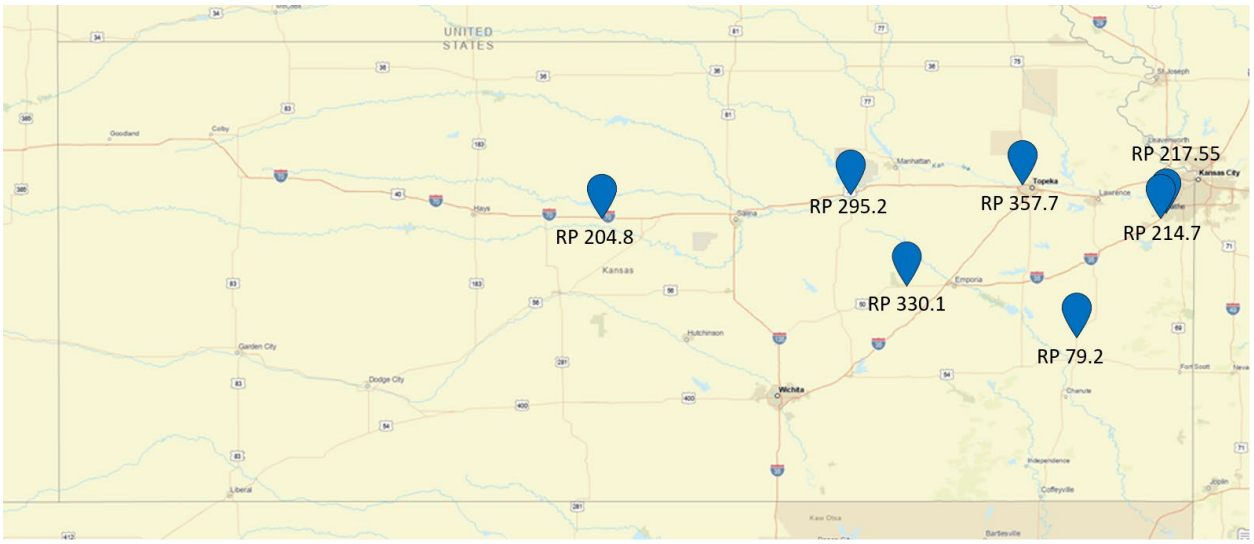

Figure 3.1: Study Locations in Kansas (Blue Markers)

Approximate locations of superelevated transitions in each study location based on design drawings are shown in Figures 3.2–3.8, where a yellow line designates the beginning of the runoff length, a partial red line designates the location of the zero-cross slope (beginning of the runout length), and a green line represents the end of the runout length when the curve reaches full superelevation. The coordinate location for each study location is marked with a red pin.

Figure 3.2: Approximate Superelevated Transitions at 169-2 RP 79.2

As shown in Figure 3.2, the 169-2 RP 79.2 location is near a crest curve of 800 ft that peaks at an intersection. The entire intersection in northbound-southbound direction is superelevated, and this location uses a rotated crown superelevation. The longitudinal grade-in from the south is +1.02%, and the grade to the north of the intersection is -0.4%.

Figure 3.3: Approximate Superelevated Transitions at 70-84 RP 204.8

As shown in Figure 3.3, the location at 70-84 RP 204.8 has a sag curve of 600 ft that occurs near the transition area east of the marker where the longitudinal grade-in is -0.78% and the grade-out +0.98%.

Figure 3.4: Approximate Superelevated Transitions at 35-46 RP 214.7

As shown in Figure 3.4, the inner lane of the site at the 35-46 RP 214.7 location superelevates, causing a zero-cross slope to occur at the median barrier and the cross slope to drain to the inside lane. Only one median drain is present at the zero-cross slope at this location within 200 ft in either direction, which could lead to drainage problems. The bottom of a sag curve occurs after the section reaches full superelevation.

Figure 3.5: Approximate Superelevated Transitions at 35-46 RP 217.55

Similar to the 35-46 RP 214.7 location, the location at 35-46 RP 217.55 experiences a zero-cross slope at the inside lane by the median barrier (Figure 3.5). However, this area has more median drainage than the former location, and a large sag curve occurs approximately 200 ft from the beginning of the superelevation transition.

Figure 3.6: Approximate Superelevated Transitions at 70-31 RP 295.2

As shown in Figure 3.6, the on-ramp acceleration lane of the 70-31 RP 295.2 location occurs at the zero-cross slope. The end of the acceleration lane taper ends as the curve transitions to full superelevation. Traffic travels downhill in this location.

Figure 3.7: Approximate Superelevated Transitions at 50-9 RP 330.1

As shown in Figure 3.7, the location at 50-9 RP 330.1 contains a 600-ft sag curve (red marker) where a stream flows under the roadway. The longitudinal slope heading into the curve is -0.60%, while the slope exiting the curve is +3.60%.

Figure 3.8: Approximate Superelevated Transitions at 70-89 RP 357.7

As shown in Figure 3.8, the location at 70-89 RP 357.7 is a weave segment in which the superelevation transition occurs over a short distance. This area transitions from full superelevation that slopes to the outside weave lanes, ending with cross sloping to the median. This location has two drains at the median barrier of the weave and another drain at the median barrier between the zero-cross slope and the point of full superelevation.

3.1.1 Site Visits

Locations near 35-46 RP 214.7, 35-36 RP 217.55, 70-31 RP 295.2, 50-9 RP 330.1, and 70-89 RP 357.7 were visited throughout this study to thoroughly investigate each location. Site visits confirmed that unique factors at each location could lead to slow drainage and subsequent possible hydroplaning (Figures 3.9–3.14).

Figure 3.9: Gore Area Facing Southbound Direction Near 35-46 RP 214.7

As shown in Figure 3.9, the research site at 35-46 RP 214.7 faces the southbound lanes. A gore area next to Exit 214 at this location attributes to a large contribution area that could increase the amount of flow the exit lane experiences during rain events. Slopes that drain flow to the right of the roadway and flow down the ramp could potentially occur at this location.

Figure 3.10: Northbound Direction Near 35-46 RP 217.55 (Left) and Evident Dampness at the Southbound Direction Near 35-46 RP 217.55 (Right)

Figure 3.11: Washout Near Guardrail Near 35-46 RP 217.55

As shown in the right-hand picture of Figure 3.10, the southbound direction of the location near 35-46 RP 217.55 contains a high water table, as also evidenced by the washout along the guardrail shown in Figure 3.11. Groundwater at this location could rise to inundate low-lying roadway areas and cause hydroplaning. Hydroplaning mitigation at this location may require eliminating water seepage due to groundwater rather than correcting the superelevated transition. A more thorough investigation is needed to determine which issue has the largest impact on hydroplaning at this location.

Figure 3.12: Eastbound (Left) and Westbound Direction (Right) Near 70-31 RP 295.2

As shown in the left-hand picture of Figure 3.12, eastbound traffic heads downhill towards a horizontal curve at the location near 70-31 RP 295.2, with an on-ramp immediately preceding

the curve. Flow traveling downhill (eastbound) could increase hydroplaning potential due to increased sheet flow potential at the on-ramp.

Figure 3.13: Eastbound (Left) and Westbound Direction (Right) Near 50-9 RP 330.1

The culvert underneath the 50-9 RP 330.1 location did not appear to impact drainage of the roadway surface because the roadway is elevated far above the culvert area, as shown in Figure 3.13. This location contains a sag curve with a large drainage area from both the eastbound and westbound directions. However, the westbound lane shoulder by the guardrail was discolored, potentially due to it being the area of a surface milling project to correct poor drainage. Decreased roadway friction could also occur at this location due to normal use or poor drainage over time.

Figure 3.14: Westbound (Left) and Eastbound Direction (Right) Near 70-89 RP 357.7

As shown in Figure 3.14, roadway geometry appears to be the main cause of hydroplaning at the westbound location near 70-89 RP 357.7. Near Exit 357B, the westbound roadway slope is

uphill, with a 2.723% longitudinal grade, and during rain events, flow reportedly funnels towards traffic. As vehicles move uphill, they spray water back uphill in the direction of traffic, causing flow accumulation that travels downhill against traffic. During extensive rainfall, hydroplaning potential increases in this area.

3.2 Datasets

After investigating and photographing study locations, subsequent conversations with KDOT engineers were initiated. Because design plans of highway segments did not accurately resemble current conditions, accurate highway profiles were needed to understand cross slope for proper drainage. Several methods can be used to create highway profiles for as-built infrastructure, and each has a unique combination of collection safety, cost, measurement time, and accuracy. For example, conventional surveying of a location is time consuming and often requires lane closures and surveying crews must be in close proximity to road traffic (Souleyrette et al., 2003). Stereo photography is accurate but time consuming and expensive. A viable method for this application was mobile laser scanning (MLS), which utilizes a collection vehicle to collect many lanes of data in a single pass at highway speeds (Shams et al., 2018).

KDOT collected light detection and ranging (LiDAR) data for most of the Kansas highway system from March 2021 to April 2021 (KDOT, 2021b). Available data from the KDOT Mobile LiDAR Project include LiDAR files and data from the laser crack measuring system (LCMS). Although the KDOT Mobile LiDAR Project was conducted primarily with roadway asset collection (KDOT, 2021b), previous studies have shown that LiDAR data can be used to create roadway profiles. Studies by Zhang and Frey (2006), Tsai et al. (2013), Holgado-Barco et al. (2014), and Shams et al. (2018) have shown that the use of mobile LiDAR is an accurate and effective method for measuring highway cross slope. Notably, research by Gurganusa et al. (2021) used mobile LiDAR to delineate basins on highway areas with hydroplaning speeds below posted speed limits.

In addition to roadway scanning and mapping, this study utilized design plans for the study locations as well as crash data for the entire highway system of Kansas. Highway design plan sheets for the study locations included typical sections, horizontal and vertical alignment, and their

superelevation transitions. Crash data for the entire state was also used in addition to crash data from the study locations.

3.2.1 Digital Terrain Mapping

Data from laser digital terrain mapping (LDTM) scanners creates a 3D point cloud using laser line projectors (Pavemetrics, n.d.-b) that can be used to better understand the slope of a roadway. As the collection vehicle travels down the roadway at highway speed, it captures the roadway surface and the surrounding area. LDTM data from the LiDAR project was collected using a Pavemetrics LDTM scanner that collected 112 million data points per second with a vertical accuracy of +/- 3 mm and a 1 sigma standard deviation for straight and curved roadways (Pavemetrics, n.d.-b). This data identified specific areas at the study locations where flow was likely to accumulate, and the expected direction flow would drain.

3.2.2 Laser Crack Measuring System Data

Similar to LDTM, LCMS data is typically collected via laser line projectors with an array of scanners to create a profile of the roadway (Pavemetrics, n.d.-a). In this study, data from the LCMS was collected using Pavemetrics LCMS-2 with a transversal resolution of 1 mm over a width of 4 m, a vertical accuracy of 0.25 mm, and a vertical resolution of 0.05 mm at a 95% confidence interval (Pavemetrics, n.d.-a).

3.2.3 State Crash Data

To evaluate areas of wet-weather related crashes at the study locations, KDOT crash data were requested for the entire state, including public data reports, from January 1, 2011, to December 31, 2021 (Bureau of Transportation Safety, n.d.). Information such as dates, times, coordinate locations, crash locations on the road (e.g., shoulder, intersection, etc.), travel directions, crash type, crash mechanisms, vehicles involved, weather types, and lighting conditions were included in the crash reports. Location data of crashes are typically recorded using smartphone Global Positioning System (GPS) (KDOT, 2019).

3.3 Methods

This study employed various data-analysis methods. State crash data were used to identify crashes at the study locations, while ArcGIS Pro software (Esri, 2022) was used to evaluate flow direction and flow accumulation at each of the areas of concern. OpenRoads Designer (ORD) software (Bentley Systems, n.d.) helped identify areas of long-flow path using slope length. Each of these methods is discussed in greater detail in the following sections.

3.3.1 Hydroplaning Remediation

Cost-effective, systematic approaches are essential for hydroplaning remediation at transition areas with increased potential for hydroplaning. Remediation strategies include correcting areas with poor drainage and correcting areas with poor texture. Roadway areas with poor drainage can be identified using flow direction and accumulation models, as well as examining cross slopes and longitudinal slopes, while areas with poor texture can be identified by measuring MTD on roadway sections. Table 3.4 lists workable solutions to both problem areas.

Table 3.4: Methods of Hydroplaning Remediation

Poor Drainage Remediation and Poor Texture Remediation	
Overlay and overbuild	
Surface tining or groove cutting	
Milling or diamond grinding	
Seals, bonds, and resurfacing	
Poor Drainage Remediation	Poor Texture Remediation
Permeable pavements	High friction surface treatments
Geometry redesign (adjust slopes or configuration adjustment)	
Drainage redesign (adding additional drainage)	

Although the table lists permeable pavements as a remedy for poor drainage, these pavements are not recommended for use in Kansas due to the state's harsh winter conditions. However, permeable pavements do allow water to flow through them; thereby, decreasing a roadway's WFT (Noyce et al., 2007). A more extreme mitigation strategy, redesigning the roadway to improve drainage, is usually only considered as a last resort correction method because

highway geometric redesign projects are costly. However, proper highway geometry is required to achieve maximum effectiveness from any pavement treatment (Merritt et al., 2015).

3.3.2 Flow Direction and Flow Accumulation

This study utilized LDTM to determine flow direction and inspect accumulation on superelevated transitions of the study areas to recommend efficient remediation efforts. Data was delivered in a zipped LAZ LiDAR file, and then LAStools software (rapidlasso GmbH, 2021) was used to convert LAZ files to LAS files to create 3D models of the data. Scale of the LAS scans and georeferenced metadata of points within the LAS data was not available, but location and scale are not necessary for qualitative flow direction and flow accumulation applications from slope. All LAS data were processed using the ArcGIS Pro software to filter out noise and isolate the roadway surface and the ground. A digital elevation model (DEM) of the roadway was then created using the LAS Dataset to Raster option in the ArcGIS Pro software. Interpolation was set to binning, cell assignment was set to average, and a linear void filling method was used. A sampling value of 0.01 was used to preserve the accuracy of the 3D scan without compromising processing time. The z factor remained unchanged.

Once a DEM of the study areas was created, the roadway surface was isolated, and the isolated roadway DEM was pit filled, using no z limit to avoid indeterminant flow that would complicate processing for resampling. Flow direction was then found using the D8 method, where edges were not forced to flow outward. Directional arrows were placed on top of the flow direction based on results of the D8 method. Then a flow accumulation was performed to identify roadway areas with stagnated flow drainage and potential drainage collection areas. The resulting flow direction and flow accumulation rasters were upscaled to a rectangular cell size of 0.05 by 0.05, using the majority of the value that occurred most often in a block of cells.

3.3.3 Roadway Texture and Slopes

LCMS data from the KDOT LiDAR project revealed five different scans along the roadway at a single interval with location coordinate data for each scan according to the five standard AASHTO scanning bans of the center, right, and left wheel paths and outside section of roadway (Laurent et al., 2008). Various data points were collected at each interval, including MTD, cross

slope, longitudinal slope, latitude, and longitude coordinates. Each interval's MTD and cross slope and the coordinates of each scan were averaged. Only one longitudinal slope was given per scan interval. Scan intervals were plotted, and the locations of each interval were numbered along a map of the roadway to track changes over distance and into transition areas.

3.3.4 Highway Redesign Using Slope-Path Length

Options for the redesign of a highway section are dependent upon current design factors and goals. Design solutions are weighed with road surface drainage efficiency and cost effectiveness. Hydroplaning mitigation solutions for a geometric redesign of a highway transition vary based on the highway section considered.

In this study, the site at 70-31 RP 295.4 was selected as an example location for a geometric redesign due to evidence of high water accumulation near the superelevation transition. This location is also based on an original design from 1989, meaning design revisions could be made based on current design practices. In the eastbound direction, the 70-31 RP 295.4 location also has an acceleration lane near the transition that has reported hydroplaning. Further investigation was conducted to determine if the acceleration ramp lane contributes to increased potential for hydroplaning. Figure 3.15 shows an aerial view of this location.

Figure 3.15: Superelevated Transition at the 70-31 RP 295.4 Location

The highway section at 70-31 RP 295.4 has a design speed of 70 mph, and traffic flows in an eastbound direction. This segment features 12-ft-wide lanes, with an inside shoulder width of 6 ft, an outside shoulder width of 10 ft, and an outside shoulder width of 8 ft at the acceleration lane. The acceleration lane has a design speed of 30 mph, which is identical to the design speed for the other ramps at this interchange. This section features a parallel-type entrance with an entrance ramp radius of 1432.39 ft, a parallel acceleration lane entrance length of 810.00 ft

(measured from where the right edge of the traveled way of the ramp joins the traveled way of the roadway to the beginning of the acceleration lane taper), and a taper ramp length of 300.00 ft. The superelevated highway transition occurs near the start of the taper of the acceleration lane, with full superelevation of 6.5% in the outermost lane near the end of the taper.

In the direction of road travel, the longitudinal slope is -2.66%. A sag curve occurs approximately 160 ft from the end of the superelevation transition, where the longitudinal slope shifts from -2.66% to -0.05%. The transition meets design criteria of the May 2014 edition of the KDOT *Highway Design Manual*. Given the 2864.79-ft radius of horizontal curve, this study used an e_{max} of 8.0%, a runout length of 75 ft, and a runoff length of 275 ft, with 75% of the runoff distance occurring before the point of curvature (PC).

At the 70-31 RP 295.4 location, the cross slope of the acceleration lane slopes in the same direction as the right through lane for proper drainage, resulting in slow drainage when the acceleration lane tapers to an end just as it must match the cross slope as the right lane heads into a superelevation transition. The roadway design specifications of this section were reproduced in 3D in the commonly used ORD software. Figures 3.16 and 3.17 show examples of the completed corridor section in ORD.

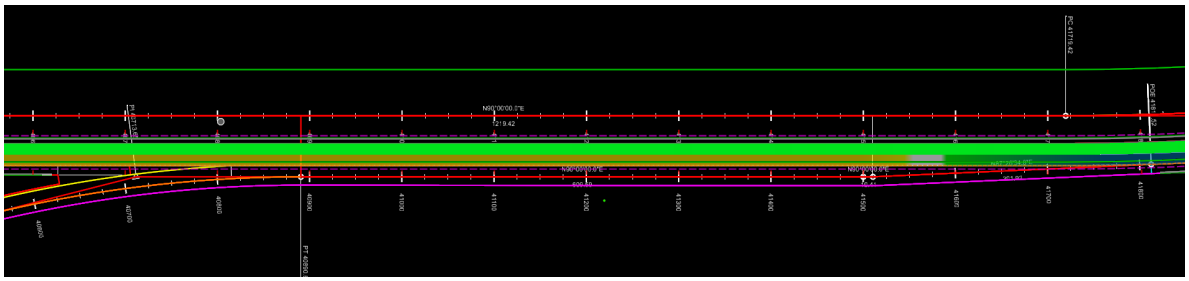

Figure 3.16: Horizontal Alignment of 70-31 RP 295.4 Location in ORD

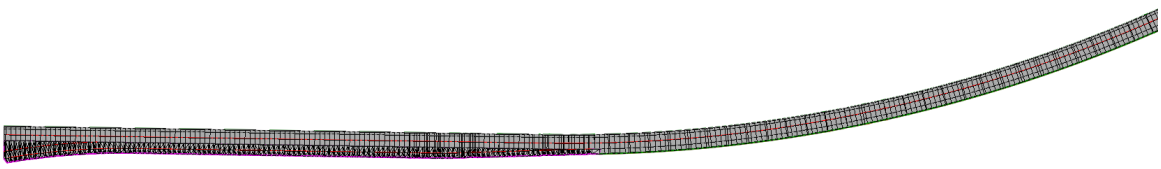

Figure 3.17: 3D Corridor Model of 70-31 RP 295.4 Location in ORD

The roadway was reproduced by first creating a horizontal alignment and assigning a vertical alignment to the section. A corridor template was made for the section and added to the alignment at an interval of 10 ft to accurately identify areas of poor drainage. To design the on-ramp, variable slope offsets were applied to cross sections of the ramp to project the elements in 3D space. A terrain mesh of the roadway was created by selecting the handles of each road element to create an accurate roadway surface.

The superelevation transition of the section is shown in Figure 3.18, where the right lane transitions to a zero slope as the taper of the acceleration lane begins. The left-hand panel of the figure shows a change in the cross slope, while the right-hand panel shows a heatmap that uses yellow to green to indicate the transition of the right lane before the horizontal curve. According to the design plans, the traveled way is revolved about the centerline profile.

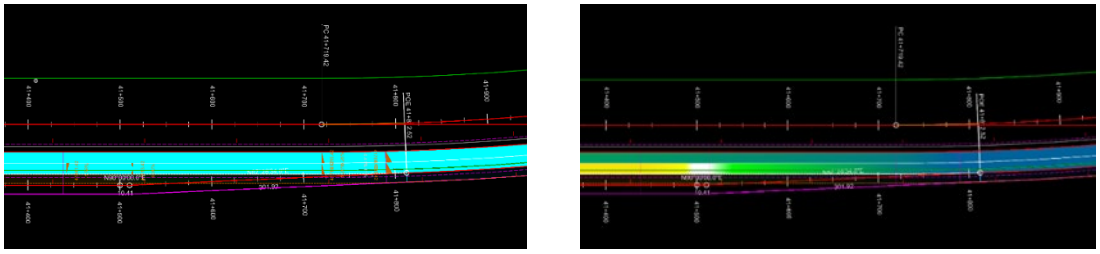

Figure 3.18: Superelevation Transition of the 70-31 RP 295.4 Location in ORD

This study used this ORD model to develop several geometric redesigns for the selected location. These redesigns incorporated relatively uncomplicated changes to provide examples of possible solutions. The examples do not constitute an exhaustive set of solutions for either this location or all study locations. Therefore, site-specific potential design solutions that maximize drainage performance should be considered.

Chapter 4: Digital Model Results

4.1 Analysis Results

Each KDOT location was analyzed for hydroplaning potential by considering MTD, cross slope, longitudinal slope, flow direction, and accumulation. The following sections quantify the potential risk of hydroplaning using LCMS and LDTM results based on MTD, flow direction, and accumulation for each location and summarize the overall hydroplaning potential and mitigation strategies at each location. In Figures 4.1, 4.3, 4.5, 4.7, 4.9, 4.11, and 4.13, intervals are labeled along the roadway sections where MTD and slopes were measured. In Figures 4.2, 4.4, 4.6, 4.8, 4.10, 4.12, and 4.14, arrows present flow direction via the D8 method, and flow accumulation is shown in the heatmaps, where green indicates low accumulation and red indicates high accumulation.

4.1.1 Results for the 169-2 RP 79.2 Location

Figure 4.1 presents the scan locations, MTD results, cross slope, and longitudinal slope of the 169-2 RP 79.2 location, and Figure 4.2 illustrates the flow direction and flow accumulation at that location.

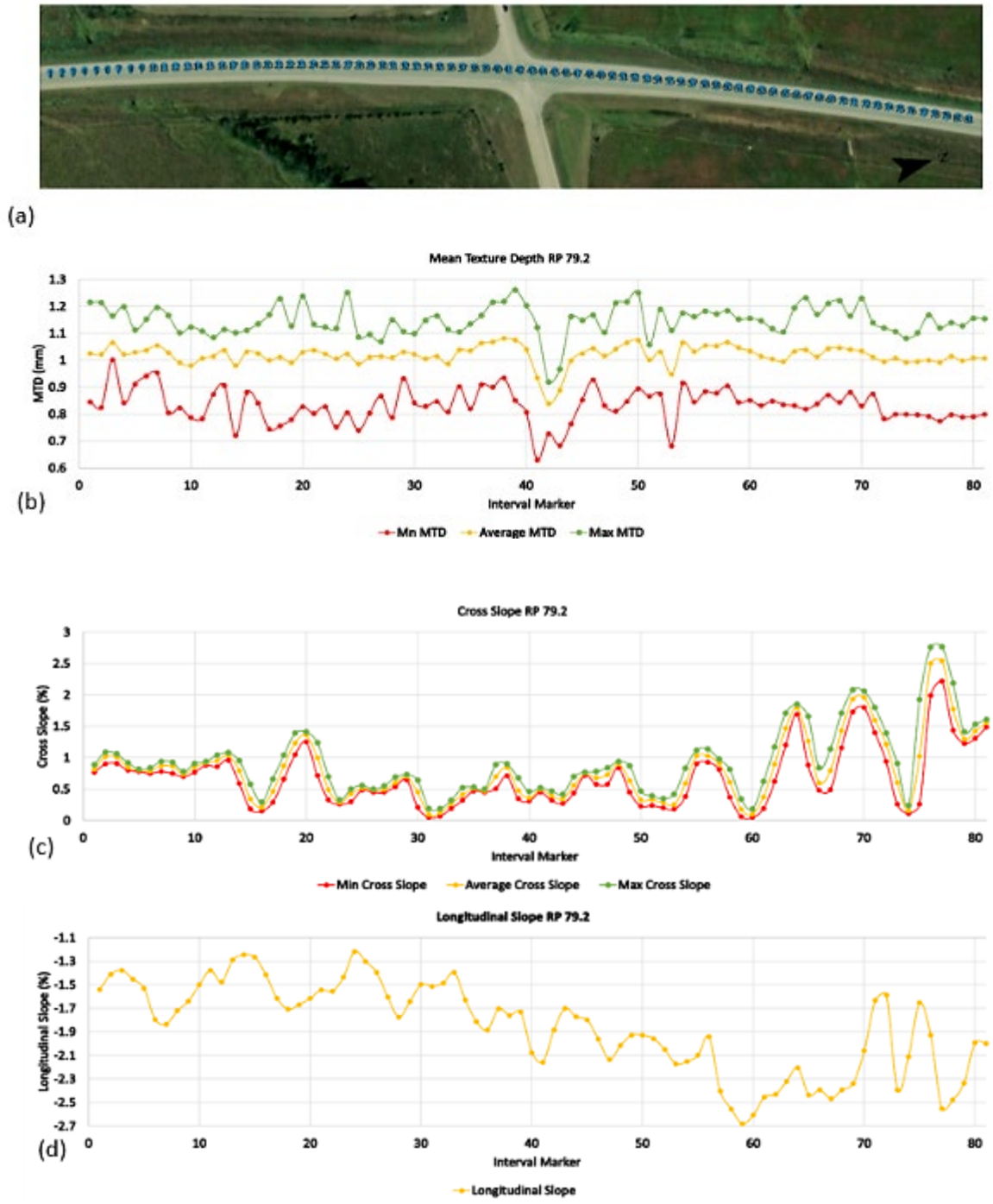

Figure 4.1: Results for the 169-2 RP 79.2 Location: (a) Scan Locations, (b) MTD, (c) Cross Slope, and (d) Longitudinal Slope

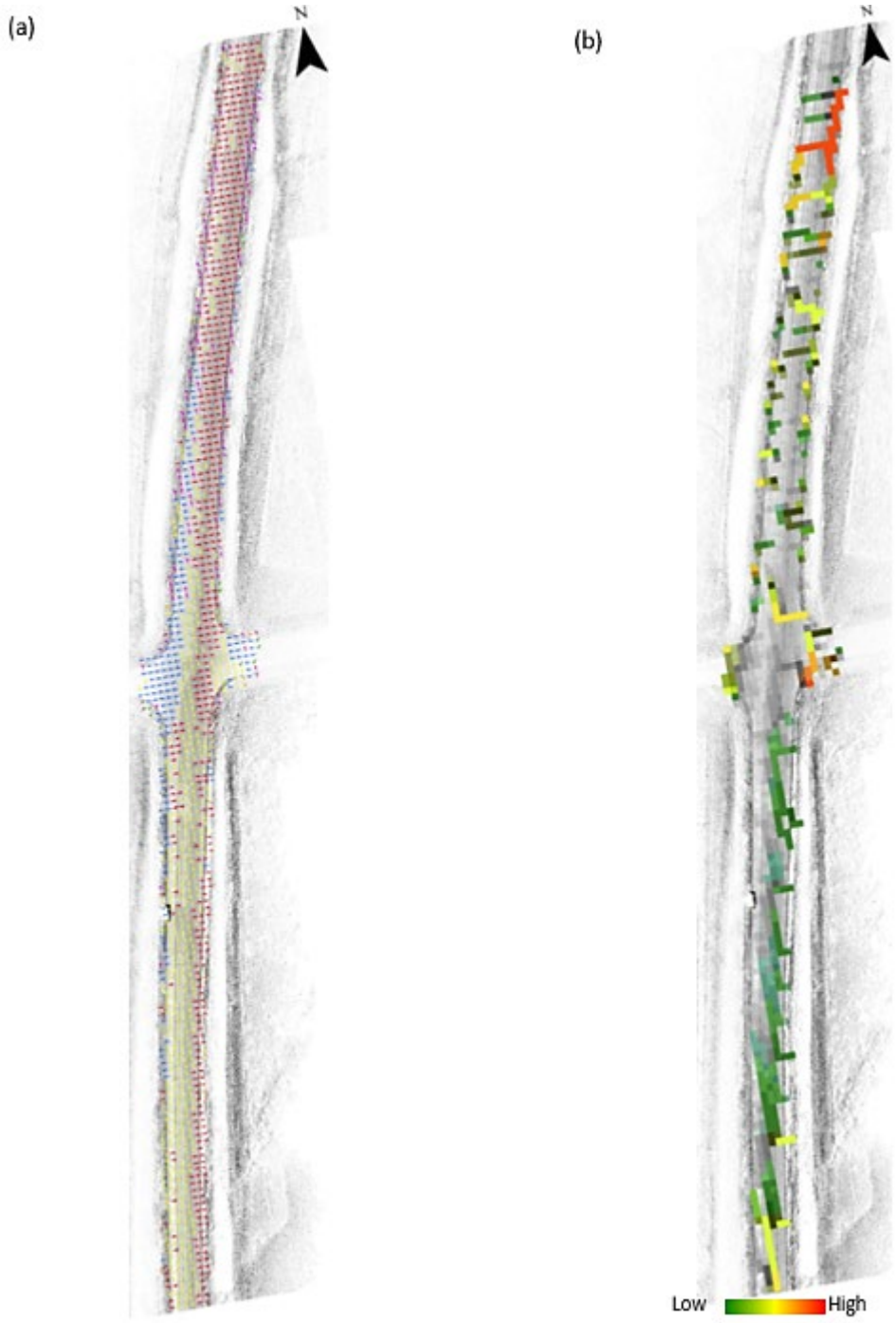

Figure 4.2: (a) Flow Direction, (b) Flow Accumulation

As shown in Figures 4.1b–d, a dip occurs near the intersection where cross slope and longitudinal slope begin to decrease. Because vehicles travel in all directions at the intersection, this decrease in texture is expected. The average MTD of the section is 1.1 mm, and the lowest MTD is 0.6, but the minimum MTD begins to dip below 0.8 mm at the superelevated transitions.

As shown in Figure 4.2a, flow direction travels in nearly the same direction as traffic on the south end of the study area, while Figure 4.2b indicates flow accumulation in the turning lane traveling north, with the highest accumulation near the transition of the north end of the location. Since MTD was found to be adequate at this location, a drainage improvement can be recommended.

4.1.2 Results for the 70-84 RP 204.8 Location

Figure 4.3 presents the scan locations, MTD results, cross slope, and longitudinal slope of the 70-84 RP 204.8 location, and Figure 4.4 illustrates the flow direction and flow accumulation at that location.

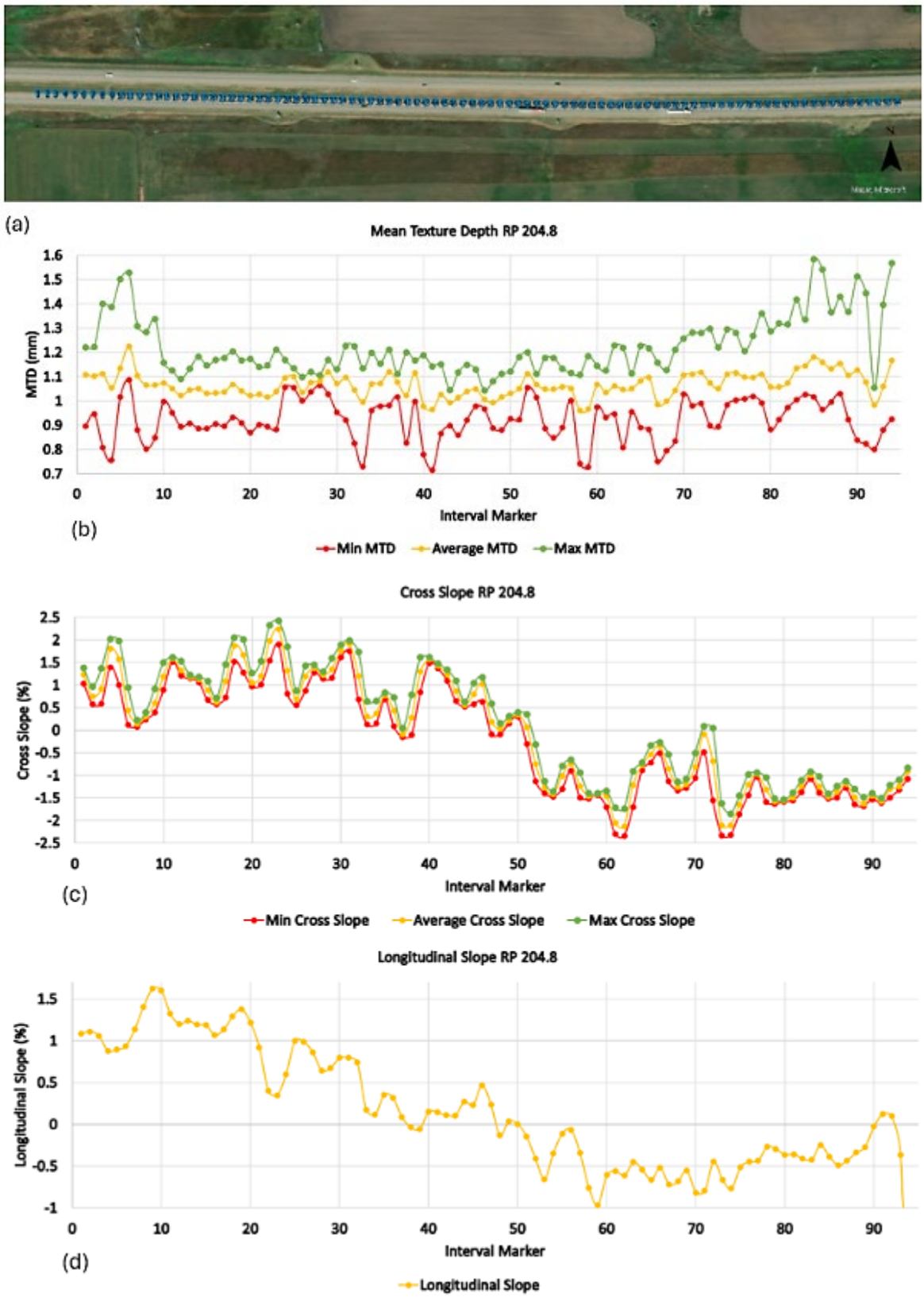

Figure 4.3: Results for the 70-84 RP 204.8 Location: (a) Scan Locations, (b) MTD, (c) Cross Slope, and (d) Longitudinal Slope

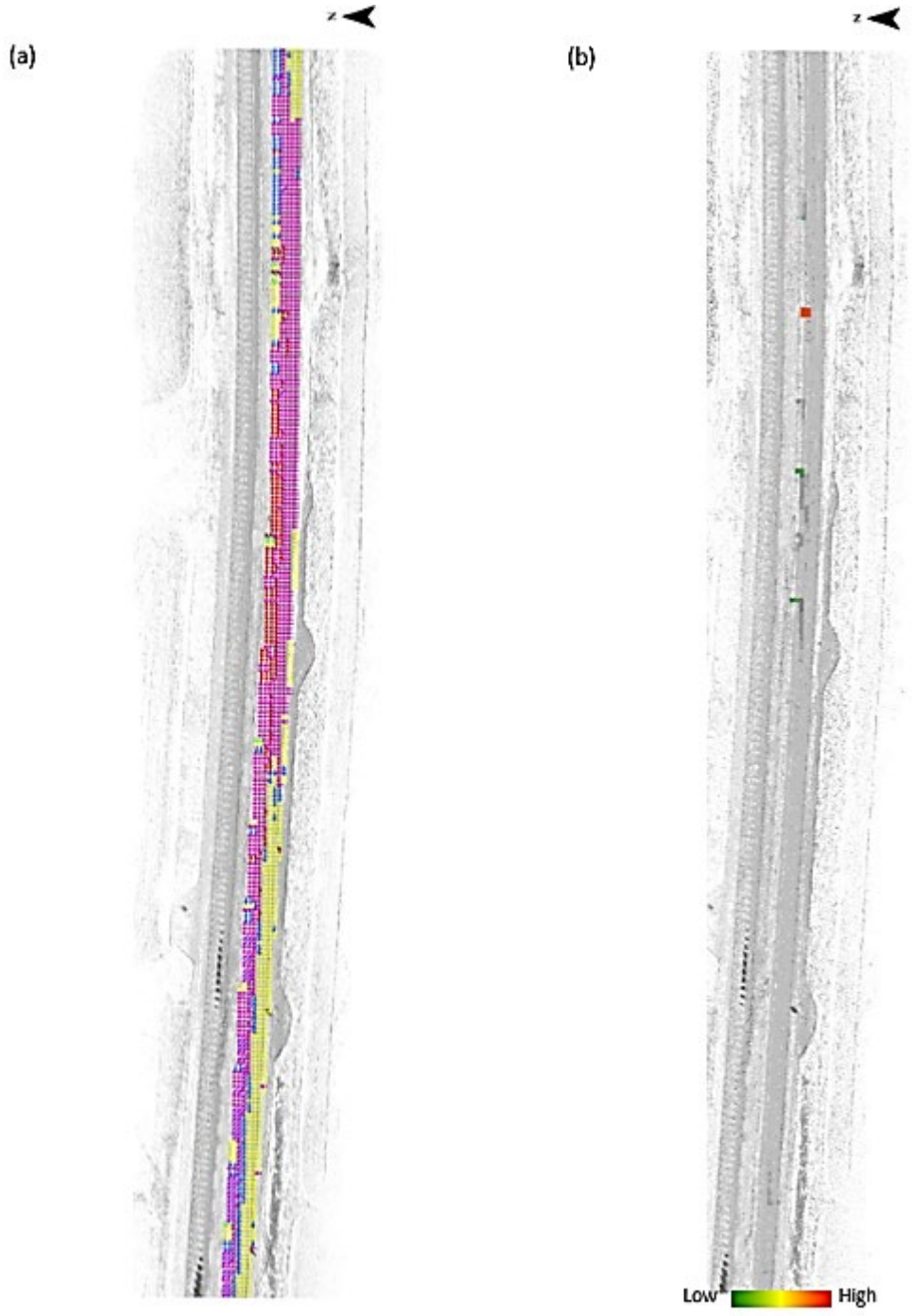

Figure 4.4: (a) Flow Direction, (b) Flow Accumulation

As shown in Figure 4.3b, the MTD decreases into and out of the horizontal curve, where the minimum texture drops below 0.8 mm. The MTD is adequate for texture in this section, with an average of 1.06 mm and a minimum of 0.5 mm. Notably, Figures 4.2c–d show that the cross slope and the longitudinal slope, respectively, are near zero at the 50th scan interval, at which point

Figure 4.4b indicates a slight amount of flow accumulation. As shown in Figure 4.4a, the flow direction travels across both lanes at the superelevation transition on the east side of the section and within the horizontal curve at full superelevation. However, the flow direction begins to change on the west side of the horizontal curve before the transition. A drainage solution should be proposed to correct geometry at this location.

4.1.3 Results for the 35-46 RP 214.7 Location

Figure 4.5 presents the scan locations, MTD results, cross slope, and longitudinal slope of the 35-46 RP 214.7 location, and Figure 4.6 illustrates the flow direction and flow accumulation at that location.

(a)

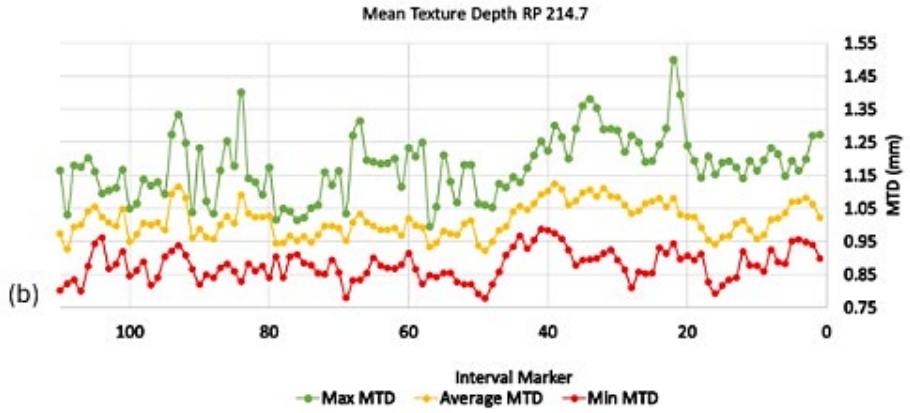

(b)

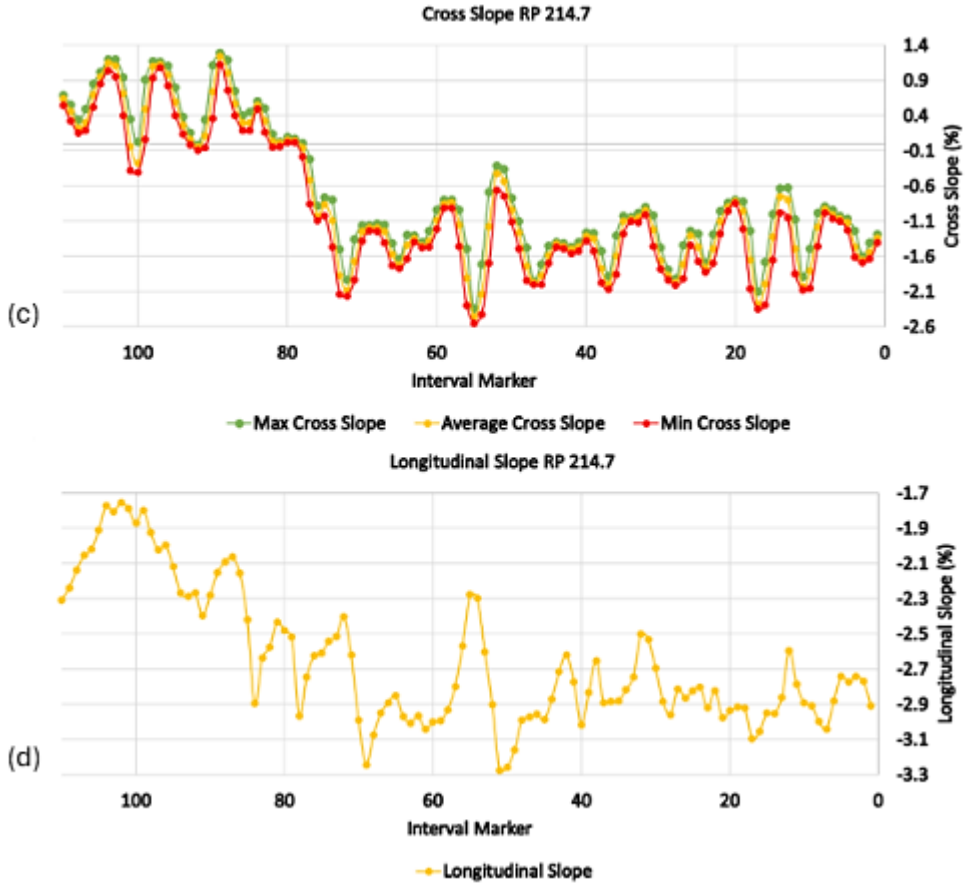

(c)

(d)

Figure 4.5: Results for the 35-46 RP 214.7 Location: (a) Scan Locations, (b) MTD, (c) Cross Slope, and (d) Longitudinal Slope

Figure 4.6: (a) Flow Direction, (b) Flow Accumulation

As shown in Figure 4.5b, the MTD decreases towards the off-ramp; although, the MTD is adequate for friction, with an average MTD of 1.0 mm and a minimum MTD of 0.80 mm. Figure 4.5d shows the longitudinal slope as uphill at a high magnitude in the pathway of travel, indicating that splash and spray may increase hydroplaning potential at this location. The flow direction

results (Figure 4.6a) also indicate flow towards the median, as demonstrated by high water accumulation at the location of the weave (Figure 4.6b). Adequate MTD and a flow direction against traffic would create a drainage solution to correct geometry at this location.

4.1.4 Results for the 35-46 RP 217.55 Location

Figure 4.7 presents the scan locations, MTD results, cross slope, and longitudinal slope of the 35-46 RP 217.55 location, and Figure 4.8 illustrates the flow direction and flow accumulation at that location.

(a)

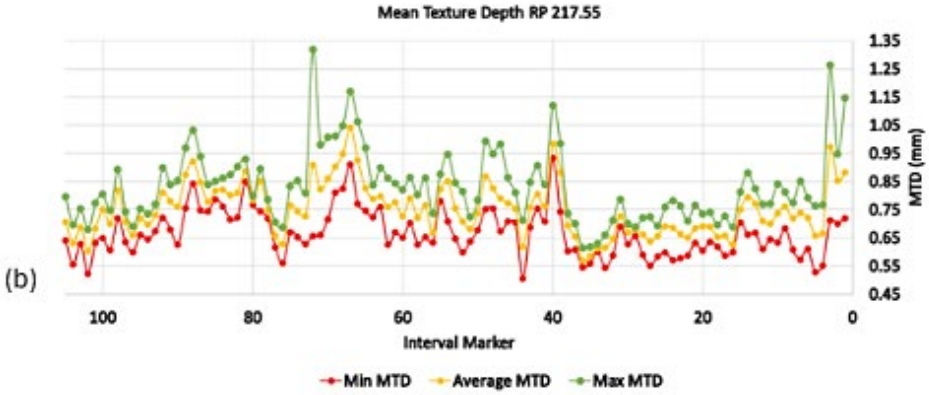

(b)

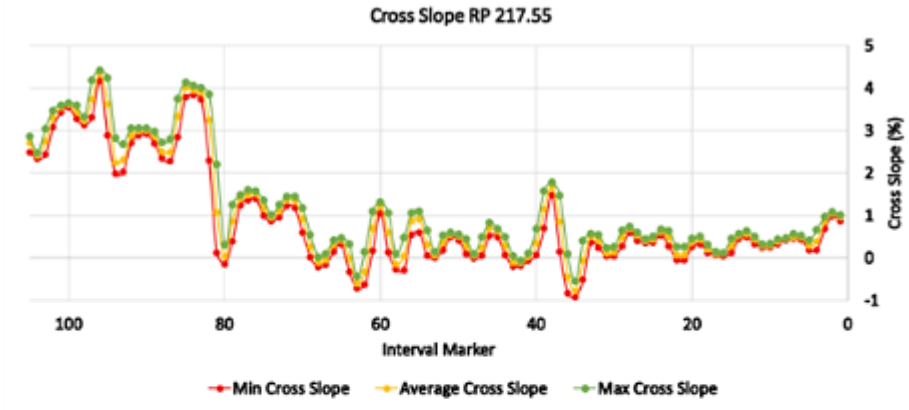

(c)

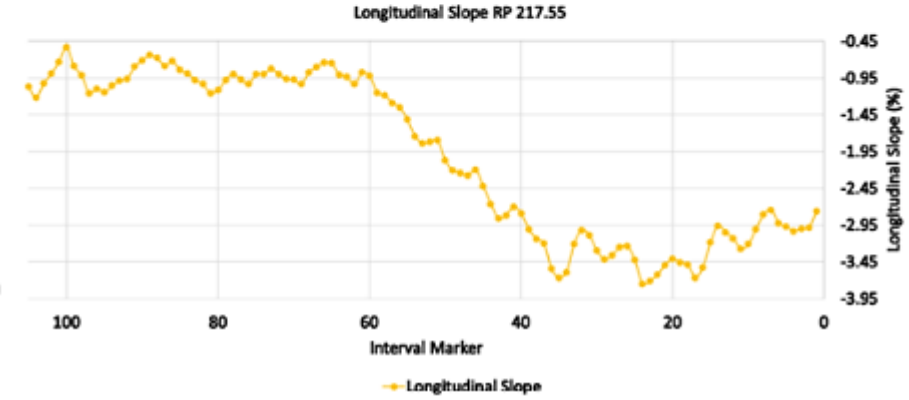

(d)

Figure 4.7: Results for the 35-46 RP 217.55 Location: (a) Scan Locations, (b) MTD, (c) Cross Slope, and (d) Longitudinal Slope

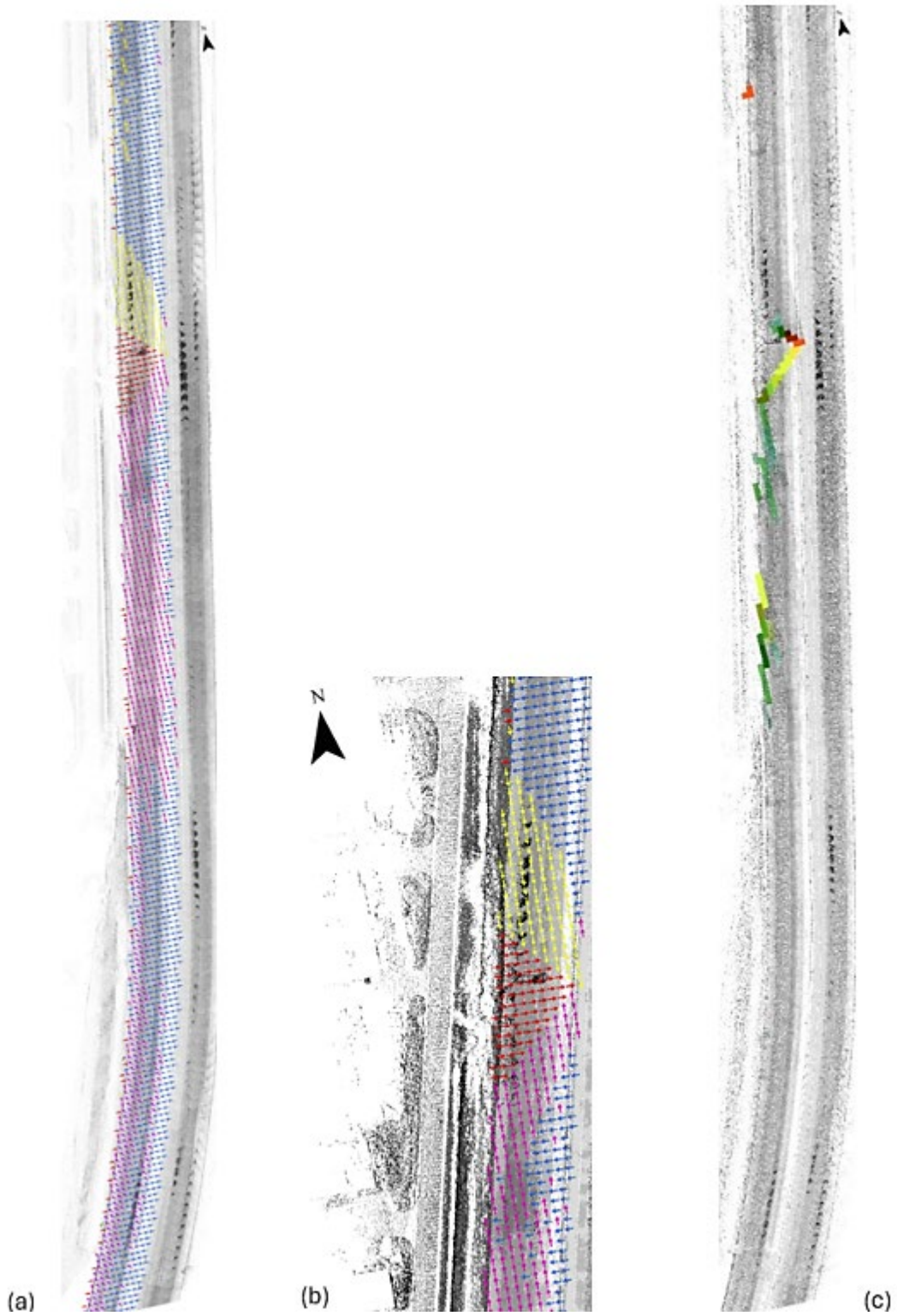

Figure 4.8: (a) Flow Direction, (b) Enlarged View of Flow Direction, and (c) Flow Accumulation

As shown in Figure 4.7b, the MTD is low over the entire section of roadway, potentially indicating a lack of friction for vehicles. The average MTD of the section is 0.75 mm, with a minimum MTD of 0.51 mm. MTD remains the lowest at the area of washout described in section 3.1.1. Figure 4.8a shows that flow changes directions near the washout area and travels towards the median instead of towards the edge of the roadway. Although the texture at this location is lacking, the reversal of flow back to the roadway should be a priority before improving roadway friction, and drainage systems that protect pavment from high water tables should be considered at this location.

4.1.5 Results for the 70-31 RP 295.2 Location

Figure 4.9 presents the scan locations, MTD results, cross slope, and longitudinal slope of the 70-31 RP 295.2 location, and Figure 4.10 illustrates the flow direction and flow accumulation at that location.

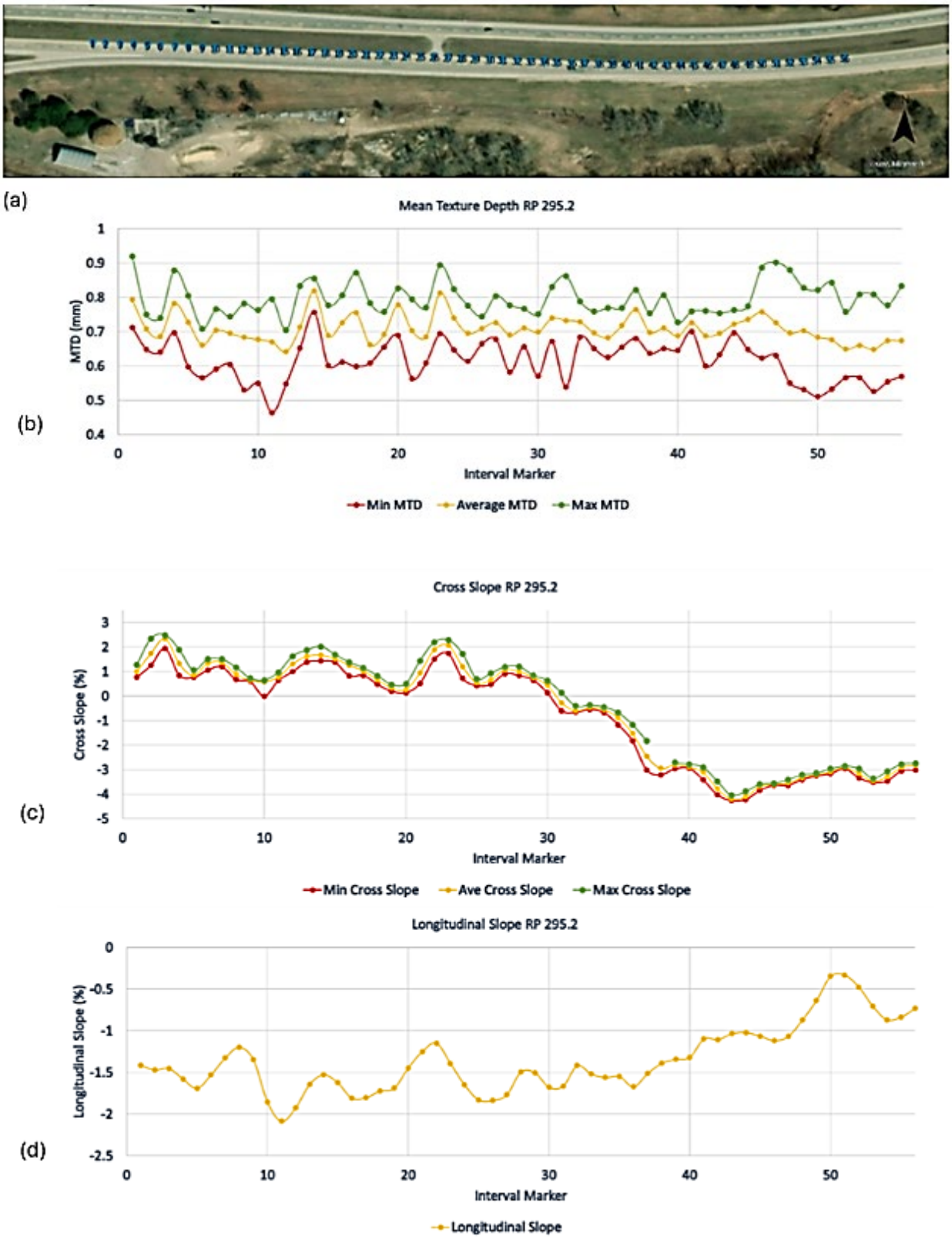

Figure 4.9: Results for the 70-31 RP 295.2 Location: (a) Scan Locations, (b) MTD, (c) Cross Slope, and (d) Longitudinal Slope

Figure 4.10: (a) Flow Direction, (b) Flow Accumulation

As shown in Figure 4.9b, the MTD remains low along the section, potentially indicating a lack of texture. The average MTD of this section is 0.71 mm, and it only exceeds 0.8 mm twice, as shown, while the MTD falls below 0.5 mm only once (0.46 mm). Figure 4.10a indicates flow across the roadway at the end of the merging on-ramp, and flow accumulation results (Figure 4.10b) are high near the transition area. Texture improvement at this location is recommended to increase the MTD.

4.1.6 Results for the 50-9 RP 330.1 Location

Figure 4.11 presents the scan locations, MTD results, cross slope, and longitudinal slope of the 50-9 RP 330.1 location, and Figure 4.12 illustrates the flow direction and flow accumulation at that location.

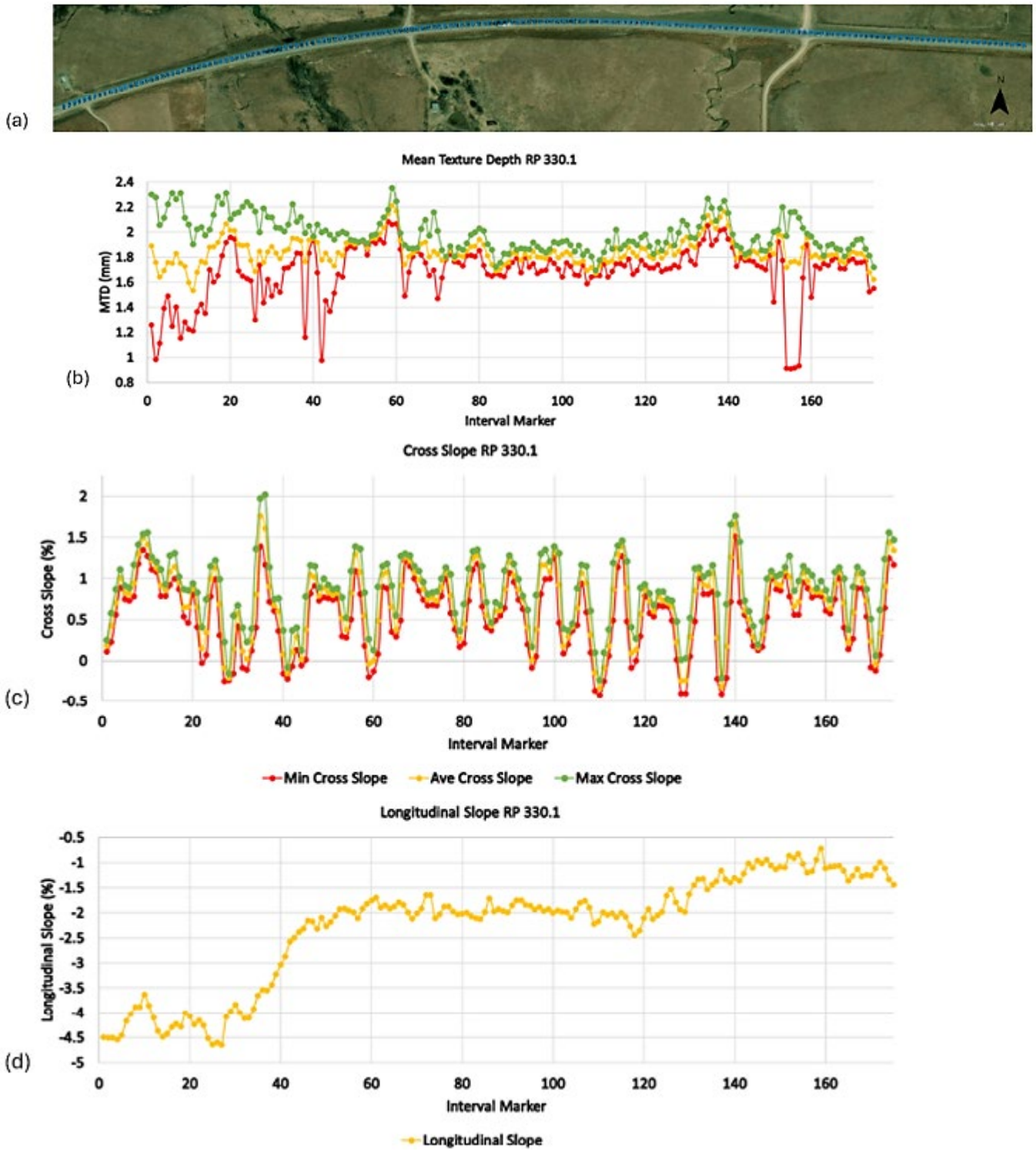

Figure 4.11: Results for the 50-9 RP 330.1 Location: (a) Scan Locations, (b) MTD, (c) Cross Slope, and (d) Longitudinal Slope

Figure 4.12: (a) Flow Direction, (b) Flow Accumulation

Of all the study sites, the 50-9 RP 330.1 location has the highest MTD, with an average MTD of 1.80 mm and a minimum MTD that never falls below 0.5 mm (Figure 4.11b). However, the results show that the MTD decreases near the bridge and creek, as well as near the transition

area heading east. Figure 4.12a indicates that flow direction shifts at the bottom of the sag curve, while the flow accumulation remains high in many areas (Figure 4.12b). However, digital banding from the LDTM results creates a uniform flow direction and flow accumulation on the east side of the section.

4.1.7 Results from the 70-89 RP 357.7 Location

Figure 4.13 presents the scan locations, MTD results, cross slope, and longitudinal slope of the 70-89 RP 357.7 location, and Figure 4.14 illustrates the flow direction and flow accumulation at that location.

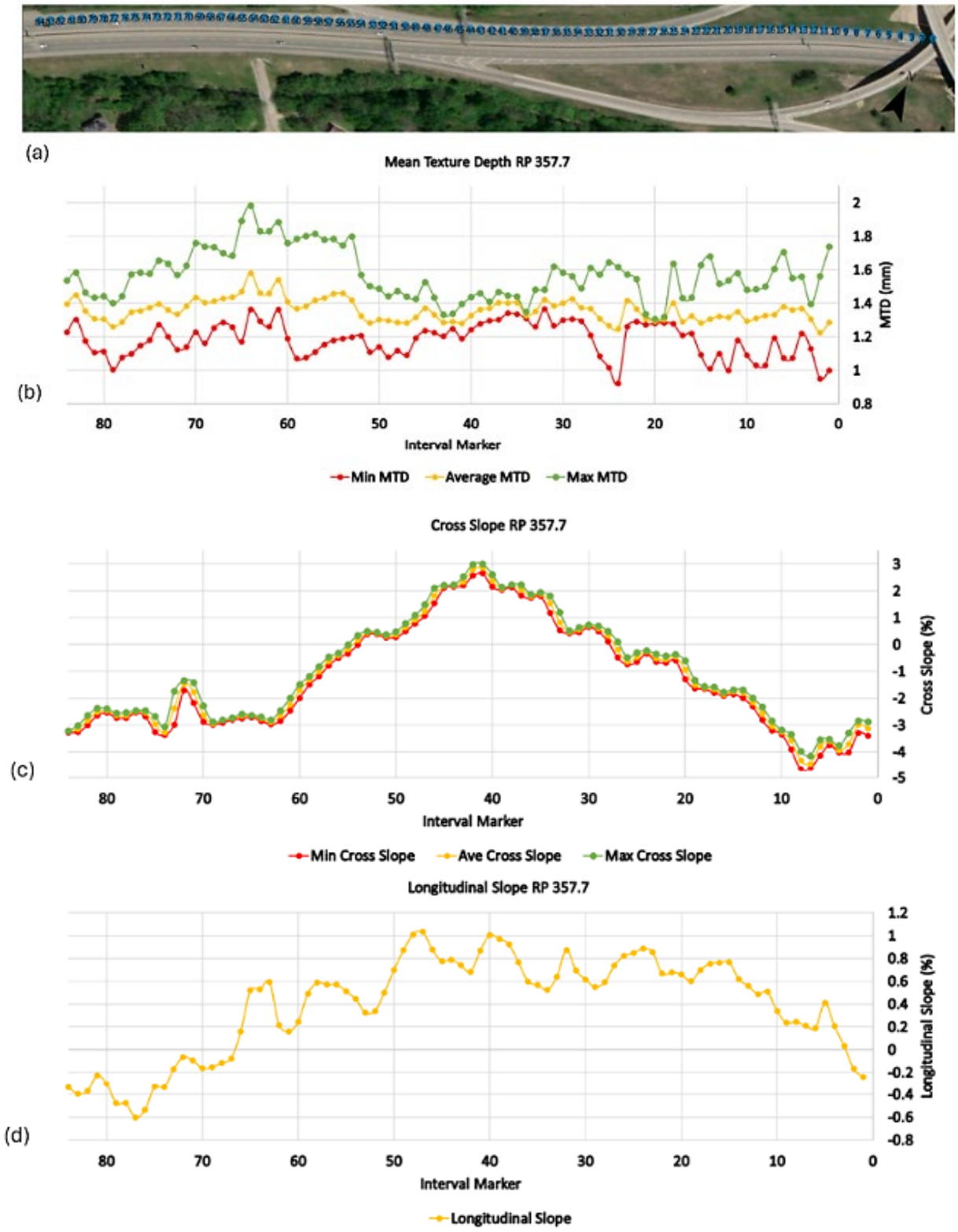

Figure 4.13: Results for the 70-89 RP 357.7 Location: (a) Scan Locations, (b) MTD, (c) Cross Slope, and (d) Longitudinal Slope

Figure 4.14: (a) Flow Direction, (b) Flow Accumulation

Figure 4.13b shows that, although the MTD is suitable throughout this location, it dips slightly near the weave terminal. The average MTD in this area is 1.36, never falling below

0.5 mm. As shown in Figures 4.13c and 4.13d, the cross slope and longitudinal slope, respectively, are also near zero just after the off-ramp, potentially indicating slow drainage. The flow direction results in Figure 4.14a show a flow reversal that is nearly against traffic and into the median, while the flow accumulation results in Figure 4.14b do not reveal where water may drain on this roadway.

4.2 Overall Hydroplaning Potential and Mitigation

A summary of the analysis at each KDOT location, including proposed solutions, is shown in Table 4.1. Suggestions for each location were based on observations of texture, slope, flow accumulation, and direction. Drainage improvements and/or low-cost geometry remedies such as milling, grinding, and overlays should be considered prior to expensive geometric redesign solutions.

Table 4.1: Study Location Results

Location	Average MTD (mm)	Minimum MTD (mm)	Observations	Suggested Solutions for Investigation
RP 79.2	1.10	0.60	High accumulation at turning lane	Drainage and geometry improvement
RP 204.8	1.06	0.71	Low slope	Drainage and geometry improvement
RP 214.7	1.01	0.80	Drainage flow against traffic	Drainage and geometry improvement
RP 217.55	0.75	0.51	Drainage flow against traffic	Drainage and geometry improvement
RP 295.2	0.71	0.46	High accumulation at superelevated transition and low texture	Texture improvement
RP 330.1	1.85	0.91	High accumulation	Drainage and geometry improvement
RP 357.7	1.35	0.92	Drainage flow against traffic and low slope	Drainage and geometry improvement

4.3 Crash Rate

This study calculated a crash rate to explore the relationship of traffic volume to the number of crashes at each KDOT location. Crash rates were calculated using the following equation from FHWA-SA-11-09 by Golembiewski and Chandler (2011):

$$R = \frac{C \times 100{,}000{,}000}{V \times 365 \times N \times L}$$

Equation 4.1

Where:

R = roadway segment departure crash rate (crashes per 100 million vehicle-miles of travel),

C = total number of roadway departure crashes in the study period,

V = traffic volumes using AADT volumes (based on 2021 AADT data),

N = number of years (11) in the study period data, and

L = length of the segment in miles (0.5 miles).

Table 4.2 and Figure 4.15 present the crash rate and accident rate during wet weather for each location. Wet-weather crash rates only considered crashes that occurred during rain, mist, or drizzle precipitation according to weather conditions reported in the crash records. In addition, only crashes that occurred in the direction of travel at the study location were included. A distance radius of 0.5 miles from the KDOT-specified marker was used to identify crashes, and crashes that occurred within the approximate superelevated transition locations, but that were not within 0.5 miles of the marker were also included. Extraneous crashes that occurred at intersections or on unrelated on- or off-ramps were not included in crash rates.

Table 4.2: All-Weather and Wet-Weather Crash Rates for Study Locations

Reference Point (RP)	Total Crashes Near RP and Superelevated Transition	Ratio of Crashes Reported During Rain, Mist, or Drizzle	Annual Average Daily Traffic as of 2021 (Vehicles/Day)	Segment Crash Rate (Per 100-Million Vehicle-Miles of Travel)	Wet-Weather Segment Crash Rate (Per 100-Million Vehicle-Miles of Travel)
79.2	18	0.28	4160	215.5	59.9
204.8	4	0.00	13500	14.8	0.0
214.7	65	0.31	52800	61.3	18.9
217.55	88	0.36	62900	69.7	25.3
295.2	88	0.26	26800	163.6	42.8
330.1	9	0.00	5180	86.5	0.0
357.7	58	0.21	57800	50.0	10.3

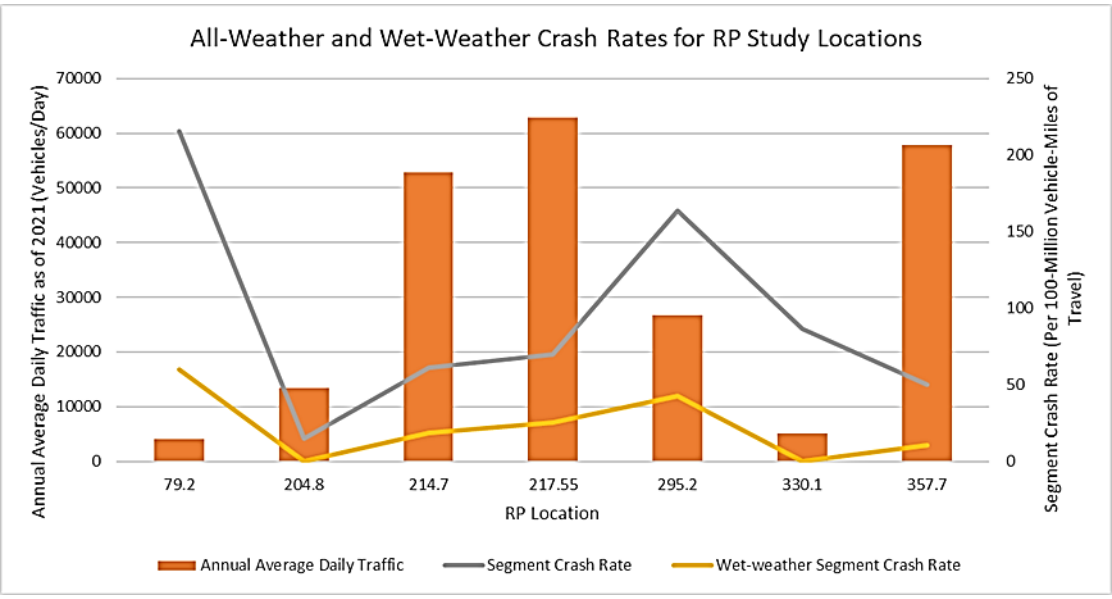

Figure 4.15: All-Weather and Wet-Weather Crash Rates for Study Locations

4.4 Geometric Redesign to Mitigate Hydroplaning

The results in Table 4.1 indicate that all but the 70-31 RP 295.2 location of the KDOT study locations experience poor drainage and require solutions that adjust roadway geometry to improve drainage and reduce the potential for hydroplaning. Therefore, this study created a proof-of-concept highway redesign example in ORD of the 70-31 RP 295.2 location.

4.4.1 Identifying Poor Drainage Using Flow Paths in ORD

Although the literature presents flow path reduction length as a means to mitigate flow at superelevated transitions (Anderson et al., 1998; Brown et al., 2009; Flintsch et al., 2021), implementation descriptions using modern design tools in areas with complicated elements (i.e., ramps, weaves, and intersections) are limited. Therefore, this study developed a general method for tracing flow paths using slope in ORD to evaluate the effectiveness of the redesign.

The Aquaplaning command in ORD was used to identify problematic flow paths in the design. A similar method draws perpendicular flow lines between elevation contours, or uses flow arrows, but the Aquaplaning tool allows the user to observe concerning flow paths in a highway design. However, the empirical equations included in the aquaplaning tool demonstrate poor effectiveness in areas of complicated geometry, so they were not used for this report.

The Aquaplaning command was used with a flow interval of 10 ft, rainfall intensity of 2.00 in./hr, shallow ridge slope of 0.00%, maximum film depth of 0.007 ft (2.1 mm), maximum slope of 20.0%, and a texture depth of 0.002 ft (0.7 mm). The Gallaway equation was selected, and the "use equal area slope" option was unselected. Because this location is a two-lane roadway in the same direction, proper design should allow the flow to drain to each edge from the crown. The "trace slope" tool displays this as two separate directional lines that travel away from the crown of the road.

Figure 4.16 illustrates the roadway profile with flow lines plotted every 10 ft at the crown of the road. In the figure, the roadway lanes are black, the crown is red, and the flow lines are shown in green, with blue flow lines indicating areas with flow above the maximum flow depth (according to the Gallaway formula). The orange line designates the beginning of the superelevated transition, the red line shows when the right lane experiences a slope of zero, the yellow line indicates when 75% of the superelevation is reached in the runoff length, and the purple line signifies full superelevation. The flow slope lines were isolated for clarity.

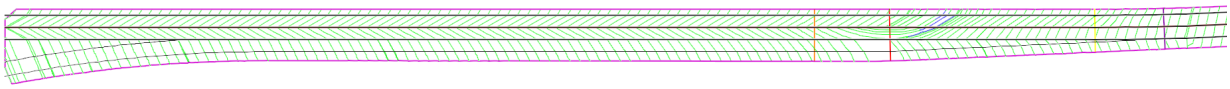

Figure 4.16: Flow Slope Paths of Original 70-31 RP 295.2 Design

As shown in the figure, the slope direction from the crown is a pathway to the roadway edges and across the acceleration lane. Near the superelevation transition, the slope lines begin to group together instead of forming parallel bands, indicating flow accumulation in areas where slope flow lines overlap if they originate in different locations. Additionally, as shown, the flow paths become longer near where the roadway slope becomes zero. Since the flow lines are also in the direction of traffic, vehicles would push water down the roadway in a splash-and-spray scenario and potentially exacerbate the drainage issue. A closer view of the transition area is shown in Figure 4.17.

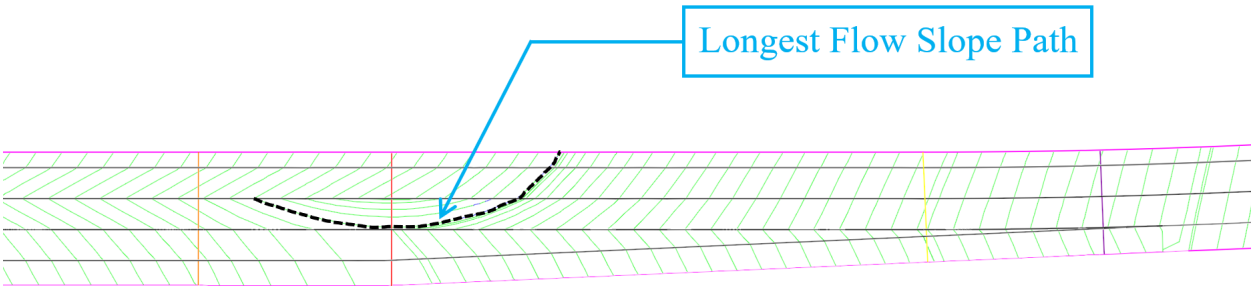

Figure 4.17: Flow Slope Path of Transition Area of Original 70-31 RP 295.2 Design

The change in flow slope path direction was then visually compared to the roadway sections before the superelevation transition, as illustrated in Figure 4.18.

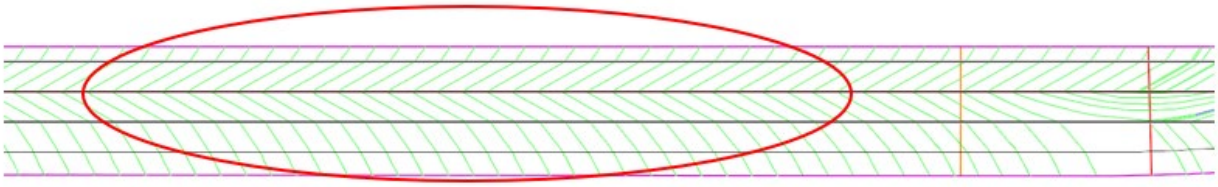

Figure 4.18: Flow Slope Path of Tangent Section of 70-31 RP 295.2 Location

Although adjusting a current, built design to improve drainage should only occur as a last resort, the following design changes proposed to this location could be considered for future design of superelevated transitions. For example, a shorter superelevated transition length at this location could reduce the length of roadway where the cross slope is near zero; thereby, allowing water to drain from the transition area faster since cross slopes surrounding the transition would increase, resulting in shorter flow slope lines. This study calculated the transition length (i.e., minimum runoff length) using the Green Book (7^{th} edition) (AASHTO, 2018), in which a design speed (V_D) of 70 mph, an e_{max} of 8.0%, a design superelevation (e_d) of 6.5%, and a maximum relative gradient (Δ) of 0.50 for a design speed over 50 was used. The radius of the horizontal curve was identical to the design curve at 2864.79 ft. The following equation was used to find a minimum runoff length (L_r) of 194.2 ft:

$$L_r = \frac{(wn_l)e_d}{\Delta}(b_w)$$

Equation 4.2

Where:

w = lane width (12 ft),

n_l = number of lanes rotated (1.5, including the acceleration lane), and

b_w = the lane adjustment factor (0.83).

The minimum runout length (L_t) was found to be 46.61 ft using the following equation:

$$L_t = \frac{e_{NC}}{e_d}L_r$$

Equation 4.3

Where:

e_{NC} = normal cross slope rate (1.56%),

e_d = design superelevation (6.5%) and

L_r = minimum runoff length (194.22 ft).

This study also utilized a method to attain superelevation that matched the original design plans, with 75% of the runoff length occurring before the PC (Figure 4.19).

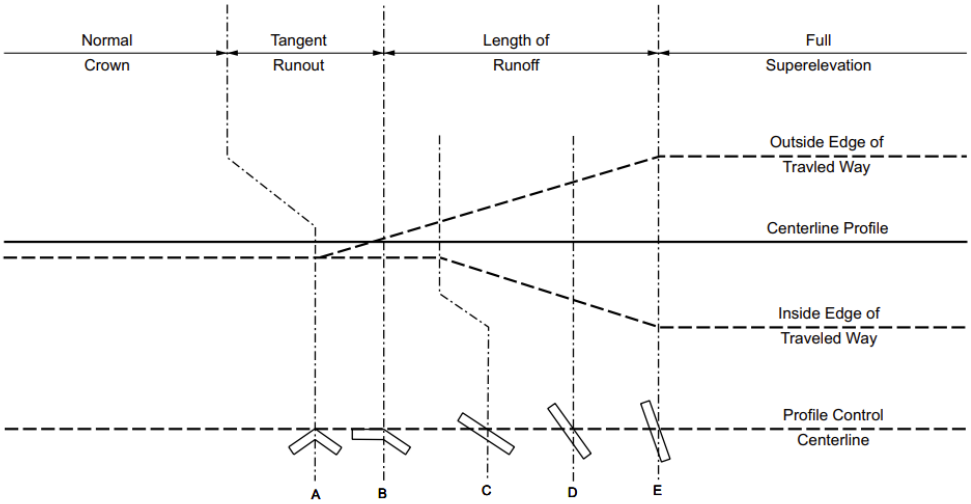

Figure 4.19: Method to Attain Superelevation for Transition Redesign
Source: (AASHTO, 2018)

Because a superelevation transition of the minimum length could be jarring and visually unattractive for drivers, this study created example transitions that were shorter than the original design but larger than the minimum required length. The original runout and runoff lengths were

shortened individually. Shortened Transition 1 had runout and runoff lengths that were each 85% of the original design length, while Shortened Transition 2 had runout and runoff lengths that were 90% of the original design length. Although the runout length used in Kansas is typically 75 ft (according to the KDOT *Highway Design Manual*), shorter lengths were used to demonstrate flow path length reduction. Statistics about the calculated transitions are listed in Table 4.3.

Table 4.3: Comparison of Transition Designs For 70-31 RP 295. Location In ORD

Transition	Rounded Runout Length (ft)	Rounded Runoff Length (ft)	Total Amount Shortened Compared to Original Design (%)
Minimum	45	195	- 31.4
1	64	234	- 14.9
2	68	248	- 9.7
Original Design	75	275	N/A

Other configurations that did not change the transition length of the original design included shifting the placement of the transition along the roadway and increasing the design superelevation. The placement of the transition was adjusted by moving how much of the runoff length occurred before and after the PC. The Green Book indicates that the proportion of runoff length placed on the tangent varies from 50% to 80%, and the majority of state agencies place 67% of the runoff length before the PC (AASHTO, 2018). The original design was adjusted so that 50% and 67% of the runoff length were placed before the PC compared to 75% in the original design. An additional transition redesign example was created using Shortened Transition 2 with 67% of the runoff length placed before the PC.

Another configuration of the original design with an increased superelevation of 7.0% was also evaluated. Equations 4.2 and 4.3 were used to ensure that a superelevation of 7.0 would be suitable for the runout and runoff lengths of the original design. Using a design superelevation rate of 7.0% and values identical to the original design in Equations 4.2 and 4.3, a minimum runout length of 56.16 and a minimum runoff length of 252 were found, respectively.

Heading into the horizontal curve, the longitudinal slope of this section of roadway transitions from -2.66% to -0.05%. Referencing the vertical alignment of the design in Figure 4.20,

the superelevated transition occurs at the beginning of the sag vertical curve; the beginning and end of the transition is marked with vertical pink lines. As shown, the longitudinal slope at the beginning of the transition is -2.66%, while the longitudinal slope at the end of the transition is -1.06%.

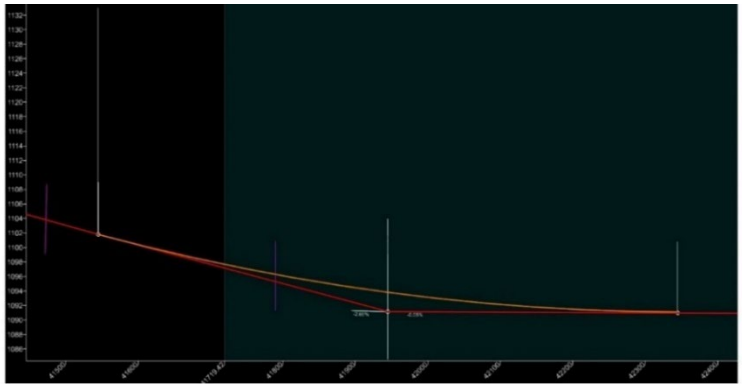

Figure 4.20: Vertical Alignment for the 70-31 RP 295.2 Location

The bottom of the vertical sag curve created by this transition occurs near the middle of the horizontal curve. Grade near the transition to the sag curve can be deemed suitable for drainage using Section 3.3.8.9 in the Green Book (AASHTO, 2018). The first consideration for this section is to ensure that minimum profile grade of 0.5%; within the transition area, the profile grade exceeds 0.5%. The second consideration is to ensure that a minimum 0.2% edge-of-pavement grade for uncurbed sections is used, as verified by the following equations:

$$\Delta^* = \frac{(\boldsymbol{wn_l})\boldsymbol{e_d}}{\boldsymbol{L_r}}$$

Equation 4.4

$$\boldsymbol{G} \leq -\Delta^* - \boldsymbol{0.2}$$
$$\boldsymbol{G} \geq -\Delta^* + \boldsymbol{0.2}$$
$$\boldsymbol{G} \leq \Delta^* - \boldsymbol{0.2}$$
$$\boldsymbol{G} \geq \Delta^* + \boldsymbol{0.2}$$

Equation 4.5

Where:

Δ^* = effective maximum relative gradient (%),

w = width of one lane (ft),

n_l = number of lanes rotated,

e_d = design superelevation (%),

L_r = superelevation runoff length (ft), and

G = profile grade (%).

Using values from the original design, the effective maximum relative gradient was 0.57%, and the bounds of the control grades were -0.77% and +0.77%. Considering an increased design superelevation of 7.0%, the resulting effective maximum relative gradient was 0.61. The grade within the transition area remained outside the range of these values, meaning the transition met the criteria for proper drainage at the beginning to the horizontal curve for a design superelevation of 6.5% and 7.0%. Other design verifications that increased the design superelevation were not conducted, and the design superelevation was increased only to compare flow path lengths.

One redesign solution was to adjust the acceleration lane to decrease splash and spray from vehicles merging to the mainline. Section 10.9.6.4.7 in the Green Book describes taper and parallel entrance terminal lane design for on-ramps and off-ramps, as illustrated in Figure 4.21 (AASHTO, 2018).

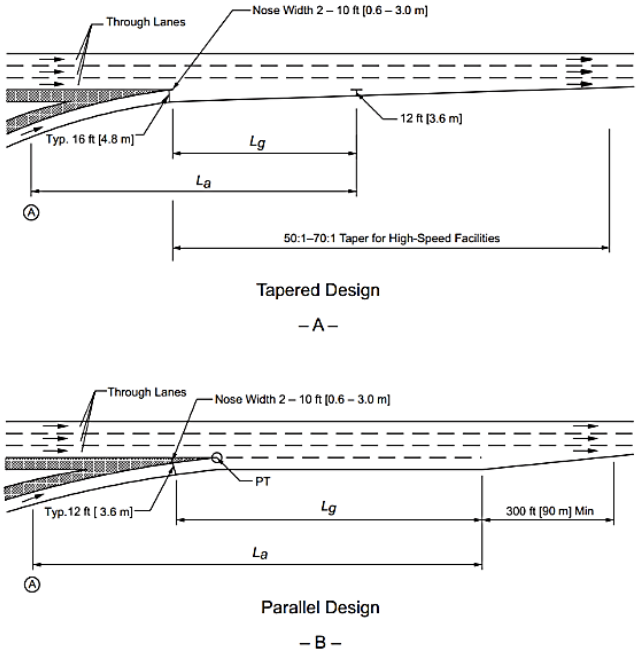

Figure 4.21: Entrance Terminal Examples
Source: AASHTO (2018)

Adjusting the acceleration lane to ensure it does not merge with the through lanes at the superelevated transition would improve drainage and prevent merging vehicles from spraying water onto the mainline during a rain event. However, decreasing the length of the acceleration

lane is not possible in this area because a tapered design does not allow enough space before the horizontal curve. In addition, shortening the ramp is not preferred because its current length is suitable for the design speeds in Table 10-4 in the Green Book (AASHTO, 2018), as summarized in Table 4.4.

Table 4.4: Minimum Acceleration Lane Lengths

Acceleration Lane Length, L_a (ft) for Design Speed of Controlling Feature on Ramp, V' (mph)										
Highway		**Stop Condition**	**15**	**20**	**25**	**30**	**35**	**40**	**45**	**50**
Design Speed, V (mph)	**Merge Speed, V_a (mph)**	**Average Running Speed (i.e., Initial Speed) at Controlling Feature on Ramp, V'_a (mph)**								
		0	14	18	22	26	30	36	40	44
30	**23**	180	140	-	-	-	-	-	-	-
35	**27**	280	220	160	-	-	-	-	-	-
40	**31**	360	300	270	210	120	-	-	-	-
45	**35**	560	490	4.4	380	280	160	-	-	-
50	**39**	720	660	610	550	450	350	130	-	-
55	**43**	960	900	810	780	670	550	320	150	-
60	**47**	1200	1140	1100	1020	910	800	550	420	180
65	**50**	1410	1350	1310	1220	1120	1000	770	600	370
70	**53**	1620	1560	1520	1420	1350	1230	1000	820	580
75	**55**	1790	1730	1630	1580	1510	1420	1160	1040	780
80	**57**	2000	1900	1800	1750	1680	1600	1340	1240	980

Source: AASHTO (2018)

However, a potential adjustment for this location could be the addition of an entrance ramp on the horizontal curve to prevent the acceleration lane from merging with the mainline during the superelevation transition, as described in the Green Book (AASHTO, 2018) and illustrated in Figure 4.22.

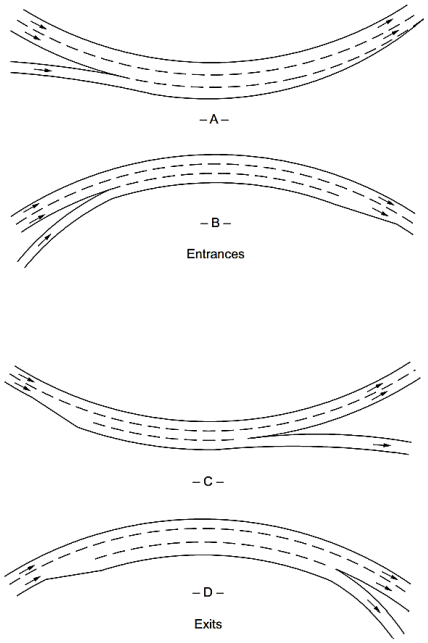

Figure 4.22: Entrance Types within Horizontal Curves
Source: (AASHTO, 2018)

Entrance ramp A in Figure 4.22 could be used at this study location in conjunction with the horizontal curve present at 70-31 RP 295.2 location. Section 10.9.6.6.3 of the Green Book also provides a design guide for these types of entrances and exits. This study followed the method to taper the speed change lane to complete the redesign example for the 70-31 RP 295.2 location.

4.4.2 Design Check of Slope Flow Path Length

Transition length, longitudinal grade, and roadway reconfiguration were calculated using slope path flow reduction to evaluate each design. The current design was found to have adequate longitudinal slope, so no redesign was conducted for this focus. Results for transition length adjustment and acceleration lane reconfiguration are shown in Table 4.5. Because reducing the transition length did not result in a linear decrease in flow path, multiple variations of a design should be evaluated when minimizing slope flow paths. Figures 4.23–4.29 show various flow slope paths for this study location.

Table 4.5: Slope Flow Path Length Comparison of Transition Redesign

Transition	Length of Longest Flow Path on Transition (ft)	Flow Path Length Reduction Compared to Original Design (%)	Total Transition Length Reduction Compared to Original Design (%)
Minimum Length	93.4	- 30.1	- 31.4
Shortened Transition 1	121.8	- 8.8	- 14.9
Shortened Transition 2	121.9	- 8.8	- 9.7
7.0 % Superelevation	127.0	- 4.9	0.0
Runoff 50 % Before PC	121.0	- 9.4	0.0
Runoff 67 % Before PC	122.0	- 8.6	0.0
Shortened Transition 2 and Runoff 67 % Before PC	120.9	- 9.5	- 9.7
Original Design	133.6	N/A	N/A

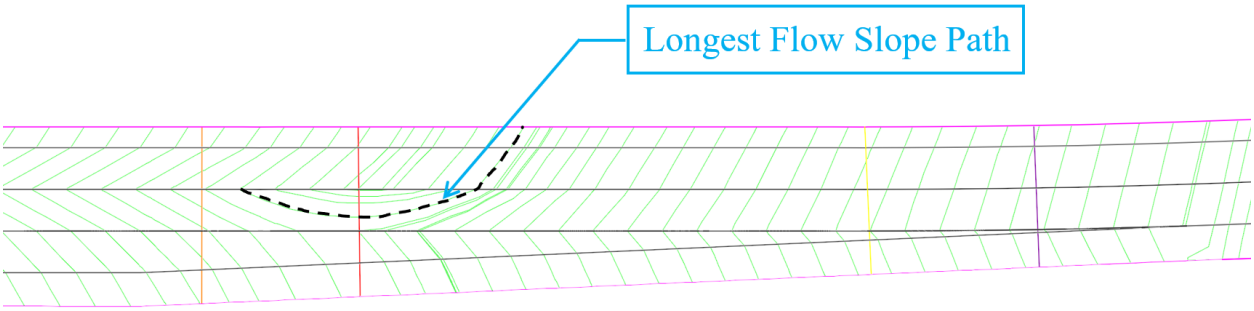

Figure 4.23: Flow Slope Paths of Minimum Transition Length for 70-31 RP 295.2 Location

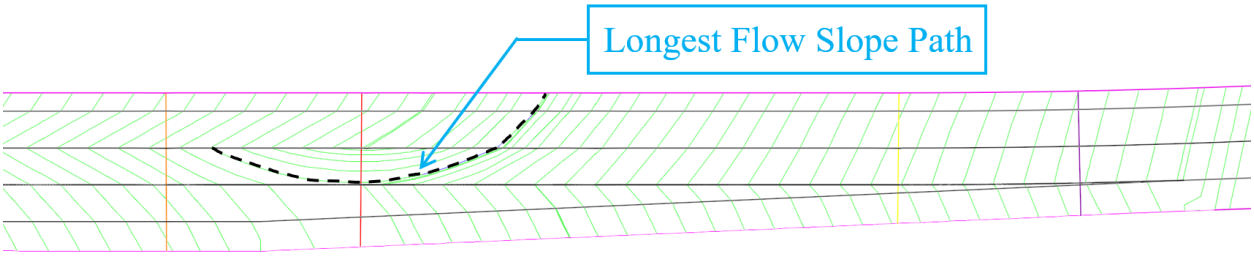

Figure 4.24: Flow Slope Paths of Shortened Transition 1 for 70-31 RP 295.2 Location

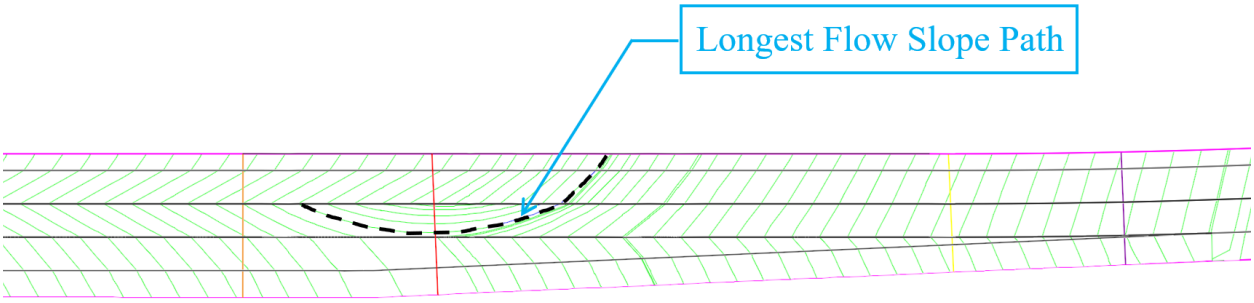

Figure 4.25: Flow Slope Paths of Shortened Transition 2 for 70-31 RP 295.2 Location

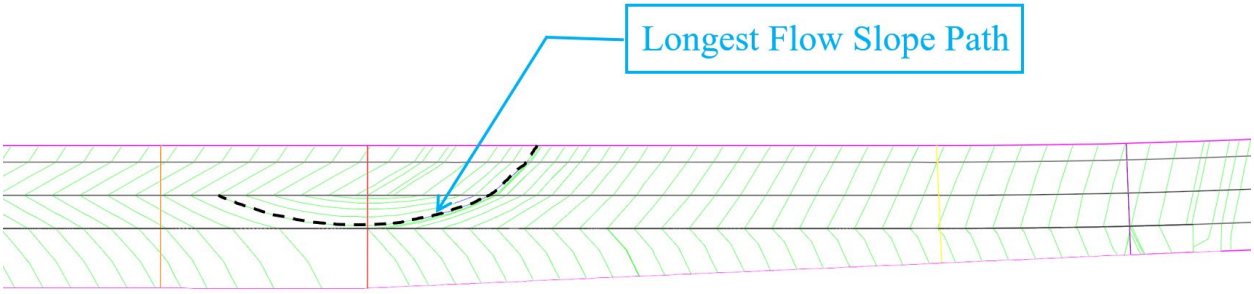

Figure 4.26: Flow Slope Paths of 7.0% Superelevation Transition for 70-31 RP 295.2 Location

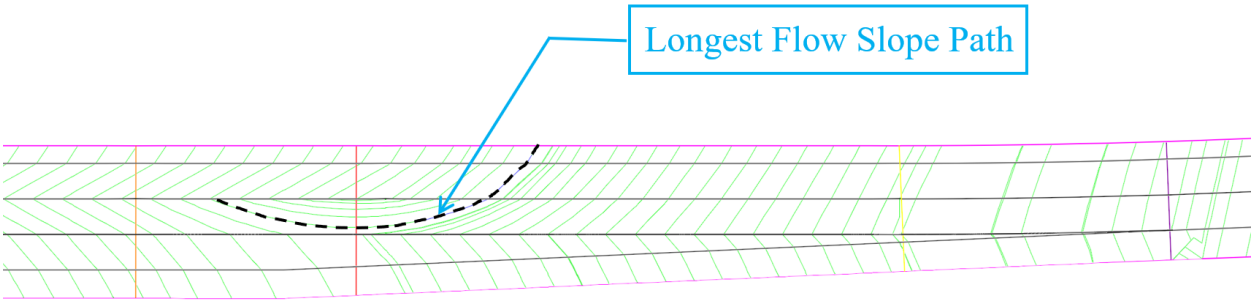

Figure 4.27: Flow Slope Paths of 67% Runoff Before the PC for 70-31 RP 295.2 Location

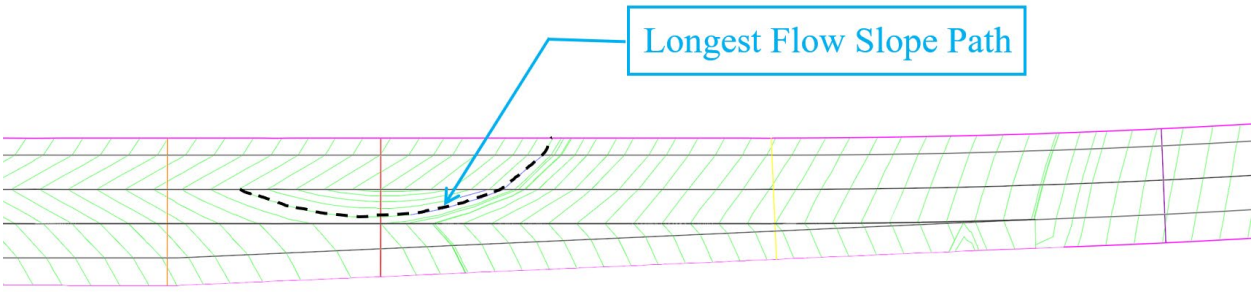

Figure 4.28: Flow Slope Paths of 50% Runoff Before the PC for 70-31 RP 295.2 Location

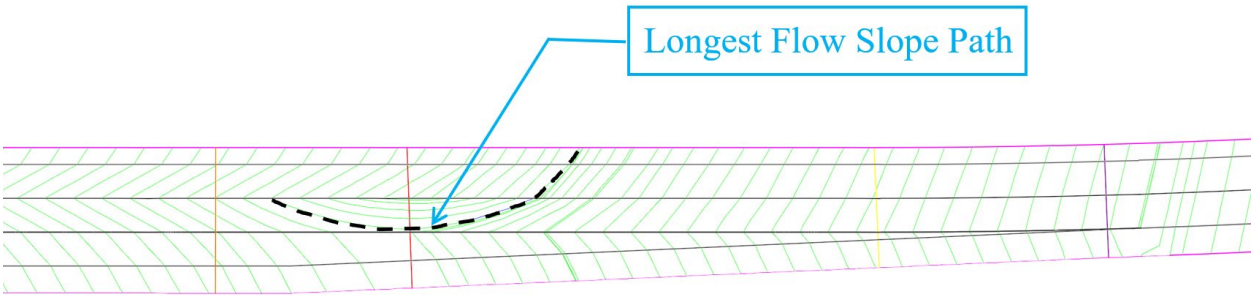

Figure 4.29: Flow Slope Paths of Shortened Transition 2 with 67% Runoff Before the PC for 70-31 RP 295.2 Location

This research also investigated on-ramp configuration adjustments, as illustrated in the ORD example of roadway mesh in Figure 4.30. As shown, the acceleration lane occurs completely within the horizontal curve, ending at three-quarters the length of the horizontal curve with a taper of 50:1 and the same profile as the on-ramp of the original design.

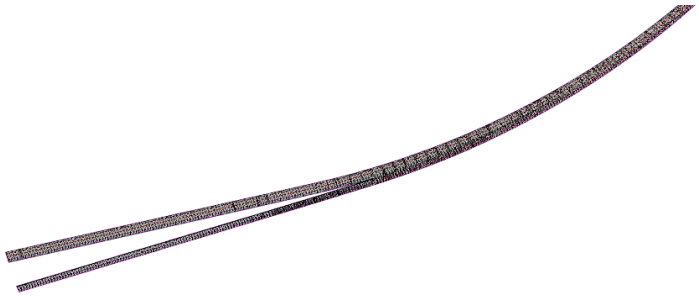

Figure 4.30: Acceleration Lane Reconfiguration at 70-31 RP 295.2 Location

Instead of correcting the flow lines in the original design, this configuration moves the acceleration lane to the horizontal curve to avoid the superelevation transition, potentially improving splash-and-spray drainage in the area. Consequently, a longer flow path was created when the shoulder was added to the transition instead of the acceleration lane that sloped to the outward edge during the transition. Slope paths representing drainage flow are shown in Figure 4.31, with slope paths drawn every 10 ft using the Aquaplaning tool in ORD.

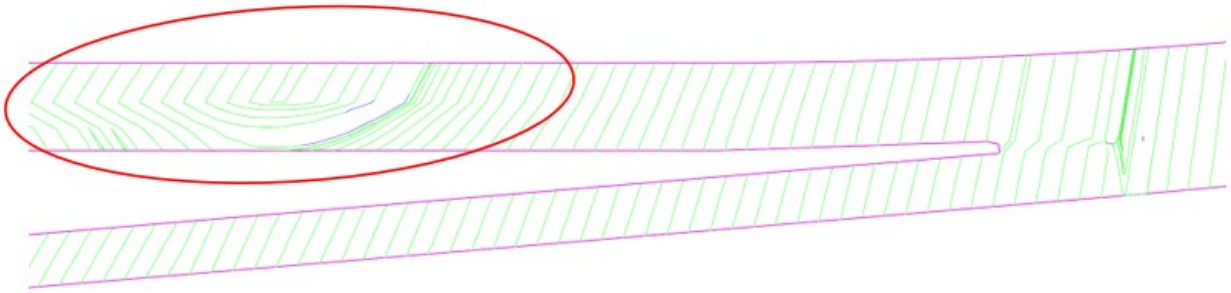

Figure 4.31: Slope Flow Path Length for Acceleration Lane Reconfiguration at 70-31 RP 295.2 Location

However, because the length of the flow path in the reconfiguration significantly exceeds the flow path length of the original design, other redesign options may be preferable to this configuration.

Chapter 5: Discussion

5.1 Hydroplaning Remediation Recommendations for Study Locations

Based on the analysis of each study location, suggested solutions were categorized as drainage and geometry improvements or pavement texture improvements. Drainage and geometry improvements were suggested for the 169-2 RP 79.2, 70-84 RP 204.8, 35-46 RP 214.7, 35-46 RP 217.55, 50-9 RP 330.1, and 70-89 RP 357.7 locations, and texture improvements were recommended for the 70-31 RP 295.2 location. Pavement texture was lacking in areas at many locations, but drainage, geometry and poor texture can be corrected simultaneously using a solution that adds or removes material for the roadway, including overlay and overbuild; surface tining or groove cutting; milling or diamond grinding; and seals, bonds, and resurfacings (Table 3.4). Proper cost-benefit analyses should be considered before selecting the optimal solution.

Several observations regarding the crash rates for each study location were also noted. As shown in Table 4.5, higher average daily traffic does not result in a linear increase of vehicle crashes for each location. In fact, crash rates are higher at locations of lower average daily traffic, such as locations 169-2 RP 79.2 and 50-9 RP 330.1 (except for the 70-31 RP 295.2 location with a high traffic rate and a high crash rate). Locations 169-2 RP 79.2 and 70-31 RP 295.2 have the highest crash rates and the highest wet-weather crash rates, while locations 35-46 RP 214.7 and 35-46 RP 217.55 have the highest wet-weather crash rates, with over 30.0% of crashes occurring during rain, mist, or drizzle weather. Comparisons of wet-weather and all-weather crash rates are useful for selecting hydroplaning remediation projects, but a cost-benefit analysis is necessary for driver safety regardless of weather and crash causes.

5.2 Geometric Redesign

The highway redesign of the 70-31 RP 295.2 location showed that a reconfiguration of this section of highway is not possible due to minimum distance and size constraints of the acceleration lane. Decreasing the length of superelevation transition, decreasing the proportion of runoff length before the PC, and increasing the design superelevation rate resulted in slope flow path lengths that were shorter than the original design. In addition, the length that the transition was shortened did not scale linearly with the distance of the slope flow path lengths of the redesigned

superelevation transitions. For maximum drainage and hydroplaning reduction, the safest superelevation transition length that can be used for driver comfort should ideally have the lowest slope flow path length. Since transition length does not scale linearly to slope flow path length, many lengths must be investigated to identify a safe transition with the lowest slope flow path length.

Study results also revealed that Shortened Transition 1 was 14.9% shorter than the original superelevated transition, resulting in a slope flow path reduction of 8.8%. Shortened Transition 2 resulted in the same slope flow path length reduction but only had a superelevated transition that was 9.7% shorter than the original design, potentially indicating that more complicated geometric factors than the transition length impact the length of the resulting slope flow paths. More research is needed to identify an ideal superelevated transition length long enough to maximize driver safety and comfort and provide a minimum slope flow path length.

This study also adjusted the proportion of runoff before the PC in the redesigned superelevated transitions. When 50% of the runoff length occurred before the PC, a 9.4% reduction in the slope flow path length was observed. Comparatively, when 67% of the runoff length occurred before the PC, an 8.6% reduction in the slope flow path length was noted. The least decrease in slope flow path length occurred when the design superelevation rate was increased from 6.5% to 7.0%, resulting in a 4.9% reduction in slope flow path length compared to the original design. When Shortened Transition 2 and a 7.0% design superelevation rate were used, the largest decrease in slope flow path length was 9.6%; however, the results of this configuration did not strongly outweigh the others.

Chapter 6: Summary and Recommendations

6.1 Summary

This study analyzed existing hydroplaning and hydroplaning mitigation research, recommended hydroplaning mitigation near superelevated highway curves in seven study locations in Kansas and identified current hydroplaning mitigation methods other state DOTs use in their design manuals. A method to identify limitations at areas of hydroplaning concern was determined using LCMS and LDTM data from the KDOT Mobile LiDAR Project. Texture and slope data were also considered, and an example highway redesign to reduce slope path and limit drainage flow paths was created in ORD. Current design manuals from all state DOTs were examined for hydroplaning mitigation and drainage improvement near areas of low pavement slope.

6.2 Recommendations and Best Practices

This study compiled several general suggestions regarding hydroplaning reduction, drainage at areas of low roadway slope, and superelevated transition design. First, the length of flat areas on roadways should be limited to reduce hydroplaning, and flow slope paths should be minimized in transition areas to reduce the amount of roadway with slope that is near 0%. Second, superelevation transitions that coincide with the bottom of sag vertical curves, the top of crest vertical curves, or relatively flat tangent grade sections should be avoided. A varying "sawtooth" vertical profile can be used to maintain minimum grades. Third, when considering drainage inlets at sag curves, KDOT should incorporate additional design guidance for inlet design, as demonstrated in Minnesota Department of Transportation (MnDOT, 2000) and Oregon Department of Transportation (ODOT, 2014) in Appendix A. In addition, a process similar to the process described in Alabama Department of Transportation (ALDOT, 2022) should be used to predict hydroplaning and WFT in areas that do not have superelevated highway transitions, and the method to compute rainfall intensity based on roadway characteristics and water depth for potential hydroplaning (ALDOT, 2022), as described in Appendix A should be implemented. Finally, to improve drainage, cross slope should be increased to shorten drainage flow paths, as

described in the VTran manual presented in Appendix A (Wark et al., 2015). VTran suggests the use of an increasing cross slope of 0.5%–1.0% for each lane exceeding three lanes.

This study also recommends highway redesign and rehabilitation projects that focus on drainage and geometry improvements, specifically a step-by-step approach for highway redesign projects with hydroplaning improvements for Kansas. In addition, universal guidelines for roadway rehabilitation related to wet-weather crashes, such as are described in Florida Department of Transportation (FDOT, 2022a), are recommended, where redesign improvements for wet weather are based on the number of crashes at a location. Additional considerations should be made for areas of low texture and slope to account for hydroplaning potential, as outlined in North Carolina Department of Transportation (NCDOT, 2013) and detailed in Appendix A. Although flow path length reduction was suggested by Anderson et al. (1998), Brown et al. (2009), and Flintsch et al. (2021), an efficient incorporation method of this reduction into design practices is not common. This study modeled this incorporation in ORD, but further investigation is necessary to reduce ponding and promote proper drainage.

6.3 Uncertainty and Limitations

Pavement and roadway modeling in this study were limited in the following areas:

- Roadway meshes created to investigate slope flow path minimizations in ORD are uniform with completely flat geometry. These ideal conditions are unrealistic when considering the non-uniformity of a roadway, and they do not account for the microtexture and macrotexture of a roadway surface.
- Although reduced texture indicates road surface wear and can decrease the surface's ability to drain water, a study of roadway friction (friction number, coefficient of friction, etc.) should be conducted before texture improvements are made at the study locations.
- Porous pavements were not considered in this research. The models created in ORD and ArcGIS Pro do not allow for porous surfaces, which

impact the results of flow accumulation, flow direction, and slope path modeling by reducing overall WFT.

- Digital banding of the digital terrain map scans impacts the results of flow direction and accumulation results, as observed in the eastern portion of the 50-9 RP 330.1 location in Figure 4.12 and could reflect collection errors associated with the LDTM and LCMS data.
- LDTM and LCMS data were collected using longitudinal bands that may not represent the entirety of a roadway section.
- Multiple redesign solutions must be compared when considering flow path minimization using slope paths in ORD. As demonstrated in the examples with shorter transitions, distances do not always result in shorter flow paths.

The following limitations impacted the identification and quantification of crash rate at the study locations:

- The accuracy of the crash reports was affected by time uncertainties, weather conditions, and crash locations and directions. These factors impacted the crash rates at each reference point.
- Crashes were only identified within 0.5 miles from location reference points and within approximate locations of the superelevated transitions associated with each reference point. Other crashes related to hydroplaning or otherwise could have occurred at other KDOT locations.
- Crashes that occurred during wet weather were assumed to have been caused by wet weather. Crashes caused by factors unrelated to hydroplaning (e.g., driver error, wildlife, roadway ice) were not filtered from the crashes related to wet weather.
- Locations with serious hydroplaning risks elsewhere in Kansas could be unidentified, such as roadways with less traffic and/or locations with low crash rates.

6.4 Future Directions

The relationship between rainfall intensity and hydroplaning could be explored further as it pertains to crash location. Areas with high numbers of wet-weather crashes should be studied to determine if increasing rainfall intensity increases crash rates, such as in Saberi and Bertini (2010). Locations with low rainfall intensities and wet-weather related crashes should be considered first for hydroplaning reduction projects since these locations could result in a higher number of crashes during wet weather. In addition, further research regarding surface texture and grooving should be conducted, and rainfall intensity and resulting WFT on roadways with low texture should be evaluated. Optimal texture for WFT could also be researched, including various roadway surface texture types and grooving methods using different roadway surface materials. Additional research should apply best practices for roadway texture and grooving considering rainfall intensity at a large scale if digital scans of roadway surfaces are available. Research could also be conducted on roadway texture and grooving as they relate to pavement drainage, and drainage comparisons could be made based on grooving direction, grooving spacing, grooving depth, shape, pavement slope, and pavement material. Similarly, pavement texture and its role in increasing drainage capacity of a roadway for low rainfall rates (TxDOT, 2019) could also be explored.

References

Alabama Department of Transportation (ALDOT). (2022). *Hydraulic manual*. https://www.dot.state.al.us/publications/Design/pdf/HydraulicManual.pdf

American Association of State Highway and Transportation Officials (AASHTO). (2018). *A policy on geometric design of highways and streets* (7th ed.).

Anderson, D. A., Huebner, R. S., Reed, J. R., Warner, J. C., & Henry, J. J. (1998). *Improved surface drainage of pavements* (NCHRP Web Document 16, Project 1-29). Pennsylvania Transportation Institute. https://onlinepubs.trb.org/Onlinepubs/nchrp/nchrp_w16.pdf

ASTM E965-15. (2019). *Standard test method for measuring pavement macrotexture depth using a volumetric technique*. ASTM International. doi: 10.1520/E0965-15R19, www.astm.org

Bentley Systems. (n.d.). *OpenRoads Designer: Road design software*. Retrieved December 16, 2022, from https://www.bentley.com/software/openroads-designer/

Boulet, M., Descornet, G., & Wambold, J. C. (1995). International experiment to compare and to harmonize pavement texture and skid resistance measurement methods. *Routes/Roads*, *288*, 22-37.

Brown, S. A., Schall, J. D., Morris, J. L., Doherty, C. L., Stein, S. M., & Warner, J. C. (2009). *Urban drainage design manual: Hydraulic engineering circular 22* (3rd ed., Report No. FHWA-NHI-10-009). Federal Highway Administration. https://www.fhwa.dot.gov/engineering/hydraulics/pubs/10009/10009.pdf

Browne, A. L. (1975). Mathematical analysis for pneumatic tire hydroplaning. In J. G. Rose (Ed.), *Surface texture versus skidding: Measurements, frictional aspects, and safety features of tire-pavement interactions* (ASTM Special Technical Publication 583, pp. 75-94). American Society for Testing and Materials, ASTM International. https://doi.org/10.1520/STP39045S

Bureau of Transportation Safety. (n.d.). *Crash facts book archive*. Kansas Department of Transportation (KDOT). https://www.ksdot.gov/about/our-organization/divisions/transportation-safety/crash-facts-book-archive

Charbeneau, R. J., Jeong, J., & Barrett, M. E. (2008). *Highway drainage at superelevation transitions* (Report No. FHWA/TX-08/0-4875-1). https://trid.trb.org/View/872428

Chesterton, J., Nancekivell, N., & Tunnicliffe, N. (2006). The use of the Gallaway formula for aquaplaning evaluation in New Zealand. In *Transit NZ and NZIHT 8th Annual Conference, Auckland*. New Zealand Institute of Highway Technology and Transit New Zealand. https://www.researchgate.net/publication/268295341

City of Lenexa. (n.d.). *Pavement management program (ongoing)*. Accessed on October 1, 2025, from https://www.lenexa.com/City-Services/Public-Improvement-Projects/Street-Sidewalk-Trail-Projects/Pavement-Management-Program

City of Salina. (2020). *City of Salina pavement management street maintenance program*. Retrieved November 30, 2022, from https://www.salina-ks.gov/filestorage/18184/18599/20877/20979/Street_Maintenance_Presentation_10-29-20.pdf

Colorado Department of Transportation (CDOT). (2018). *Roadway design guide*.

Dhaliwal, S. S., Wu, X., Thai, J., & Jia, X. (2017). Effects of rain on freeway traffic in southern California. *Transportation Research Record*, *2616*, 69-80. https://doi.org/10.3141/2616-08

Dreher, R. C., & Horne, W. B. (1963). *Phenomena of pneumatic tire hydroplaning* (Technical Note, Report No. NASA-TN-D-2056). https://ntrs.nasa.gov/citations/19640000612

Drenth, K. P., Ju, F. H., & Tan, J. Y. (2017). Sampling functional condition indices at traffic-speed. In A. Loizos, I. Al-Qadi, & T. Scarpas (Eds.), *Bearing capacity of roads, railways and airfields* (pp. 947-952). CRC Press. https://doi.org/10.1201/9781315100333-127

Esri. (2022). *ArcGIS Pro* [Computer software]. https://www.esri.com/en-us/srcgis/products/arcgis-pro/overview

Flintsch, G. W., Ferris, J. B., Taheri, S., Katicha, S., Kang, Y., Nazari, A., de Leon Izeppi, E., Velez, K., Battaglia, F., Chen, L., Kibler, D., & McGhee, K. K. (2021). *Guidance to predict and mitigate dynamic hydroplaning on roadways* (NCHRP Web-Only Document 300). Transportation Research Board. https://doi.org/10.17226/26287

Florida Department of Transportation (FDOT). (2022a). *2023 FDOT design manual*. https://www.fdot.gov/roadway/fdm/2023-FDM

Florida Department of Transportation (FDOT). (2022b). *Drainage manual*. https://fdotwww.blob.core.windows.net/sitefinity/docs/default-source/roadway/drainage/files/drainagemanual2022.pdf

Gallaway, B. M., Hayes, G. G., Ivey, D. L., Ledbetter, W. B., Olson, R. M., Ross, H. E., & Schiller, R. E. (1979). *Pavement and geometric design criteria for minimizing hydroplaning: A technical summary* (Report No. FHWA-RD-79-30). Federal Highway Administration. https://rosap.ntl.bts.gov/view/dot/67508

Gallaway, B. M., Schiller, R. E., & Rose, J. G. (1971). *Effects of rainfall intensity, pavement cross slope, surface texture, and drainage length on pavement water depths* (Report No. 138-5). Texas Transportation Institute. https://library.ctr.utexas.edu/hostedpdfs/tti/138-5.pdf

Georgia Department of Transportation (GDOT). (2020). *Drainage design for highways*.

Georgia Department of Transportation (GDOT). (2022). *Design policy manual*.

Golembiewski, G. A., & Chandler, B. (2011). *Roadway departure safety: A manual for local rural road owners* (Report No. FHWA-SA-11-09). Federal Highway Administration. https://rosap.ntl.bts.gov/view/dot/41531

Gunaratne, M., Lu, Q., Yang, J., Metz, J., Jayasooriya, W., Yassin, M., & Amarasiri, S. (2012). *Hydroplaning on multi lane facilities* (Report No. BDK84 977-14). University of South Florida. https://rosap.ntl.bts.gov/view/dot/60722

Gurganusa, C. F., Chang, S., & Gharaibeh, N. G. (2021). Evaluation of hydroplaning potential using mobile Lidar measurements for network-level pavement management applications. *Road Materials and Pavement Design*, *23*(6), 1390-1399. https://doi.org/10.1080/14680629.2021.1899962

Hall, J. W., Smith, K. L., & Littleton, P. (2009). *Texturing of concrete pavements* (NCHRP Report 634). Transportation Research Board. https://doi.org/10.17226/14318

Henry, J. J. (2000). *Evaluation of pavement friction characteristics* (NCHRP Synthesis 291). Transportation Research Board.

Hibbs, B. O., & Larson, R. M. (1996). *Tire pavement noise and safety performance: PCC Surface Texture Technical Working Group* (Report No. FHWA-SA-96-068). Federal Highway Administration. https://rosap.ntl.bts.gov/view/dot/42583

Holgado-Barco, A., Gonzalez-Aguilera, D., Arias-Sanchez, P., & Martinez-Sanchez, J. (2014). An automated approach to vertical road characterization using mobile LiDAR systems: Longitudinal profiles and cross-sections. *ISPRS Journal of Photogrammetry and Remote Sensing*, *96*, 28-37. https://doi.org/10.1016/j.isprsjprs.2014.06.017

Horne, W. B. (1968). Tire hydroplaning and its effects on tire traction. *Highway Research Record*, *214*, 24-33. http://onlinepubs/hrr/1968/214/214-005.pdf

Huebner, R. S., Anderson, D. A., Warner, J. C., & Reed, J. R. (1997). PAVDRN: Computer model for predicting water film thickness and potential for hydroplaning on new and reconditioned pavements. *Journal of the Transportation Research Board*, *1599*, 128 – 131. https://doi.org/10.3141/1599-16

Idaho Transportation Department (ITD). (2013). *Roadway design manual*.

Iowa Department of Transportation. (2019). Superelevation transition evaluation tool. In *Design manual* (Section 21M-51). https://iowadot.gov/design/dmanual/21M-51.pdf

Jayasooriya, W., & Gunaratne, M. (2014). Evaluation of widely used hydroplaning risk prediction methods using Florida's past crash data. *Transportation Research Record*, *2457*, 140-150. https://doi.org/10.3141/2457-15

Jeong, J., & Charbeneau, R. J. (2010). Diffusion wave model for simulating storm-water runoff on highway pavement surfaces at superelevation transition. *Journal of Hydraulic Engineering*, *136*(10), 770-778. https://doi.org/10.1061/(ASCE)HY.1943-7900.0000253

Kansas Department of Transportation (KDOT). (2019). *State of Kansas law enforcement crash report coding manual* (2nd ed.). https://www.ksdot.gov/Assets/wwwksdotorg/bureaus/burTransPlan/prodinfo/lawinfo/CrashCodingManual.pdf

Kansas Department of Transportation (KDOT). (2021a). *2021 traffic flow map Kansas state highway system*. Kansas Department of Transportation. https://www.ksdot.gov/home/showpublisheddocument/4195/638724462659570000

Kansas Department of Transportation (KDOT). (2021b). *2021 KDOT mobile LiDAR project data portal*. Kansas Department of Transportation. Retrieved November 17, 2022, from https://www.ksdot.org/bureaus/burTransPlan/Lidar/home.asp

Kummer, H. W., & Meyer, W. E. (1963). The Penn State road friction tester as adapted to routine measurement of pavement skid resistance. *Highway Research Record*, *28*, 1-31. https://onlinepubs.trb.org/Onlinepubs/hrr/1963/28/28-001.pdf

Laurent, J., Lefebvre, D., & Samson, E. (2008). Development of a new 3D transverse laser profiling system for the automatic measurement of road cracks. In B. Leben & M. Grondin (Eds.), *Proceedings of the 6th Symposium on Pavement Surface Characteristics (SURF 2008), Portoroz, Slovenia.*

Lee, H. S., & Ayyala, D. (2020). *Enhanced hydroplaning prediction tool* (Contract No. BE570). Florida Department of Transportation. https://fdotwww.blob.core.windows.net/sitefinity/docs/default-source/research/reports/fdot-be570-rpt.pdf

Li, P., Sun, C., Huang, M., Jiang, S., & Khan, M. D. (2023). Water accumulation and anti-sliding decay characteristics of freeway pavement at superelevation transitions. *Road Materials and Pavement Design, 24*(7), 1837-1852. https://doi.org/10.1080/14680629.2022.2106294

Li, S., Zhu, K., Noureldin, S., & Jiang, Y. (2006). Surface friction on longitudinally tined concrete pavements: New findings from field testing and finite element analysis simulation (Paper No. 06-1824). In *Transportation Research Board 85th Annual Meeting compendium of papers*.

Lottes, S. A., Sitek, M. A., & Sinha, N. (2020). *Computational analysis of water film thickness during rain events for assessing hydroplaning risk, part 1: Nearly smooth road surfaces* (Report No. ANL-20/36). Argonne National Laboratory. https://doi.org/10.2172/1674976

Martinez, J. E., Young, R. D., & Faatz, W. C. (1976). *Effects of pavement grooving on friction, braking, and vehicle control* (Report No. FHWA-RD-76-166). Federal Highway Administration. https://rosap.ntl.bts.gov/view/dot/30118

Merritt, D., Himes, S., & Porter, R. J. (2021). *High friction surface treatment site selection and installation guide* (Report No. FHWA-21-093). Federal Highway Administration. https://highways.dot.gov/sites/fhwa.dot.gov/files/2022-06/HFST_Guide_HPA.pdf

Merritt, D. K., Lyon, C. A., & Persaud, B. N. (2015). *Evaluation of pavement safety performance* (Report No. FHWA-HRT-14-065). Federal Highway Administration. https://rosap.ntl.bts.gov/view/dot/35858

Minnesota Department of Transportation (MnDOT). (2000). *Drainage manual*. https://www.dot.state.mn.us/bridge/hydraulics/drainage-manual-2000.html

Nebraska Department of Transportation (NDOT). (2022). *Roadway design manual*.

North Carolina Department of Transportation (NCDOT). (2013). *Roadway design manual*.

Noyce, D. A., Bahia, H. U., Yambo, J., Chapman, J., & Bill, A. (2007). *Incorporating road safety into pavement management: Maximizing surface friction for road safety improvements* (Report No. MRUTC 04-04). Midwest Regional University Transportation Center. https://digital.library.wisc.edu/1793/53397

Ong, G. P., & Fwa, T. F. (2007). Wet-pavement hydroplaning risk and skid resistance: Modeling. *Journal of Transportation Engineering, 133*(10), 590-598. https://doi.org/10.1061/(ASCE)0733-947X(2007)133:10(590)

Ong, G. P., Fwa, T. F., & Guo, J. (2005). Modeling hydroplaning and effects of pavement microtexture. *Transportation Research Record*, *1905*, 166-176. https://doi.org/10.1177/0361198105190500118

Oregon Department of Transportation (ODOT). (2014). *Hydraulics design manual*.

Pavemetrics. (n.d.-a). *Laser Crack Measurement System (LCMS-2)*. Retrieved November 24, 2022, from https://www.pavemetrics.com/applications/road-inspection/lcms2-en/

Pavemetrics. (n.d.-b). *Laser Digital Terrain Mapping System (LDTM)*. Retrieved November 24, 2022, from https://www.pavemtrics.com/applications/digital-terrain-mapping/laser-digital-terrain-mapping-system/

Pourhassan, A., Gheni, A. A., & ElGawady, M. A. (2022). Water film depth prediction model for highly textured pavement surface drainage. *Transportation Research Record*, *2676*(2), 100-117. https://doi.org/10.1177/03611981211036349

Pranjić, I., & Deluka-Tibljaš, A. (2022). Pavement texture-friction relationship establishment via image analysis methods. *Materials (Basel)*, *15*(3), Article 846. https://doi.org/10.3390/ma15030846

Rajaei, S., Chatti, K., & Dargazany, R. (2017). *A review: Pavement surface micro-texture and its contribution to surface friction* (Paper No. 17-06773). Presented at the 96th Annual Meeting of the Transportation Research Board.

Rapidlasso GmbH. (2021). *LAStools* [Computer software]. https://rapidlasso.de/product-overview/

Ross, N. F., & Russam, K. (1968). *The depth of rain water on road surfaces* (Report No. LR 236). Road Research Laboratory. https://trl.co.uk/publications/lr236

Saberi, M., & Bertini, R. L. (2010). Empirical analysis of the effects of rain on measured freeway traffic parameters (Paper No. 10-2331). In *Transportation Research Board 89th Annual Meeting compendium of papers*.

Shams, A., Sarasua, W. A., Famili, A., Davis, W. J., Ogle, J. H., Cassule, L., & Mammadrahimli, A. (2018). Highway cross-slope measurement using mobile LiDAR. *Transportation Research Record*, *2672*(39), 88-97. https://doi.org/10.1177/0361198118756371

Sitek, M. A., & Lottes, S. A. (2020). *Computational analysis of water film thickness during rain events for assessing hydroplaning risk part 2: Rough road surfaces* (Report No. ANL-20/37). Argonne National Laboratory. https://doi.org/10.2172/1677647

Snyder, M. B. (2006). *Pavement surface characteristics: A synthesis and guide* (Engineering Bulletin EB235P). American Concrete Pavement Association.

Snyder, M. B. (2019). *Concrete pavement texturing* (Tech Brief; Report No. FHWA-HIF-17-011). Federal Highway Administration. https://rosap.ntl.bts.gov/view/dot/43538

Souleyrette, R., Hallmark, S., Pattnaik, S., O'Brien, M., & Veneziano, D. (2003). *Grade and cross slope estimation from LIDAR-based surface models* (Project No. MTC-2002-02). Midwest Transportation Consortium, Iowa State University. https://cdn-wordpress.webspec.cloud/intrans.iastate.edu/uploads/2018/03/LIDAR_Grade.pdf

Texas Department of Transportation (TxDOT). (2019). *Hydraulic design manual*. http://onlinemanuals.txdot.gov/TxDOTOnlineManuals/txdotmanuals/hyd/index.htm

Tsai, Y., Ai, C., Wang, Z., & Pitts, E. (2013). Mobile cross-slope measurement method using Lidar technology. *Transportation Research Record*, *2367*, 53-59. https://doi.org/10.3141/2367-06

Wark, N., Smith, K., Kennedy, M., Widing, S., San Antonio, J., & Wildey, R. (2015). *Hydraulics manual*. Vermont Agency of Transportation. https://vtrans.vermont.gov/sites/aot/files/highway/documents/structures/VTrans%20Hydraulics%20Manual.pdf

West Virginia Division of Highways (WVDOH). (2007). *West Virginia Division of Highways drainage manual* (3rd ed.). West Virginia Department of Transportation.

Young, G. K., Walker, S. E., & Chang, F. (1993). *Design of bridge deck drainage: Hydraulic Engineering Circular 21* (Report No. FHWA-SA-92-010). Federal Highway Administration. https://rosap.ntl.bts.gov/view/dot/745

Zahir, H., Islam, S., & Hossain, M. (2017). *Friction management on Kansas Department of Transportation highways* (Report No. K-TRAN: KSU-14-5). Kansas Department of Transportation. https://rosap.ntl.bts.gov/view/dot/32229

Zhang, K., & Frey, H. C. (2006). Road grade estimation for on-road vehicle emissions modeling using light detection and ranging data. *Journal of the Air & Waste Management Association*, *56*(6), 777-788. https://doi.org/10.1080/10473289.2006.10464500

Zuniga-Garcia, N., & Prozzi, J. A. (2019). High-definition field texture measurements for predicting pavement friction. *Transportation Research Record*, *2673*, 246-260. https://doi.org/10.1177/0361198118821598

Appendix A: Relevant Literature from Departments of Transportation

A.1 Alabama Department of Transportation

The drainage design manual (DDM) for the Alabama DOT (ALDOT) provides superior guidance for superelevation transitions and hydroplaning mitigation. Hydroplaning mitigation, (Section 6.1.2) and adjacent inlet structures (Section 6.6.5) were found in ALDOT's DDM from March 2022 (ALDOT, 2022).

ALDOT cites the FHWA's Hydraulic Engineering Circular No. 22 (Brown et al., 2009) for hydroplaning considerations, specifically that hydroplaning is a result of factors such as vehicle speed, tire conditions, pavement texture, roadway geometry, and pavement conditions. To estimate hydroplaning speed, ALDOT recommends using the Texas DOT equations based on Gallaway et al. (1979) for WFT and HPS. The ALDOT manual describes cases in which a designer could use these equations to estimate how a higher roadway texture or a lower WFT would impact the HPS of a vehicle. A rainfall intensity equation is also included in the manual to predict how much rain causes hydroplaning. The manual also recommends using the Florida DOT hydroplaning tool as supplementary guidance and that designers must use their own judgment for specific applications. These hydroplaning considerations mentioned in the ALDOT DDM, however, do not focus on superelevated transitions.

A.2 Colorado Department of Transportation

Chapter 4, section 4.12 of the Colorado DOT (CDOT) highway design manual (HDM) briefly mentions hydroplaning mitigation (CDOT, 2018). The manual says "to avoid excessively close inlet spacing, hydroplaning, and other drainage problems associated with flat pavement slopes and wide typical cross sections. Superelevation transitions and vertical curve lengths should be minimized in wide typical cross sections to reduce flat areas that may accumulate water" (CDOT, 2018). Section 4.1.3 of the HDM describes the use of longitudinal tining on Colorado highways with concrete pavements and design speeds above 40 mph.

A.3 Florida Department of Transportation

The Florida DOT (FDOT) HDM is an excellent source for general hydroplaning. Section 210.2.4.2 provides a hydroplaning risk analysis for superelevated sections (FDOT, 2022a). FDOT recommends using proper cross slope for correct drainage, but this can be weighed against the cost of using non-compliant typical sections to improve drainage. For projects with design speeds 60 mph or greater with three or more lanes sloped in one direction, the FDOT HDM recommends using guidance from section 211, which details hydroplaning risk analysis. Section 211.2.3 describes the following projects that require hydroplaning analysis:

- Areas where an additional contributing pavement area is added to standard FDOT cross slope sections (e.g., managed lane buffer, paved shoulder, paved gore, auxiliary lane, etc.)
- Superelevated sections of merging roadways
- Bridge decks that are ungrooved and not included in the above descriptions. Grooved bridge decks are not included.

A report including a cost-benefit analysis is also included in the hydroplaning analysis, which is required for capacity improvements and new alignment projects of more than three lanes draining in one direction and for projects of three lanes where the "superelevation of lowest lane is less than 3% or when there have been 2 or more wet-weather crashes within the available 5-year crash data." Similarly, resurfacing, restoration, and rehabilitation projects on three or more lanes draining one direction require a hydroplaning analysis only when two or more wet-weather crashes have occurred within five years of the crash data. Wet-weather crashes are attributed to hydroplaning when considering crashes that necessitate hydroplaning analysis. Hydroplaning risk assessments are performed using the FDOT hydroplaning program and its accompanying report by Lee and Ayyala (2020). The FDOT HDM considers hydroplaning risk assessments for general hydroplaning and not necessarily hydroplaning at superelevated transitions. The FDOT manual also recommends that an evaluation of mitigation strategies such as "shortening transitions and staggering the cross slope transitions prior to evaluating more costly solutions (i.e., bridge replacement and pavement type changes that require additional design details and a benefit-cost analysis)" should be completed for bridge transitions.

The 2023 FDOT drainage manual was released in October 2022 (FDOT, 2022b). Section 3.9.3 discusses hydroplaning potential evaluation and highlights the FDOT HDM sections previously discussed. For drainage, the FDOT manual generally states "capture accumulated runoff from driveways, side streets and ramps to limit runoff into the mainline travel lanes or other areas where the additional sheet flow could contribute to potential hydroplaning. Design the inlet to capture 100 percent of the flow."

A.4 Georgia Department of Transportation

The HDM and DDM of the Georgia DOT (GDOT) is a decent source for hydroplaning and drainage considerations. The most recent editions of the GDOT HDM and DDM are dated December 18, 2020, and October 10, 2022, respectively (GDOT, 2020, 2022). The GDOT HDM mentions the following concerning drainage and cross slope: "If necessary, when 3 or more lanes are sloped in the same direction and the profile grade is ≤ 0.3%, a 4% cross slope may be used to facilitate roadway drainage in areas of intense rainfall. A decision to use a 4% cross slope along a tangent roadway should be documented with an engineering study and placed in the project record." Similarly, the GDOT DDM provides guidance about limiting hydroplaning on page 6-1, section 6.1.2, specifically that designers should be aware of hydroplaning associated with the zero cross slope transitions at sag and crest curves, as well as hydroplaning at turn lanes, median openings, and other locations. Hydroplaning evaluations are not needed as part of standard GDOT design procedure, and gutter spread design is sufficient. The DDM also states that, since vehicle speed is a significant contributor to hydroplaning, the driver is responsible for exercising caution in wet-weather conditions to avoid hydroplaning.

If a location warrants a hydroplaning evaluation, the GDOT DDM provides guidance from the FHWA Hydraulic Engineering Circular No. 21 (Young et al., 1993), which recommends using hydroplaning speed and water accumulation equations by Gallaway et al. (1979) and a water film depth of 0.0735 in. (1.8669 mm) for general design. The DDM also recommends using "the mean or median" value for parameters associated with calculating water film thickness, specifically a suggested vehicle speed of 55 mph, a wheel spin-down ratio of 10%, a tire inflation pressure of 27 psi, a tire tread depth of 7/32 in., and an MTD of 0.038 in. A continuation of hydroplaning speed

based on water film thickness is used in the GDOT DDM to identify a rainfall rate to induce hydroplaning, as described in the FHWA Hydraulic Engineering Circular No. 21 (Young et al., 1993). This approach uses the equations by Gallaway et al. (1979), the rational equation, and the Mannings equation to calculate rainfall intensity to induce hydroplaning for a given cross slope and longitudinal slope of a roadway. Other means for solving for water film thickness to result in hydroplaning at a selected design speed could also be substituted in this equation. Tables of hydroplaning rainfall intensities for design speeds of 55 mph and 65 mph are given for various cross slope, longitudinal slopes, and flow path lengths for pavement surfaces.

While it does not necessarily account for hydroplaning at superelevated transitions, the GDOT DDM recommends using the following measures to reduce hydroplaning:

- maximize transverse slope;
- maximize pavement roughness to increase roadway drainage capacity;
- use graded course (porous pavements) solutions;
- decrease inlet spacing to limit gutter spread;
- limit ponding duration and depth at sag curves;
- limit depth and duration of overtopping flow;
- although uncommon, use hydroplaning warning signage as a last course of action.

A.5 Idaho Transportation Department

The Idaho Transportation Department (ITD) HDM provides relevant information on highway design. The current revision of the manual is from August 2013 (ITD, 2013), and information regarding superelevation begins on section 535.00. For drainage, the ITD HDM mentions that “curves in cut sections and grades flatter than 1.2% should be rotated around the inner edge of the traveled way” and that “drainage must be checked for adequacy on grades flatter than 0.75%.”

The ITD HDM manual also contains a section on superelevation runoff between adjacent curves. Reverse curves are labeled as “birdbaths,” where two adjacent horizontal curves overlap. The manual cites that “roadway tangent length between two adjacent horizontal curves would

normally be two-thirds (2/3) of the sum of the superelevation runoff lengths plus the tangent runoff lengths (Z) for the two respective curves." Additionally, 200 ft between curves is desired between consecutive horizontal curves.

A.6 Minnesota Department of Transportation

The DDM of the Minnesota DOT (MnDOT) contains brief suggestions for improved pavement drainage (MnDOT, 2000). Although the current version of this manual is from August 30, 2000, it still provides several general practices for highway design, and section 8.5.2 provides relevant design recommendations for drainage. When considering longitudinal slope, MnDOT states that minimum longitudinal grade is more important for curbed pavement than uncurbed pavement due to stormwater spread against curbed sections. A similar problem can also occur on flat gradients on uncurbed sections if vegetation is allowed to build up along the pavement edge. A minimum gutter grade of 0.35% is desirable to ensure adequate drainage.

MnDOT also offers the following general design suggestions on pavement cross slope to provide proper drainage:

- Considering drainage and wet pavement safety, the crowned cross section with drainage both ways from the crown is preferred. This cross section will drain the pavement quickly, and the difference between the high and low points will be minimized. However, this requires alternate drainage design for both sides of the highway and may complicate at-grade intersection traversability due to the repeated ups and downs of the cross section, which can be lessened by transitioning to flatter cross slopes through the intersection. Therefore, this alternative is most suited for divided highways with wide depressed medians and full or partial control of access.
- A uni-directional slope towards the outside edge will reduce traversability problems at at-grade intersections, but it requires drainage design for one side of each roadway. With each lane contributing runoff, the potential for hydroplaning increases. During freeze-thaw periods,

snow that has been plowed to the median melts and drains across the travel lanes, causing a safety hazard. Slippery conditions can be created when the melting runoff refreezes.

MnDOT also states that the length and quantity of flat sections of pavement in superelevation transition areas should be minimized, although a method or best practice to limit superelevation transition length is not provided in the MnDOT DDM. In addition to standard inlet design, the MnDOT DDM also provides in-depth guidance on inlets for sag curves, including drainage capacities, drainage lengths, efficiencies, and placement calculations for grate, curb, and slotted drain types at sag curves where poor drainage can cause hydroplaning.

A.7 Nebraska Department of Transportation

The HDM of the Nebraska DOT (NDOT) contains several relevant suggestions about minimum grades for drainage with superelevated highway transitions (NDOT, 2022). The NDOT was revised in May 2022, and relevant material begins on page 3-21, section 3.A.2. A portion of the NDOT HDM is presented below:

1. Rural Curbed Roadways and Bridges: A minimum grade of 0.50% is acceptable. Flatter grades may cause stormwater runoff to spread across the traveled way.
2. Urban Curbed Roadways: A minimum grade of 0.35% is acceptable. Flatter grades down to and including 0.20% may be used with Unit Head approval. As an alternative to a grade flatter than 0.35%, rolling the gutterline and warping the centerline grade line at a minimum slope of 0.35% may be considered.
3. Non-curbed Roadways: Level longitudinal gradients are acceptable where the pavement is crowned 2% or more if consideration is given to the need for special ditches.
4. Superelevation Runout: To facilitate pavement drainage, a minimum grade of 1.5% shall be maintained through the area where the adverse

crown has been removed. A flatter grade down to and including 0.5% may be used with Unit Head approval.

A.8 North Carolina Department of Transportation

The HDM of the North Carolina DOT (NCDOT), dated July 22, 2013, contains a general method for addressing hydroplaning (NCDOT, 2013), detailed in section 1-16. The following Hydroplaning Awareness Outline from the manual is a source for a hydroplaning remediation process:

I. Contributing Factors

A. Water film and thickness

B. Pavement cross slope and longitudinal slope

C. Pavement roughness

D. Vehicle speed

E. Tire condition and so forth

II. Identification of Problem Areas

A. Existing conditions

1. Skid testing

2. Accident Reports

3. Visual Observation

4. Reports from Department personnel and citizens

B. Proposed/Design Condition

1. Design Analysis

2. Accident Reports and so forth upon project completion (see Existing)

III. Remedial and Countermeasures

A. Existing Condition

1. Improve pavement surface – open graded asphalt friction courses

2. Improved surface water removal

a. Improved drainage systems

b. Improved longitudinal and transverse pavement and shoulder slopes

3. Warning signs

B. Proposed/Design Condition – Roadway Design

5. Typical section

a. Pavement Cross Slope

b. Shoulder cross slope

c. Rooftop section

6. Grades

a. Minimum of 0.3% (tangent and along VC)

b. Vertical Curves

1. Sag (K factors greater than 167 can create drainage problems)

2. Crest (avoid 0.3% except within 50 ft. of high or low point)

7. Superelevation

a. Resolve SE about centerline instead of median EOP

b. (sic)

c. Avoid long SE transition areas

8. Combination of the above factors

B. Proposed/Design Condition – Hydraulic Design

1. Hydrology

a. Design Storm Frequencies

b. Drainage Areas (size, shape, cover, slope, future development)

c. Discharge Rates (Hydrological Method)

2. Highway Geometry

a. Longitudinal Slopes and Cross Slopes

b. Grade Elevations

c. Typical Sections

3. Critical Locations for Collecting Runoff

a. Cross Drainage

b. Points for Reducing Spread

c. Sags

d. Upgrade of Zero Cross Slopes

e. Upgrade of Street Entrances

f. Upgrade of Bridges

g. Driveway Entrances

4. Highway Drainage Structures

a. Cross Pipes, Culverts, Bridges

b. Storm Drainage Systems (Catch Basin, Drop Inlets, Berm Inlets)

c. Funnel Drains

d. Bridge Scuppers

Section 5-21 of the NCDOT HDM, dated January 2, 2002, includes additional suggestions for shoulder drains, such as using continuous drains along the full length of sag vertical curves and along the full length of the low side of superelevated curves. Implementation for a continuous drain system is left to the discretion of the highway designer.

A.9 Oregon Department of Transportation

The DDM of the Oregon DOT (ODOT) contains extensive guidance about inlet drainage near sag curves (ODOT, 2014) beginning on page 13-D-58, Section 6.0, dated April 2014. Calculations and placement for inlets at sag curves for grate inlets, curb inlets, slotted inlets, sweeper combination inlets, trench drain systems, and flanking inlets are available in this manual.

A.10 Texas Department of Transportation

Chapter 10, section 4 of the Texas DOT (TxDOT) DDM, dated September 12, 2019, contains information about hydroplaning and its association with pavement grooving and surface texture (TxDOT, 2019). The DDM contains the following summarized points and recommendations:

- Proper cross slope is needed to facilitate better drainage. Longitudinal slope has a lower impact on decreasing hydroplaning.

- Although proper inlets are needed to reduce and eliminate water that creates ponding on pavement surfaces, “transverse drains should not be used without serious consideration for small-wheeled vehicles.”
- High macrotexture surface courses and permeable surface courses impact pavement-tire interactions as well as water film thickness. Hydroplaning can be somewhat minimized with rough texture, as inlet interception can be improved. Conversely, very rough pavement texture can cause a “wider spread of water in the gutter” and can also retain water that hinders runoff.
- Grooving can be used to mitigate localized hydroplaning and can help to remove smaller amounts of water (such as a light drizzle). Transverse grooving yields better results than longitudinal grooving, which can prevent water from draining off to the side of the roadway surface and create vehicle handling problems.

A.11 Vermont Agency of Transportation

Section 8.3.4.3, page 8-5 of the DDM of the Vermont Agency of Transportation (VTrans), dated May 28, 2015, contains relevant guidance on cross slope and longitudinal slope (Wark et al., 2015). For roadway slope, the DDM states that longitudinal slope has a greater impact on curbed drainage due to larger impacts from stormwater spread compared to transverse slope. Additionally, vegetation should be cleared from edges of uncurbed pavements to limit stormwater spread. The VTrans DDM also recommends use of a 2% cross slope with a central crown line for normal use, but in areas where intense rainfall is a concern, cross slope with a central crown line can be increased to 2.5% to facilitate drainage. If three or more lanes are inclined in the same direction on multi-lane pavements, successive lanes in the same direction should have increasing cross slopes. Lanes adjacent to the crown line should have normal cross slope, but successive lane pairs (or portions of lanes) should have increasing cross slopes by 0.5%–1.0%. When more than three lanes occur in a single direction, maximum cross slope is 4.0%. VTrans also states that breaks in cross slope should be provided at two lanes, with three lanes being the upper limit. Although it is

not recommended, inside lanes can be sloped towards the median, if necessary, but these lanes are usually higher speed and experience lower allowable water depth.

A.12 West Virginia Division of Highways

The West Virginia Division of Highways (WVDOH) DDM contains several points about pavement texture and structure relevant to drainage (WVDOH, 2007). A section about hydroplaning begins in section 5.3.2.7, page 5-11, and the addendum of the DDM is dated June 2015. The WVDOH DDM states that proper macrotexture can channel water on the roadway to reduce WFT build-up and reduce hydroplaning. High macrotexture can be attained using transverse and longitudinal grooving. According to the WVDOH DDM, "combinations of longitudinal and transverse grooving provide the most adequate drainage for high-speed conditions." WVDOH also recommends using pavement structure suitable for areas of poor drainage when a high water table exists. To protect the pavement subgrade from high water tables, a system like "a free draining base course, which usually includes an underdrain system connected to a free draining base trench," can be utilized.

K-TRAN

KANSAS TRANSPORTATION RESEARCH AND NEW-DEVELOPMENT PROGRAM

AD ASTRA PER ASPERA

Kansas

Department of Transportation